# Data modeling and simulation approaches for Urban Greenery Systems in the context of climate change

Sareh Peyman

A Thesis

in

the Department

of

Building, Civil and Environmental Engineering

Presented in Partial Fulfillment of the Requirements

for the Degree of Master of Science in Building Engineering at

Concordia University

Montréal, Québec, Canada

Supervisor: Prof. Dr. Ursula Eicker

March 2022

**CONCORDIA UNIVERSITY**

**School of Graduate Studies**

This is to certify that the thesis prepared

By: Sareh Peyman

Entitled: Data modeling and simulation approaches for Urban Greenery System in the context of climate change

and submitted in partial fulfillment of the requirements for the degree of

**Master of Building Engineering**

complies with the regulations of the University and meets the accepted standards with respect to originality and quality.

Signed by the final Examining Committee:

______________________________ Chair

Dr. F. Nasiri

______________________________ Examiner

Dr. F. Nasiri

______________________________ Examiner

Dr. M. Ouf

______________________________ Thesis Supervisor

Dr. U. Eicker

Approved by

______________________________

Dr. R. Berger, Graduate Program Director

April 14, 2022

______________________________

Dr. M. Debbabi, Dean of Faculty

# ABSTRACT

Data modeling and simulation approaches for Urban Greenery System
in the context of climate change

Sareh Peyman

Buildings' construction, operation, and maintenance consume more than 40% of primary energy in most countries. Heat loss through a building's envelope makes up a large portion of the operational phase. Several materials have been developed to reduce thermal transmittance through building enclosures, despite their heavy environmental impact. Moreover, the unregulated and rapid expansion of urban environments caused many problems. Greenery systems can be a potential solution for improving, among other things, thermal demands and reducing urban heat islands. However, vegetation as a construction material is often overlooked in urban settings because of its design process and operation uncertainty. Thus, their performance should be studied in depth under different configurations and climates.

First, a data model for greenery systems based on a UML class diagram was developed using Eclipse to be integrated into an energy simulation workflow based on EnergyPlus as the dynamic building energy modeling engine. Such a data model facilitates the data storage and organization to analyze and optimize green infrastructure.
Moreover, an urban energy simulation platform can incorporate such a data model and facilitate the appraisals of the green envelope within whole buildings and city integrated greenery system. The data model allowed the study of the impact of each parameter on the system's behavior regarding energy consumption. The optimization study was conducted on the parametrization of a green roof and a rooftop farm system to identify their response under variable initial conditions. An analysis of the essential parameters in the vegetation model was performed. Consequently, the Leaf Area Index( LAI), the substrate thickness, leaf surface albedo, and finally, the moisture content of the substrate layer showed the highest effect. Compared to the heritage building and a retrofitted scenario, the largest reduction in heating and cooling demand, took place in the rooftop farm scenario due to the more LAI and soil thickness resulting in more shading and insulation features of green roofs. In terms of its potential as a mitigation strategy for the urban heat island, greenery systems in urban environments reduce the ambient temperature due to the change in the surface albedo and the cooling effect caused by the evapotranspiration process. This study aimed to investigate whether the integration of green roofs affects the surface temperature, which is not influenced by microclimatic conditions, such as wind patterns and vapor pressure deficit. The results showed a possibility of a temperature

drop of 6°-9° C on a hot summer day. On the other hand, integrating a green roof and a rooftop farm results in lower energy consumption. Therefore there is an annual equivalent carbon reduction because of energy conservation.

Because green roofs can reduce the energy consumption of buildings and sequester carbon in plants and substrates, they are considered effective for reducing atmospheric $CO_2$. However, a green roof's components (substrate, waterproofing membrane, etc.) may produce $CO_2$ during their lifetime. The annual amount of $CO_2$ emitted during the production of a modular green roof and rooftop farm systems were found to be 723.6 t $CO_2$ and 1575.76 t $CO_2$ respectively. In the green roof and rooftop farming scenarios, annual $CO_2$ reduction due to saved energy and CO2 reduction were 155.53 and 349.6 t $CO_2$ respectively. Therefore the CO2 payback time of the extensive green roof and rooftop farming were between 4 and 6 years, which indicates that green roofs contribute to $CO_2$ reduction within their lifespan. The same happened to the initial investment in green roofs assembly implementation. The cost could be paid back by the annual cost saving on energy consumption reduction which were 11 years for the extensive green roof and 23 years for the rooftop farming.

Research shows that a greenery system can replace artificial insulating materials as a passive alternative for reducing energy demands in buildings. A decrease in the ambient temperature and a reduction in the negative impacts associated with the urban heat island effect can also be achieved based on the surface temperature findings.

# Acknowledgment

The completion of this study could not have been possible without the support of my beloved Supervisor, Professor Ursula Eicker. I am honored to be a part of her team and improve my knowledge with her and my teammate's guidance and help.

I would like to appreciate my mom’s love and support during my life being.

I dedicate this thesis to my sons, Pouyan and Houman, to let them know how much I love and appreciate their presence in my life and how proud I am to be their mother.

Sareh Peyman

Montreal, March 2022

**Table of Contents**

## Table of Contents

## List of Figures

## List of Tables

# 1. Introduction

## 1.1 Motivation

According to the United Nations report, the population living in cities is expected to increase up to 67% by 2050[24]. Urbanizations contribute to several environmental issues, including global warming, natural resource depletion, acid rain, and air pollution contributing to Urban Heat Island (UHI). “Urban areas consume about 75 percent of global primary energy and emit between 50 and 60 percent of the world's total greenhouse gases” [24]. Buildings are responsible for the primary energy use and the second GHG emission after cities' transportation sector. Therefore, multiple methods are needed to control high energy consumption and tackle environmental effects in urban and building sectors, both in the design and construction process like using renewable energy sources, refurbishment methods in building, and sustainability control with codes and standards[25]. These approaches focus on the performance of buildings and carbon reduction goals while considering that a building has an evident influence on its environment. Photovoltaic panels, wind turbines, heat pumps, and highly efficient insulation materials are examples of these measures considered and implemented in Net-Zero energy designs. However, according to the life cycle assessment, most technologies have an environmental impact, e.g., photovoltaic panels have a carbon footprint during cradle-to-gate mechanism, starting from the extraction of raw materials until the disposal or recycling of the solar P.V. [26].

Greenery systems have a rather low ecological footprint and contribute to improving a city’s microclimate and may add to the insulation of buildings. The use of greenery in buildings is not a new concept, and several studies have been conducted about its benefit for several decades[9][27][28]. The integration of greenery systems, including green roofs, facades, and living walls, balconies, and rooftop farms to the buildings, not only influence the indoor condition but also have a contribution to increasing the quality of the urban environment, such as improving water and air quality, stormwater management, decreasing temperature and carbon emissions, as well as minimization of heat island effect[29].

Although the greenery system brings many proven benefits, there are controversial opinions regarding costs, complexity, and weather conditions dependency. Therefore, there is hardly a single ideal system that fulfills all conditions. Climate variability and plants diversity available to a specific location may cause a complex design problem, leading to reduced performance of the systems and making it not profitable economically. Despite lots of development on integrating greenery systems through cities, a deeper understanding is still required on different aspects and identifying the greenery system's optimal implementation while considering the influence of different climate types[11]. The goal and purpose of this thesis are to increase the knowledge regarding greenery systems to help create a more sustainable, healthy, and comfortable living environment in urban areas.

## 1.2 Problem Context

The rising population in urban areas due to the convenient living condition of the big cities result in many crucial problems such as pollution, especially water, air and noise, global warming, urban heat island, and insufficient greenery. These all impact directly on health and sustainable living conditions. Shortage of green space coverage causes increasing environmental temperatures, affecting both indoor and outdoor thermal comfort conditions[13]. Even though many sustainable approaches have been applied to urban infrastructure, greenery systems within the building envelope are considered one of the best solutions for solving urban heat island-related problems. Building integration with vegetation adds an extra layer that performs like an insulation layer to the building. Besides that, it provides additional benefits to the public, such as social and economic aspects[30]. Even though their implementation increases, greenery systems are still limited when analyzing the associated problem context described below.

### 1.2.1 Urbanization

Today, most of the world's population lives in cities, and there is a growing tendency to move from rural to urban areas year after year. Approximately 50% of the world's population lives in urban areas that occupy nearly 2.8% of the planet's total land [31]. It results in increasing resource demand to provide a high standard of living. Besides that, it makes cities denser, needing an appropriate urban design to minimize the urbanization effects and keep the balance between society and the environment. Many of the new approaches related to urban services within so-called "smart cities."The Smart City definition is far from being limited to applying technologies to cities [32]. Smart City is a high-tech intensive and advanced City that connects people, information, and city elements using new technologies to create a sustainable, greener city, competitive and innovative society, and increased quality of life. Therefore, the role of individual buildings as an essential urban element in the cities increases to profoundly impact the entire system's behavior to decrease harmful conditions like the Urban Heat Island effect, air and noise pollution, and a lack of biodiversity for its inhabitants. However, satisfying the minimum requirements for long-term health and comfort for humans and wildlife alike will become challenging.

### 1.2.2 Energy demand

The comfort conditions of the occupants play a key role in the total energy consumed in the building sector. In this respect, the building sector is vital, and mitigation efforts are required to reduce energy consumption and minimize building-related greenhouse gas emissions [33]. Fig.1.1 indicates End-use demand in Quebec in 2017. The largest sector for energy demand was industrial at 39% of total demand, followed by transportation at 30%, residential at 20%, and commercial at 10% [1]. In recent years, many policymakers and governments have systematically taken decisive measures to reduce carbon emissions and energy use in buildings. Some of these measures are directly relevant to building energy regulations proposed and implemented by developed and developing countries such as North America, the European Union, and China.[34][35]. Nevertheless, the dependency on local climate raises the complexity of the problem, and energy efficiency standards will not be sufficient to achieve international goals and large-scale standardization. Besides the climate variability, climate change causes more extreme climatic conditions. According to the information presented by The Fifth Assessment Report of the Working Group I in the Intergovernmental Panel on Climate Change (IPCC) [36], the global temperature has increased between 1880 and 2012 by about 0.85°C. In Canada, the annual temperature rise ranged from 0.5°C to 4°C for 16 major cities from 1900 to 2013.

In the building and construction industry, climate change can impact buildings' energy consumption and demand. Architects, building engineers, and energy modelers need to consider climate conditions at the building design stage to ensure that buildings and their associated energy systems can operate as expected under extreme conditions, including heatwaves [37]. Climate change and urbanization, specifically UHI, can cause crucial environmental disruptions. In practice, passive and active measures have been developed to counter the building sector's environmental impacts. The most important are thermal insulation with high-performance glazing, heating systems coming next, and finally, solar collectors and P.V. panels[38]. For optimal energy demands of a building, considering the relationship between the exterior climate and interior conditions is highly recommended by previous studies like [39],[40],[41].

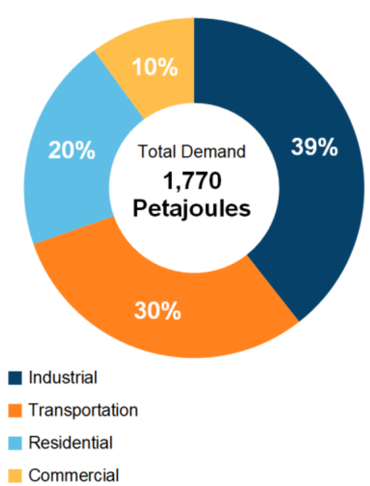


*Figure 7.1 End-Use Demand by Sector (2017)in Quebec*[1]

### 1.2.3 Climate Change and Global Warming

Climate change is a long-term alteration in global or regional climate patterns. Climate is sometimes mistaken for the weather. Climate includes seasonal temperature and rainfall averages, and wind patterns are measured over a long period, whereas weather can change daily or yearly [42]. Weather patterns can become less predictable due to climate change, including increased summer temperatures, precipitation seasonality, weather patterns, and sea-level rise. Current climate change is mainly caused by human activity, such as burning fossil fuels, and releasing greenhouse gases into Earth's atmosphere. The heat from the sun is trapped inside the atmosphere as a result of these gases, causing Earth's average temperature to rise or global warming. Throughout Earth's history, the climate has changed slowly over hundreds and thousands of years. However, man-made climate change from the mid-20th century to the present is occurring faster.

Therefore, appropriate solutions must be taken in action to prevent irreversible damage to human societies and the environment will require a more significant commitment from policymakers to meet environmental goals. As stated in previous sections, the building sector is responsible for significant global energy consumption resulting in $CO_2$ emissions. Resources are required to integrate strategies ranging from structural timber to greenery systems to more advanced technological techniques to allow direct carbon sequestration. Applying them can have a considerable influence on moderating the impacts of climate change in urban areas.

### 1.2.4 Urban Heat Island (UHI)

Urban Heat Island occurs when pavement, buildings, and other surfaces that absorb and retain heat, cover vegetation and nature in the urban area[29]. For investigating the UHI effect, we need to understand the process of energy exchange and energy balance in urban areas caused by urbanization. Fig.1.2 refers to the energy balance in urban environments influenced by the energy gains and losses and the energy level stored in urban elements, such as buildings, cars, and pavements [2]. One of the consequences of high-energy gain and low-energy loss is the Urban Heat Island phenomenon contributing to the temperature difference between urban and surrounding rural areas.

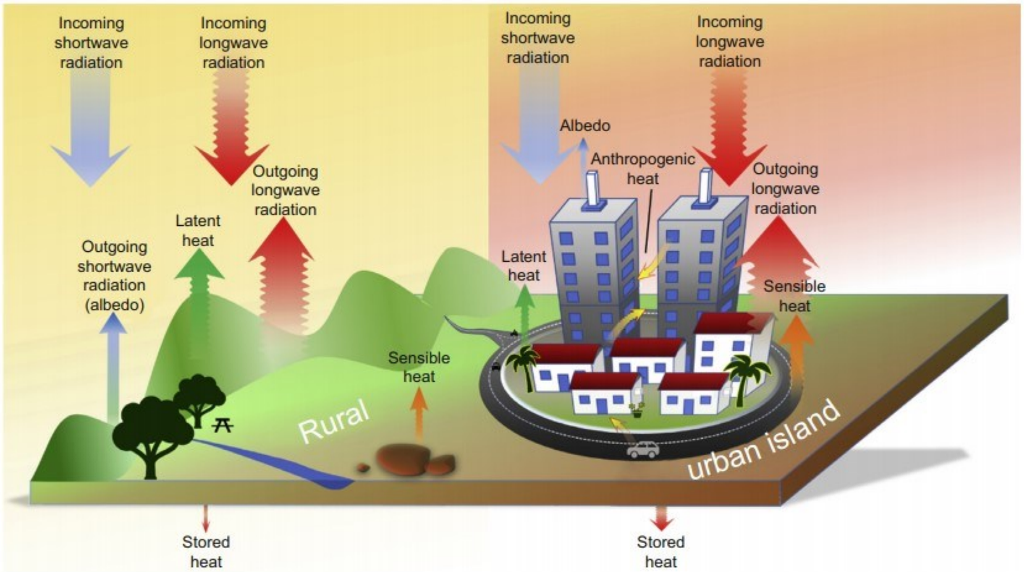


*Figure 1.8 Schematic depiction of energy flux in the urban area. Graphic by Alison Vieritz adapted from Oke, T.R., 1988. The urban energy balance.* [2]

Lots of research has been conducted to see the effect of UHI in many urban areas, such as the Greater Athens area [43], Nicosia [44], Malacca [45], and Melbourne,[46],[47] found that it can reach as high as 10 °C difference between urban and rural areas. Besides the increasing temperature, the UHI has other causes that illustrate in Fig.1.9, such as [3]:

1. Absorption of short-wave radiation from the sun in low albedo materials and trapping by multiple reflections between buildings and street surface.

2. Air pollution in the atmosphere absorbs and re-emits longwave radiation.

3. Obstruction of the sky by buildings results in the intercept of longwave radiative and absorbed or radiated back to the urban environment.

4. Combustion processes, such as caused by traffic, space heating, and industries, release Anthropogenic heat.

5. Increased heat storage by building materials with sizeable thermal admittance.

6. Waterproofed surfaces, less permeable materials, and minor vegetation decrease the evaporation from urban areas. As a consequence, less latent heat for cooling is used.

7. The turbulent heat transport within streets is decreased by a reduction of wind speed.

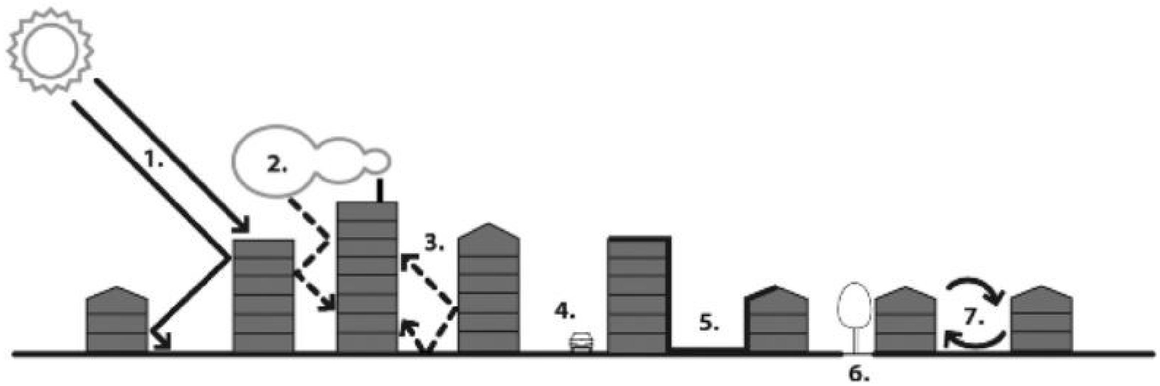


*Figure 1.9 Causes urban heat islands.*[3]

This affects the circulation of the urban hydrological and ecological systems, increases cooling energy consumption, and more significant mortality rates. Many of the causes can be associated with the configuration, materials, and surface of the envelope of buildings. A proper building envelope design can mitigate the effects of UHI and increase the environmental and physical quality of urban space[41].

Increasing vegetation, such as applying greenery systems in buildings, is a widely recommended mitigation strategy for UHI. Susca and his colleague monitored the urban heat island in four areas of New York City. They found a difference in an average of 2 °C temperature between the vegetated area and land without vegetation [48]. Several studies have been conducted to investigate the effectiveness of green infrastructure in UHI mitigation. For example, applying a green façade to a building has a much lower heat absorption, resulting in less heat radiated back into the atmosphere during the evening and at night [49]. It should be mentioned that these systems have a seasonal behavior. The efficiency of vegetation layers in reducing ambient temperatures is higher during summer than in winter.

### 1.2.5 Air and Noise Pollution

Domestic and industrial sources and, primarily, motorized traffic are responsible for pollutant emissions and noise that degrade the quality of life in cities. In this context, evaluating and monitoring urban environmental quality has become essential for making and planning more liveable and sustainable cities. The industrialization of cities resulting in biomass or fossil fuel combustion produces different particles in the air, causing air pollution. These emissions greatly influence air quality and climate change, which is not caused only by human industrial activity; natural events like volcanic eruptions and forests fires have led to the release of many pollutants into the atmosphere like $SO_2$, $H_2S$, and CO [50]. Transportation, industrial processes, and energy production take a prominent role in the emission of pollutants in the atmosphere, such as $CO_2$, $CH_4$, $N_2O$, and $PM_{2.5}$. Air pollution can lead to visibility impairment, ecosystem degradation, and health risks such as asthma, cardiovascular, respiratory diseases, and even cancer[50] [51].

Various factors and agencies are responsible for controlling air pollution and improving urban air quality as a global problem, such as urban planners. The solutions in the three general parts are as follows [52] [53]:

1) Urban transport control
2) Adaptation of roads to improve air quality
3) Control of air pollution through vegetation

To control the pollution caused by vehicle fuels, a solution is to increase the usage of electric cars. Using public transport and encouragement to expand it can help to reduce air pollution [54]. The shape of the road configuration influences the flow of passing air and thus the dispersion of air pollutants[55]. Therefore, designing the shape of the roads, considering the appropriate routes for cyclists [56], and optimizing the car parking system on the street [57] can effectively reduce air pollution. The results of the street canyon's simulations show that the ratio of the height of buildings and the speed and direction of wind flow is significant in reducing the concentration of air pollutants [58]. Vegetation, such as trees, can directly remove $CO_2$ by sequestration and intercept particulate matter in the air. Indirectly, they can also reduce the air temperature through shading and evapotranspiration, reducing the energy demand for cooling in summer and decreasing the amount of pollutants from energy production [59]. Fig.1.4 indicates Quebec's Air Quality Health Index, which is vital for qualifying healthy air. Air Quality Health Index is measured on a scale from 1 to 10+, which corresponds to low to very high health risk. To measure the overall mixture, three specific pollutants have been selected as indicators, such as O3, PM2.5, and NO2.[60].


*Figure 1.10 The Quebec's Air Quality Health Index (AQHI)*[4]

Noise pollution is one of the four primary sources of pollution globally. Due to the high density of transportation services, industries, and construction sites in urban environments, there is a significant contribution from noise pollution to an urban lifestyle. Environmental noise like traffic noise can cause numerous health problems such as sleep disturbance, high blood pressure, and psychophysiological symptoms [61][62]. According to World Health Organization (WHO), traffic noise causes 33% of individuals to be annoyed during the daytime, and 20% have disturbed sleep at night. Traffic-related noise is becoming the most health-threatening environmental stressor in Europe, and more people are exposed to traffic-related noise than any other environmental stressor [61]. Fig.1.5 indicates the noise level ranging from 10-140 decibels (dB) that a person might be subjected to different levels of risk from Faint to Painful.

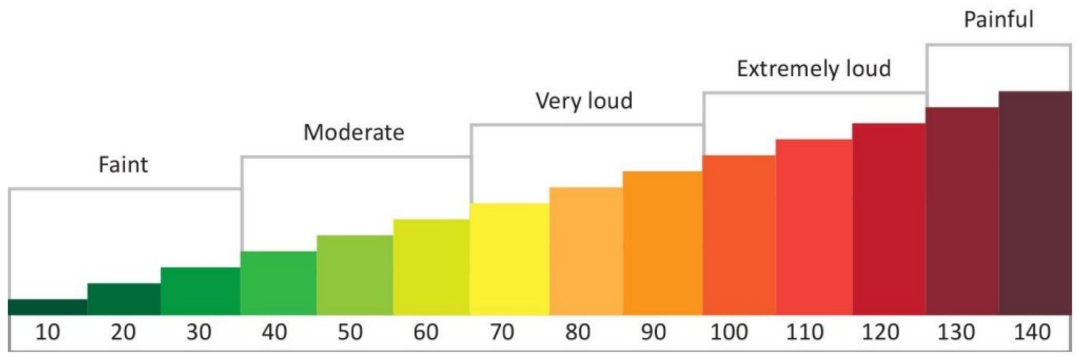


*Figure 1.11: Noise levels adapted from* [5]

### 1.2.6 Biodiversity

As people move into cities to take advantage of employment opportunities, the direct impacts of urbanization on biodiversity have increased. Although biodiversity can significantly impact environmental health in cities, urbanization undermines biodiversity directly through habitat degradation [63]. During the last decades, the aggressive expansion and use of artificial materials in cities have led to a significant decrease in greenery, replacing it with concrete or asphalt surfaces. However, the indirect footprint of urban areas on resource use and biodiversity is far greater than just using the land. Climate change and Habitat loss due to resource extraction and food production, mainly for consumption in cities, are primary causes of biodiversity loss [64]. By 2030, urban land cover is expected to triple what it was in 2000, leading to the loss of locally significant or threatened habitats, especially in highly biodiverse regions of the world [65].

Greenery in the built environment can decrease the impermeable surface fractions with concrete or asphalt, providing diverse environments. A greener urban environment will improve its population's quality of living conditions. Also, increasing the amount of plant and animal species can provide a closer and more balanced relationship between nature and cities.

## 1.3 Passive Design

Passive design defines solutions to reduce the environmental impact of urban construction by using bioclimatic design to connect nature and architecture. This means that the architect seeks cohesion between design and natural elements like sun, wind, rain, and vegetation. However, an optimal solution should satisfy both sides: the designer-architecture and benchmark regulations. Adopting one optimal passive design recommendation for each climate is a fundamental way to help the buildings become energy efficient, especially for residential buildings. The optimal passive design solution is related to many factors such as the local climate, building utilization, topography, and landscape design [66]. Appropriate geometry, orientation, and vegetation can significantly reduce a building's demands to satisfy thermal comfort and energy requirements.

According to the European standard EN 15251: "An energy declaration without a declaration related to the indoor environment makes no sense. Therefore, there is a need for specifying criteria for the indoor environment for design, energy calculations, performance and operation of buildings" [67]. Therefore, thermal comfort is the primary criterion in every design procedure. Fig.1.12 shows one of the examples of passive and bioclimate design in Mexico. This project put the Earth on its priority. That is why they have decided only to occupy a maximum of 30% of the land, respecting the existing trees and providing even more green surfaces to increase the total green area by 130% [6]. They reduce resources usage and economic savings to achieve a more sustainable and environmentally friendly housing product. Furthermore, Passive design strategies are proposed to reduce energy consumption and increase the efficiency of the building, renewable energies for lighting, heating, and cooling.

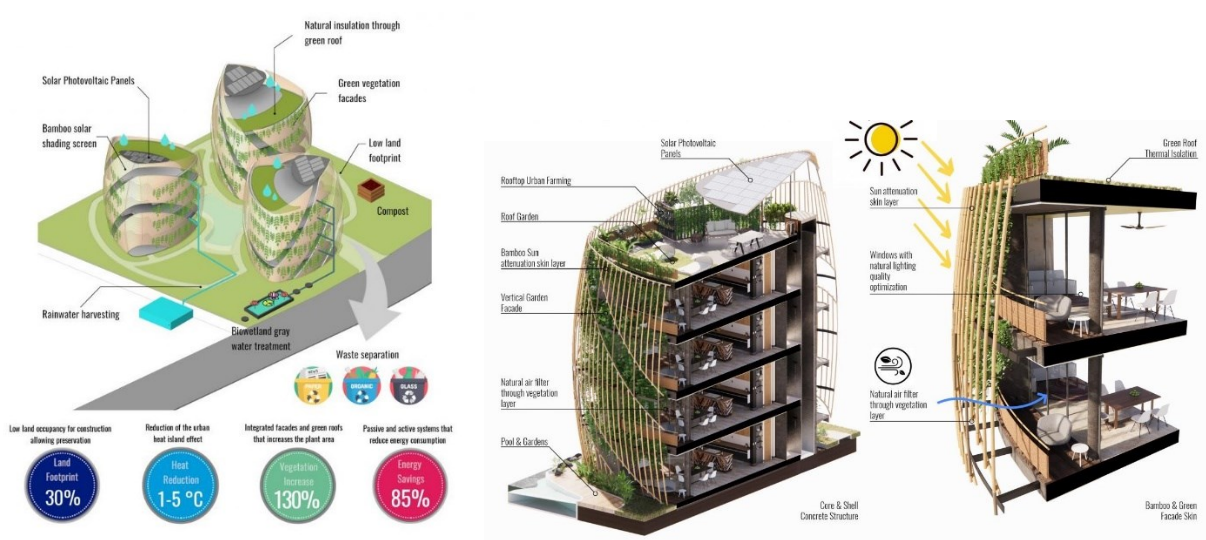


*Figure 1.12 Bio-climatic design adapted from* [6]

Nowadays, researchers and stakeholders aim for Net-zero energy buildings (NZEBs). A NZEB is a low energy building in which the yearly energy production balances energy consumption through renewable energies [68]. It has attracted much attention because of the alternative renewable energy generation aspect that complements the minimized energy requirement; however, advanced bio-climatic and passive design is complex.

## 1.4 Summary

Ever-increasing urbanization rates have created many city-wide problems. Problems such as noise and air pollution, increasing demand for resources, the urban heat island effect, and a diminishing amount of green spaces and biodiversity within cities have caused an array of issues that directly affect adequate health and sustainable living conditions. From this point of view, greenery systems integration into the buildings in urban areas has a great potential to increase the quality of the urban environment, such as improving water and air quality, stormwater management, temperature and carbon emissions reduction, as well as minimization of heat island effects. Besides the profound effects on the environment, the greenery systems benefit the public, including social and economic aspects. The presence of greenery has a significant psychological impact on urban dwellers, enhancing the visual aesthetics of the cities and developing real estate worth.

Moreover, greenery systems can be devised as passive design solutions that provide additional benefits such as insulating impact in winter and shading features in summer. Therefore, it is emphasized that the microclimatic conditions of existing buildings can be adjusted in a cost-effective and eco-friendly manner by utilizing different types of greenery systems. However, there is still a need to scale up greenery systems within urban areas to significantly improve microclimate and carbon sequestration.

# 2. Problem statement, research questions, and methodology

Increasing urban densification causes pressure on the existing infrastructures and damaging impacts on urban environmental and social conditions; therefore, sustainable strategies are required. To tackle the urbanization problems and meet the United Nations Sustainable Development Goals [69], greening the urban environment can be essential. Greenery systems, like green walls, green roofs, and rooftop gardens, have multiple associated environmental, social, and economic benefits that improve buildings' performance and the urban environment. Even though it has proven to provide substantial benefits to a building's performance, green roofs, green walls, and especially rooftop gardens have not reached large-scale implementation due to lack of knowledge, high initial cost, high maintenance costs, technical difficulties, and limited local research. The lack of comprehensive experimental studies on integrating greenery envelopes, especially green walls and rooftop gardens, means that there is hardly any information on optimizing greenery systems under different circumstances like climate conditions, suitable vegetation, and substrate layers for various scenarios.

Moreover, many building owners and stakeholders are unaware of the benefits of the greenery system. There is a need to share information about the benefits to the building's owners and stakeholders and encourage them to apply green envelopes. The other benefit of experimental studies is increasing the database for the greenery envelope, providing input datasets for many scenarios in analogy to the existing building physics catalogs for various archetypes. A comprehensive building input library is The Building Component Library( BCL), which contains building data for building energy models. The data are broken down into components representing parts of a building and measures describing changes made to a building[70]. In terms of the construction type, a web tool called TABULA has been developed for the European residential building construction benchmarks based on the size and age classes of buildings[71]. Regarding the green roofs and facades, educational institutes and commercial companies provide several tools and information. For example, greenroofs.org [57] or purple-roof.com [58] models water retention based on the construction type, location, and climate condition. One of the goals of this work is to assemble and structure datasets for green envelopes to enable performance modeling.

## 2.1 Aims and focus

This study aims to determine the efficiency of greenery systems in different scenarios when appropriately designed. A Greenery system is considered a passive, eco-friendly, and feasible solution to reduce energy demands in buildings. This research project tries to identify the most relevant parameters influencing the behavior of greenery systems to create a data model and catalog to be used for building simulation software, for example, using the *EnergyPlus* software or related workflows with *Grasshopper*, *DesignBuilder*.

Building energy performance optimization is not a simple task. Buildings are complex systems with multiple factors interacting with each other. Even without including greenery systems, finding the optimal energy efficiency solution requires significant knowledge of building science. As greenery systems are associated with additional parameters, the complexity increases by integrating greenery systems. The thermal behavior of any greenery system depends on many parameters, including vegetation and soil substrate properties, leaf area index (LAI), radiation-related properties like leaf reflectivity and emissivity, and leaf minimum stomata resistance (s/m). For the soil substrate properties, the influence of soil density, moisture content, and thickness need to be considered. Greenery systems provide a passive alternative to improve buildings' energy efficiency for both heating and cooling seasons and provide a better micro-climatic environment for the people in their surroundings.

## 2.2 Research questions

The main research questions are how to best structure and classify greenery systems so that a data model can be derived and how to integrate the data into a workflow for building energy performance modeling.

**Sub-research questions**

- What is the procedure for creating a data model for the greenery system that can be combined with a larger urban data model?
- Are there possibilities of replacing green roofs with rooftop farming?
- Which are the parameters with the most substantial influence on the performance of the greenery system?
- To what extent is the insulation, evapotranspiration, and shading effect capable of reducing a building's energy demand?
- How does a greenery system respond under the urban heat island effect study and $CO_2$ sequestration in an urban environment?

## 2.3 Methodology and chapter layout

This section will detail the methodology that will be the basis for the definition of the research and the steps taken to answer the previous questions. The research done within this thesis can be divided into the following steps: Step 1 introduces the topic and provides the relevant background information that led to the development of this project. It describes the aims, focus, and research questions for this research. The methodology shows the investigation's procedure, including the scope and limitations of the project (chapters 1 and 2). Step 2 shows the theoretical framework. A literature review has been performed on the greenery system's historical development, classification, and characteristics.

Additionally, a review of the energy balance of the Green Roof and Green Façade systems is done to identify the relevant parameters governing their performance (Chapters 3 and 4). Step 3 refers to creating a Greenery System data model and applying the knowledge gathered in Step 2 to an experimental setup. A simplified analytic model and analysis are created to show the effects of Rooftop Farming on the energy demands and Building surface temperature. Further on, higher complexity models will be defined in the Rhino/Grasshopper software package for Montreal climate conditions, using the inputs gathered in the data model (Chapters 5 and 6). Step 4 will state the answers to the research questions, conclusions, recommendations, and final remarks while discussing further research on the topic (Chapter 7). The outline for this thesis is shown in Figure 2.1.

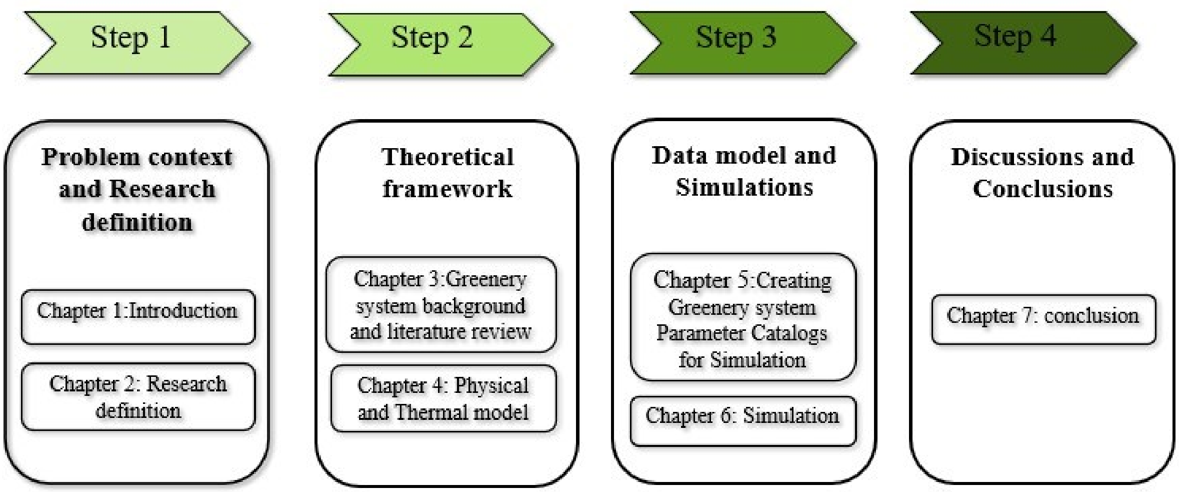


*Figure 2.1 Overview of research outline*

# 3. Greenery system background and literature review

In this chapter, a literature review and an overview of existing greenery systems are presented. It focuses on their characteristics, benefits, drawbacks and provides tables regarding the conducting project in the previous studies.

## 3.1 Background

Greening the urban environment has long been recognized as having a positive effect on the environment, contributing to urban sustainability. It is well known for absorbing carbon and helping to moderate the climate.[72] In this light, to adapt our built environment to the natural environment, Yeang suggests that"our constructions must imitate ecosystems in all aspects" (p. 412) [73]; therefore, there is a need to consider"going green" in modern building envelopes. In recent years, greenery systems have become more common due to their aesthetic influence on buildings and their numerous benefits at both the building and urban scales. In particular, the reduction of energy demands, lowering ambient temperatures, and the mitigation of the urban heat island effect stand out [74]. Furthermore, they can add urban vegetation without occupying valuable street space while increasing urban biodiversity, stormwater management, and air quality. [9].

By integrating green envelopes into the building, passive design solutions are provided to reduce hazardous impacts of the building stock on the environment, society, and economy.[11] The first examples of the implementation of greenery in an urban environment can be found in the Hanging Gardens of Babylon in Iraq in the 7th century[75] and the Roman Empire by planting trees on the rooftops [76]. Throughout the centuries, Mediterranean countries have used greenery systems for shading, cooling, and fruit production in the façades [76]. Contemporary architecture like Le Corbusier and Frank Lloyd Wright developed greenery integration, which used green roofs extensively in their projects, focusing on the harmony between nature and humans [77]. During the last decade, greenery systems have attracted building designers, emphasizing the importance of green infrastructure integration for the future of our cities and buildings. Nevertheless, there are several disadvantages to planting vegetation in buildings, including higher initial investment, maintenance costs, and unpredictable behavior over time. [74]. Table 3.1 shows the best practices in building-integrated greenery envelopes.

*Table 3.1. Green Envelope best practices*

| Project | Location | | References |
|---|---|---|---|
| | | | |

| | | | |
|---|---|---|---|
| European largest green wall | U.K. |  | https://worldarchitecture.org/article-links/eepff/sheppard-robson-creates-europe-s-largest-green-wall-for-this-mixeduse-building-in-london.html[78] |
| Ikea | Austria |  | https://www.dezeen.com/2020/01/23/ikea-vienna-westbahnhof-car-free-store/[79] |
| Chicland Hotel | vietnam |  | https://www.dezeen.com/2020/01/13/chicland-co-trong-nghia-hotel-vietnam-architecture/[80] |
| Liuzhou Forest City | China |  | https://www.stefanoboeriarchitetti.net/en/project/liuzhou-forest-city/[81] |
| Bring urban greenery to Tokyo | Japan |  | https://soranews24.com/2019/08/29/stylish-green-and-eco-friendly-modern-urban-village-to-be-built-in-the-heart-of-tokyo-by-2023/[82] |
| Bosco residential building | Italy |  | https://www.greenroofs.com/projects/bosco-verticale-vertical-forest-milan/[83] |
| Thammasat University Urban Rooftop Farm | Thailand |  | https://www.greenroofs.com/projects/thammasat-university-urban-rooftop-farm-turf/[84] |
| Vancouver convection center | Canada |  | https://www.greenroofs.com/projects/vancouver-convention-centre-expansion-project/ |

| | | | |
|---|---|---|---|
| Ryerson University Urban Rooftop Farm, Toronto | Canada |  | https://www.ryerson.ca/university-business-services/urban-farm/[85] |
| Car park building in Melbourne | Austalia |  | https://www.greenroofs.com/2019/05/18/melbourne-car-park-to-be-turned-into-a-rooftop-skyfarm/[86] |

## 3.2 Greenery System

Green infrastructure in cities can be increasingly integrated into projects to address urban sustainability challenges. However, they face many drawbacks, including social and economic factors and incentives, lack of knowledge, technical issues, uncertainty in design due to modeling software, and the uncertainty associated with a plant's performance which slow down their implementation on a large scale. Despite this, the wide range of benefits can attract scientific and marketing attention due to their capacity to improve indoor and outdoor thermal comfort can bridge the gap between theoretical analysis and real-life implementation. Fig.3.1 illustrates the standard functions of green infrastructure like air pollution abatement, temperature regulation, carbon sequestration, increasing biodiversity, building energy efficiency, and stormwater management[7]. The strengths and weaknesses associated with the Greenery System are analyzed and discussed in the following chapters.

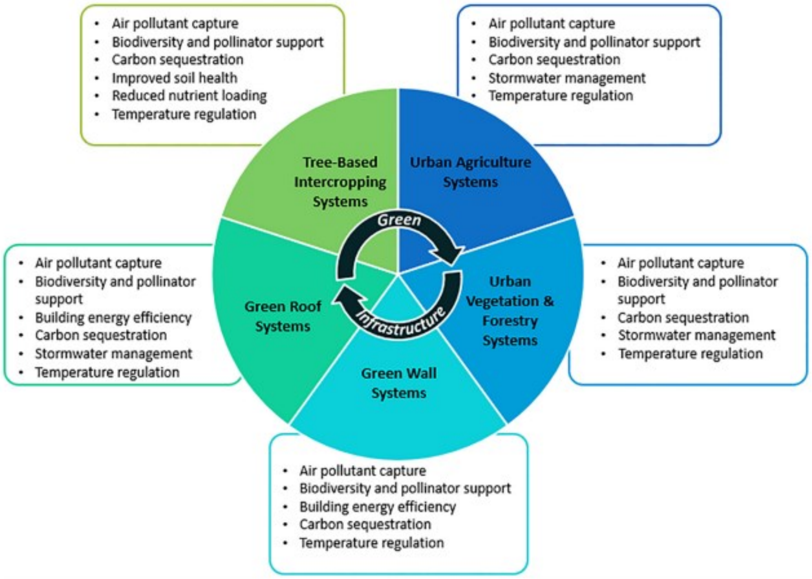


*Figure 3.1 Green infrastructure form and function*[7]

### 3.2.1 The benefit of the Greenery System

Incorporating green infrastructure into cities brings considerable benefits to the urban area, such as mitigating the urban heat island effect by reducing the temperature in urban areas. V.Sangiorgio et al. quantified the influence of each parameter affecting the phenomenon UHI for the first time. City albedo and the presence of greenery represent the most important characteristics with an influence of 29% and 21%. Population density, the width of streets, canyon orientation, and building height have a medium influence of 12%, 10%, 9%, and 8%, respectively. The remaining parameters have an overall influence of 11% [8]. Fig.3.2 displays the percentage of the influences in the piechart. The letter i refers to the weights of eleven parameters or criteria.

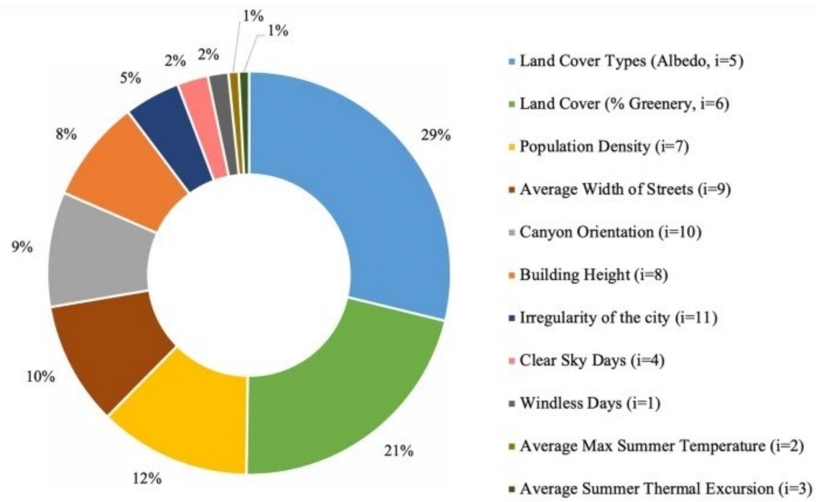


*Figure 3.2 Influence of each parameter in the absolute max UHII phenomenon*[8].

Therefore, adding greenery to urban areas has a major impact on reducing the harmful effects of UHI. Many studies have proven that urban areas with more greenery have a much higher potential to mitigate UHI [87]-[88]. In 2020 Balany et al. tried to present a review of scientific articles about Green Infrastructure published during 2009–2020. Researchers discovered that the temperature surrounding vegetation decreased from 0.2 to 2.27°C [29]. The cooling effect of vegetation on a building through shading and evapotranspiration is not limited to reducing the temperature of the building envelope. Also, it could cause a decrease in the air temperature of an entire urban street canyon outside the building [89]. It brings a large-scale change in the albedo of surfaces, significantly impacting the local ambient temperature. In 2014 Santamouris showed that the greenery system changes the surface's albedo, decreasing the amount of heat stored in vegetation, reducing the total amount of solar radiation absorbed and later released by a green canopy[28]. Table 3.2 illustrates the modeling and experimental studies evaluating the green infrastructure effect on the reducing heat island effect in the past 10 years.

*Table 3.2. Effect of the green envelope on the urban heat island effect*

| **Article** | **Method** | **Location** | **Project** | **Greenery Type** | **Temperature Reduction (°C)** |
|---|---|---|---|---|---|
| Ng et al.,2012[90] | Modeling | Hong Kong | High-density district with various building heights with coverage 100%. Green roof areas around 100 $m^2$. | Extensive Green Roof | 0.6 |
| Peng and Jim,2013[91] | Modeling | Hong Kong | Green roof coverage 100% in 31.2 hectares site area. | Extensive and Intensive Green Roof | 1.7 |
| Ouldboukhitine et al.,2014[92] | Modeling | La Rochelle, France | 100%. Green roof coverage with plant type includes *sedum*, herbs, and grass | Extensive Green Roof | 1 |
| Li et al.,2014[93] | Modeling | Baltimore-Washington | Several G.R.s coverages from 10% - 100% with *Sedum* plant | _ | 1 |

| | | | | | |
|---|---|---|---|---|---|
| | | | type. | | |
| Chen et al.,2014[94] | Modeling | Melbourne, Australia | G.R.s coverage around 50% and LAI of 1.5 | _ | 0.5 |
| Djedjig et al.,2015[95] | Experimental and Modeling | La Rochelle, France. Athens | 2 case studies for 2 different climates. | Green roof and Green wall | 2.7-4 |
| Lobaccaro and Acero,2015[96] | Modeling | Bilbao, Spain | Three urban areas with 100% coverage with grass.The total areas were 175,000 $m^{2,}$ 890,000 $m^2$ and 18,000 $m^2$ respectively. | _ | 1 |
| Meek et al.,2015[97] | Modeling | Melbourne, Australia. | green roof coverage from 42 and 90%. The total area included was around 100 $m^2$. | Extensive Green Roof | 0.9 |
| Timmermans et al.,2015[98] | Modeling | Arnhem, Netherlands | 25% Green roof coverage with Various vegetation types. | _ | 0.03 |
| Larsen et al.,2015[99] | Experimental | Ancona, Italy | The total area of the building was 8.20 m × 10.50 m. | Extensive Green Roof | 2 |
| Di Giuseppe and D'Orazio,2015[100] | Modeling | Salta, Argentina | Green Façade Considered as a shading for glazed West facade. | Green Facade | 1.5 |
| MacIvor et al.,2016[101] | Experimental | Toronto, Canada | *Sedum* green roof near 100% coverage. | Extensive Green Roof | 1.5 |
| Sun et al.,2016[102] | Modeling | Beijing, China | *Sedum* Green Roof coverage from 10% - 100%. | Extensive Green Roof | 2.5 |
| Sharma et al.,2016[103] | Modeling | Chicago, US | The grass Green Roof coverage was 25%, 50%, 75%, and 100%. | _ | 0.6 |
| Pérez et al.,2016[104] | Experimental | Lleida, Spain | double skin green facade covering the east, south, and west orientations of the experimental cubicle. | Green Facade | 10.1 |
| He et al.,2016[105] | Experimental | Shanghai, China | 4 cm substrate depth and *sedum* plant type used for this study. The overall green roof module area was 3 m × 3 m × 2.7 m. | Extensive Green Roof | 2.5 – 5.0 |
| Alcazar et al.,2016[106] | Experimental | Madrid, Spain | A total of 60,000 $m^2$ *sedum* and *Lucerne* green roof was considered for this study analysis. | Extensive Green Roof | 1 |
| Zolch et al.,2016[107] | Modeling | Munich, Germany | Grass with vegetation cover 19 and 100%. Area of 3.5 hectares | Extensive Green Roof | 0.5 |
| Berardi,2016[108] | Modeling | Toronto, Canada | Green roof coverage is 100%, and plant types used are *sedum*, *graminaceous*, and *mosses*. | Extensive Green Roof | 0.4 |
| Taleghani et al.,2016[109] | Modeling | El Monte, California, US | The residential area in California, U.S. Green roof plant type grass with 100% coverage. | _ | 0.2 |
| Morakinyo et al.,2017[110] | Modeling | Hong Kong, Cairo, Paris, and Tokyo | 4 different green roof types were evaluated at different locations. | Extensive and Intensive Green Roof | 0.6 |
| Wilkinson et al.,2017[111] | Experimental | Sydney, Australia, and Rio de Janeiro, Brazil | The green roof was combined with green walls. | Extensive Green Roof.Green Wall | 9 and 3.6 |
| Lee et al.,2017[112] | Experimental | Hong Kong | electricity substation building. | Green Wall and Green Facade | 0.52-3.49 |

| | | | | | |
|---|---|---|---|---|---|
| Solcerova et al.,2017[113] | Experimental | Utrecht, Netherlands | Green roof vegetation *sedum* was used for the study. Different soil moisture value also affects green roof performance. 4 green roofs with each dimension of 7 × 7.5 m respectively | Extensive Green Roof | 0.2 |
| Mirnezhad et al., 2017[114] | Experimental | Putrajaya, Malaysia | Extensive green roofs were used in this study. | Extensive Green Roof | 1 – 2 |
| Charoenkit et al.,2017[115] | Experimental | Phitsanulok, Thailand | 1m*0.5 m*1m Four experimental boxes. | Green Wall | 0.73-2.6 |
| Yang He et al.,2017[116] | Experimental | Shanghai, China | 3 m*3 m*2.7 m test room in Jiading campus of Shanghai Tongji University | Green Wall | 10-28 |
| Huang et al.,2018[117] | Experimental | Taiwan | Four green roof plants: *perennial herb, shrub, vine,* and *groundcove*r | Extensive Green Roof | 3.98 |
| Lalošević et al.,2018[118] | Modeling | Belgrade, Serbia | Five different scenarios were utilized for this study. | Extensive Green Roof | 1.45 |
| Piro et al.,2018[119] | Experimental | Cosenza, Italy | Plants used in this study are *Dianthus gratianopolitanus*, *carpobrotus edulis*, and *cerastium tomentosum*. | Extensive Green Roof | 2.1 |
| Castiglia Feitosa and Wilkinson, 2018[120] | Experimental | Rio de Janeiro, Brazil and Sydney, Australia | The green roof with green wall performance evaluation with the control roof (no vegetation). | Extensive Green Roof.Green Wall | 1.1 and 0.9 |
| He et al., 2018[121] | Modeling | Five different locations in China: Harbin, Beijing, Shanghai, Kunming, Guangzhou | Thermal performance evaluation of green roofs at various climatic conditions in China. | Extensive and Intensive Green Roof | 0.1 - 0.4 |
| Zhang et al., 2019[122] | Modeling | Hangzhou, China | Two districts of Tokyo. Green roof coverage 100%. | | 0.82 |
| Vidya Anderson,2018[7] | Experimental | Toronto, Canada | the extensive green roof located at the Department of Physical and Environmental Sciences building on the University of Toronto campus in suburban Scarborough | Green Roof | 0.47-0.87 |
| Vidya Anderson,2018[7] | Experimental | Toronto, Canada | located at the Instructional Centre building on the University of Toronto campus in suburban Scarborough | Rooftop Garden | 0.79-1.26 |
| Vidya Anderson,2018[7] | Experimental | Toronto, Canada | located at the corner of Military Trail and Ellesmere Road on the University of Toronto campus in suburban Scarborough | Urban Forestry | 0.29-0.64 |
| Vidya Anderson,2018[7] | Experimental | Toronto, Canada | green walls located at the Green Roof Innovation Testing Lab (GRIT) located at the Daniels Faculty of Architecture on the University of Toronto St. George campus in downtown Toronto | Green Wall | 0.51-0.62 |
| Baghaei et al.,2021[116] | Experimental and Modeling | Iran | The northern facade of a 2-story residential building. | Green Wall | 0.36 |

Moreover, the shading of the green envelope, higher insulation, and thermal mass improve the thermal performance of the building [123]. In 2020 Anwar et al. found out a building with an extensive green roof in Australia can decrease energy consumption up to 13.65% (simulated) and 11.70% (measured) compared to a non-green roof [124]. Even though the influence of greenery systems like green roofs and walls on energy saving, surface, and indoor air temperature has been widely investigated over the last decade, there is a lack of information about air conditioning spaces. Xiaoli Hao et al. investigated experimentally and computationally two rooms in Xiangtan, China, located in the hot summer and cold winter climate zone. The results indicate that during the day, the room's operative temperature with green envelope was reduced between 0.4-2.1°C compared to the room without, which is negligible during the night. The result validated by EnergyPlus simulation software showed that the energy consumption reduced by 7% to 8% during the daytime [125].

The shading effect of the greenery system played a significant role in energy-saving.In 2020, Xing Zheng et al. proposed the portable green wall that can shade beam solar radiation but allows soft daylighting. The results indicated that green shading reduced the cooling energy consumption with the correlation coefficients from 0.94 to 0.61. in terms of the shading coefficient. With 80% coverage, the shading coefficient was 0.28. The cooling energy consumption and heat flux transferred through the window glass was reduced by 11.5% and 64.8%, respectively. It found that the west-facing window had the better shading performance[126].

Aside from the energy and thermal benefits, the greenery systems can retain rainwater, manage stormwater, and delay precipitation peak flow. By reducing the water flow into existing sewer systems, the demand on these systems can be reduced, improving their service life and allowing for better stormwater management.[127] When rainwater enters the green roof, a portion of water will be absorbed by the growing substrate or retained in the pore spaces. The vegetation can also take it up and either be stored in plant tissues or transpired back into the atmosphere[128]. In general, the green roof's retention potential depends on the type and thickness of the substrate, type of drainage and its storage capacity, type of vegetation and coverage, the volume of rain event and time of previous dry period, and slope of green roof [9].

Greenery infrastructure can help achieve additional benefits such as pollution reduction and sound absorption. Vegetation can reduce the amount of air pollution caused mainly by $PM_x$, and of greenhouse gases such as $CO_2$. Plants can use these gases through photosynthesis to grow and capture them on their leaves. This procedure depends on leaf stomatal conductance and roughness, leaf surface moisture, and stickiness [59],[129] [130]. In addition, The capture level varies between the different greenery systems and vegetation types. For instance, the *Sedum* species have positive features, such as cold tolerance and a lower need for irrigation than other plants. Moreover, these plants have a very high potential to absorb carbon [131]. Shafique et al. indicated that the green envelopes reduce $CO_2$ emissions in two ways: first by $CO_2$ absorption through photosynthesis and second by energy demand reduction of buildings, resulting in lower fossil fuel consumption in the HVAC system [132]. Green envelopes are considered building materials, and a great deal of carbon dioxide is released during the manufacturing, installation, maintenance, and transportation processes. Kuronuma et al. estimated the $CO_2$ emitted during a hypothetical modular green roof production and maintenance and the $CO_2$ reduction from energy savings and $CO_2$ sequestration. The authors developed an equation to calculate the carbon dioxide payback time[133]:

$CO_2$ payback time = $CO_{2\ e\text{-}p}$ / ($CO_{2\ r\text{-}s}$ + $CO_{2\ r\text{-}e}$ - $CO_{2\ e\text{-}m}$),

where
$CO_{2\ e\text{-}p}$ equals the amount of $CO_2$ emitted during the green roof production.
$CO_{2\ r\text{-}s}$ is the reduction in $CO_2$ due to plant sequestration.
$CO_{2\ r\text{-}e}$ is the reduction in $CO_2$ due to energy savings attributed to the green roof.
$CO_{2\ e\text{-}m}$ is $CO_2$ maintenance emissions.

According to the results, the $CO_2$ payback time of extensive green roofs was between 5.8 and 15.9 years, depending on the species and irrigation method used, indicating that extensive green roofs contribute to atmospheric $CO_2$ reduction and global warming mitigation within their lifespan. In 2021, Seyedabadi et al. investigated the $CO_2$ absorption of a 4-story building green roof with *Sedum acre*, *Frankenia thymifolia* , and *Vinca* plants. These plants' annual carbon uptake through photosynthesis was estimated by 0.14, 2.07, and 0.61 kg carbon/$m^2$.year. Besides absorbing carbon through photosynthesis, the building carbon emission was reduced through reductions in energy consumption by 7.7, 7.2, and 6.4 kg carbon/$m^2$.year, respectively [131]. Table 3.3 refers to studies that have been conducted on green roof carbon sequestration.

*Table 3.3.The results of Green Roofs on sequestering carbon.*

| **Article** | **Method** | **Substrate parameters** | **Location** | **Plant type** | **Carbon sequestration** |
|---|---|---|---|---|---|
| George,2013[134] | carbon offset calculation | _ | _ | _ | 1.22[a] |
| Whittinghill et al.,2014[135] | ANOVA (Analysis of variance) model | The common substrate with depth: 20.4 cm. | Michigan, USA | *Herbaceous perennials and grasses*<br>*Native prairie mix*<br>*Succulent rock garden Vegetable and herb garden* | 3.27[b]<br>3.13[b]<br>3.22[b]<br>9.82[b] |
| Luo et al.,2015[136] | Data was analyzed by the R Project for | A local soil mixed sewage sludge soil, and various soil | Chengdu, China | *L. vicaryi* (Perennial plant)<br>*N.* | 7.11[b]<br>4.73[b]<br>4.77[b] |

| | | | | | |
|---|---|---|---|---|---|
| | Statistical Computing (v. 3.02) | depth 20, 25, and 30 cm. | | *auriculata* (Flowering plant) *L. spicata* (Flowering plant) | |
| Ondoño et al.,2016[133] | IBM-SPSS statistics (v. 20) | Compost-soil-bricks, and compost and bricks. Substrate depth:5 and 10 cm. | Spain | *S. vulgaris* *L. ovatu* | 4.40[b] 1.90[b] |
| Ondoño et al.,2015[137] | Data was analyzed by SPSS (v. 12.0) | crushed bricks, compost clay loam soil compost silica sand clay. | Spain | *Lotus creticus, Asteriscus Maritimus* | 4.60[b] 4.40[b] 1.90[b] |
| Kuronuma and Watanabe,2016[138] | ANOVA and IBM SPSS Statistics version 22.0 | Seedling propagation substrate with a depth 5 cm. | Japan | *Z. matrella* *O. japonicas* *S. mexicanum* | 0.67[b] 0.28[b] 0.34[b] |
| Heusinger and Weber,2017[139] | A-gs model | Different soil depth. | Berlin, Germany | *edum floriferum Weihenstephaner Gold, Sedum album and Allium schoenoprasum.* | 0.313[a] |
| Cascone et al.,2018[140] | EN ISO 13,786 standard | Seventeen different substrates. | Catania, Italy | *Sedum* *Salvia* | 1.35[a] |
| Kuronuma et al.,2018[133] | IBM SPSS Statistics | Various substrate depth. | Japan | *Cynodon dactylon* *Festuca arundinacea* *Zoysia matrella* *Sedum aizoon* | 1.70[a] 1.89[a] 1.80[a] 1.88[a] |
| Seyedabadi et al.,2021[131] | An infrared gas analyzer (ADC Bioscientific Limited, U.K.) | The common substrate with depth: 20 cm | Iran | *Sedum acre* *Frankenia thymifolia* *Vinca* | 0.14[b] 2.07[b] 0.61[b] |

*a kg $CO_2/m^2$ year.*

*b kg $C/m^2$ year*

Concerning sound absorption, not much research has taken place. Davis et al. evaluated the sound absorption of a vertical garden considering the substrate and plants layer effects. Their results showed that absorption of low-frequency sound waves based on the substrate's thickness and moisture content have a higher impact on the sound absorption coefficient [141]. Vegetation has a minimal influence on the sound absorption in low frequencies but provides a more considerable impact on frequencies higher than 400 Hz. Therefore the greenery system can be a sustainable solution to tackle noise pollution in an urban environment. However, Perez et al.'s research referred that the green wall has a small proportion of sound reduction compared to the traditional construction material [142]. Nevertheless, applying small changes in the greenery system like substrate thickness and the structural material can increase its acoustic properties.

Furthermore, the greenery system brings this opportunity to increase biodiversity in the urban area. During the last century, rapid urban expansion and limited conservation of natural areas have forced many animal species to find alternative sources of food and shelter, reducing the amount of fauna present in the urban environment[65]. Therefore, design for increasing biodiversity in the built environment can benefit the local ecosystem. Gonsalves and her colleagues recently investigated the impact of the green roof on beetle biodiversity. Their project indicates that green roofs can support different beetle communities compared to ground-level urban green spaces [143]. Although much research is still needed to understand the effects of building-integrated vegetation on urban biodiversity, current research has shown that implementing these systems can effectively increase biodiversity in cities. Besides that, green roofs and facades have psychological benefits and improve aesthetic appearance. It is proven that people prefer to be surrounded by green areas over those without vegetation. White and Gatersleben conducted a survey involving 188 participants determined that integrating vegetation in the built environment helps to satisfy the human need for aesthetics and restoration. In all cases, there is a clear preference for green façade over green roofs in terms of aesthetic appraisal [144]. In 2018 Vidya Anderson conducted a survey for her thesis on the Carrot Green Roof and Community Garden to investigate the impact of rooftop gardens on the residents. The 10,000 square foot Carrot Green Roof and Community Garden are managed by the Seeds of Hope Foundation, which has five community homes offering a wide variety of resources and support programs, including two learning centers, three post-rehab recovery homes, and a women's shelter. The residents can go planting and use a wide variety of fresh produce, including fruit, vegetables, herbs, and medicinal plants. Fig.3.3 referred to the survey results that admit that green infrastructure brings health benefits like recreation and physical activity for local communities.[7]

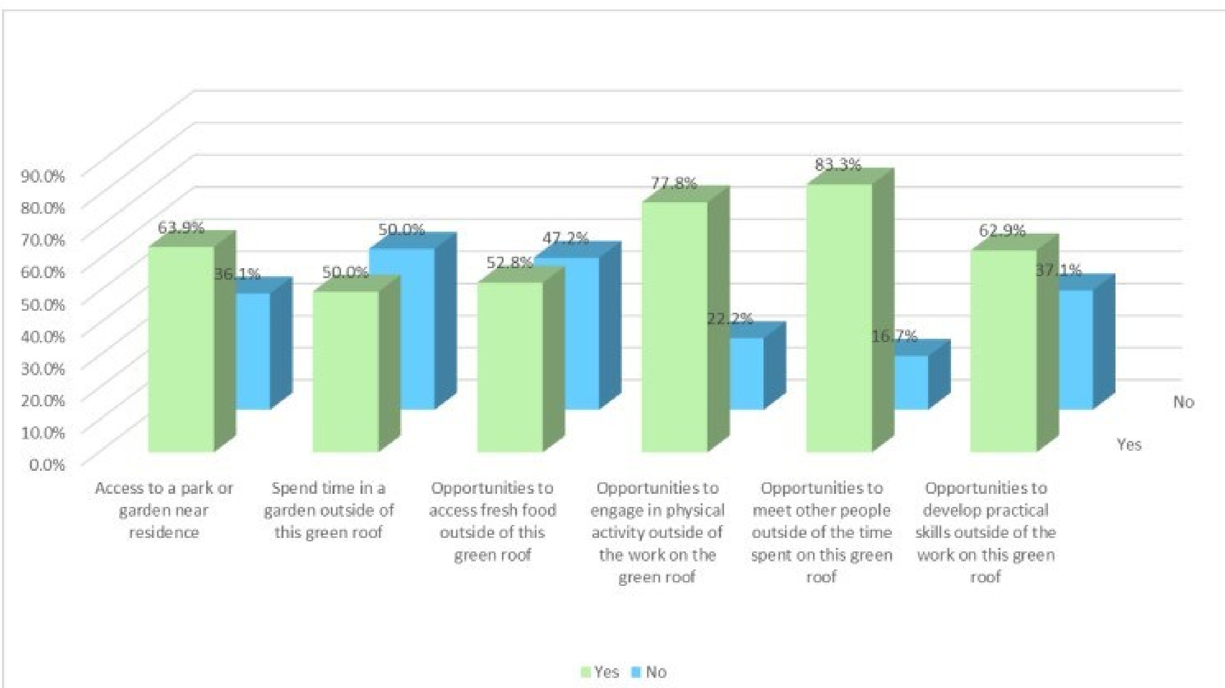


*Figure 3.3 Summary of responses to green infrastructure benefits* [7]

To complement green infrastructure benefits, investigating the Life Cycle Assessments (LCA) of the green envelope is a suitable approach to the environmental, social, economic, and technical aspects. The environmental impact evaluation was assessed through five stages of life cycle assessment (LCA): material extraction, transportation, construction, operation/maintenance, and disposal phases. Bachawati et al. compared vegetative roofs, traditional gravel ballasted roofs, and white reflective roofs life cycle assessment in Lebanon. SimaPro software and Ecoinvent library were used to evaluate 834$m^2$ roof surface area for 45 years, resulting in the extensive green roof being the suitable choice for reducing environmental impact compared to the others [145]. Similarly, Vacek et al. investigated the Life Cycle Assessment of four semi-intensive green roof assemblies, including typical assembly, assembly with added extruded polystyrene, and two assemblies with hydrophilic mineral wool for 20 years cradle-to-gate model [135]. They found that the substrate's green roof with extruded polystyrene and mineral wool has shown the highest environmental impacts over the other assemblies[146]. In 2015 Chenani et al. analyzed the environmental performance of green roof layers like water retention, drainage, and substrate layers. Results indicated that the Rockwool, the plastic drainage layers, and expanded clay had the most significant adverse environmental impact. A study found that using simple materials in the layers of green roofs improves their environmental performance in urban areas [147].

In 2020 Shafique et al. conducted a review study on Green Roof's LCA. The result indicated that a green roof is a sustainable option over a conventional roof because of several benefits in the operational phase [148]. Using recycled material for green roof components such as the substrate, waterproofing membrane, etc., can reduce the impact on the environment since those parts emit $CO_2$ during their lifespan. However, a comprehensive environmental and economic assessment needs to be carried out for future research work. In order to understand the effectiveness and environmental sustainability of the Green Wall in 2021, Salah et al. used WITNESS software to evaluate GHG emission quantification on the component's material, weight, distance traveled, and type of transportation (inventory data) was gathered from the manufacturer. The study found that in ten years of living wall service, an environmental payback period is 4.6 years, followed by years of gain in benefits [149].

To conclude the greenery system advantages, Table 3.4 summarizes the most relevant results regarding the benefits and costs of green roofs and green walls on a building and urban scale. The values in the currency of each study were converted to Euros in the year of the study[21].

*Table 3.4 summary of the green roof and wall benefits* [21]

| | | Ecosystem Services | | | | |
|---|---|---|---|---|---|---|
| | | Green Roofs | | | Green Walls | |
| Measurable | | Extensive | Semi- Intensive | Intensive | Green Façades | Living Walls |
| Building/ Local | Energy savings (Maximum values) | 100% Cooling (Cfb N-Ins.) 73% Heating (Csa Ins.) | 67% Cooling (Cfb N-Ins.) 68% Heating (Csa Ins.) | 84% Cooling (Cfb N-Ins.) 71% Heating (Csa Ins.) | 34% Cooling (Csa) | 66% Cooling (Csa) |
| | PV performance | 1.35%–3.35% increase | | | | |
| | Sound transmission | <5 dB–20 dB | No data available | No data available | | |
| | Greywater treatment | No data available | | | | <80%–90% TSS <90% BOD <30–50% TN <15–30% TP <30–70% COD <20–80% E. coli |
| | In-service life | 28 years–47 years | | | Avg = 50 years | |
| | Property value | 16,2% | | | 2%–5% | |
| | Risk of fire | No data available | | | | |
| | Incentive policies | No data available | | | | |
| | | | | | | |
| Urban | UHIE | 0.97 ∘C – 2.29 ∘C | | | Avg = 1.37 ∘C | |
| | Urban noise | ≈10 dB | No data available | | | 0 dB–10 dB |
| | | | | | | |
| | Water Stormwater management runoff | <33% - < 81% | No data available | Avg < 85% | No data available | |
| | Rainwater | Avg = 8% Cd | | | | |
| | retention | Avg = 5% Pb | | | | |
| | | Avg = 80% NO3 | | | No data available | |
| | | Avg = 68% PO4 | | | | |
| | Peak runoff | <49% - < 90% | No data available | | | |
| | Air quality (Maximum values) | Avg < 20% O3 | | | <40% O3 | |
| | | Avg < 29% NO2 | | | <11,7–40% NO2 | |
| | | Avg < 79% PM10 | | | <42%–60% PM10 | |
| | | Avg > 37% SO2 | | | <3,5% SO2 | |
| | | | | | <1,34% CO | |
| | | | | | <1,34% PM2.5 | |
| | Urban farming | No data available | | | | |
| Intangible | | | | | | |
| | Health/well-being | Use alternative methodologies of measurement as enquiries, multicriteria analysis, etc | | | | |
| | Biodiversity | | | | | |
| | Aesthetic value | | | | | |
| | Recreational value | | | | | |
| | | Costs | | | | |
| | Installation (€/m2) | 67 - 128 | 112 - 148 | 156 - 627 | 114 - 266 | 408 - 1091 |
| | Operation/Maintenance (€/m2/ year) | 0.84–9.16 | Avg = 7.77 | 0.72–12.75 | 2.06 –9.07 | Avg = 18.98 |
| | Disposal (€/m2) | Avg = 12 | No data available | Avg = 26 | 44 - 146 | Avg = 239 |

### 3.2.2 Weakness associated with the Greenery System

In implementing greenery systems, it is important to consider several barriers such as initial high construction cost, polymer material production and disposal, high maintenance costs, limited local research, roof leakage problems, and lack of cooperation between different fields[30]. Fig.3.4 illustrates several factors relating to the limits and risks of Green Infrastructure integration.

The high initial cost is the biggest challenge in the green envelope with long-term investment (costs) [21], which depends on many factors such as location, labor costs, type, material, etc. Installation and maintenance costs of green roofs and green walls are typically higher when compared to most conventional systems, based on Life-cycle Costs (LCC) [13]. The green wall systems have a higher initial cost than the green facades, and they are hardly cost-effective[150]_[151]. A study performed by Perini et al. evaluated the cost-benefit of applying green walls and concluded that the green façade types could be economically sustainable, considering only the system's air purification and carbon reduction capacity [150]. In comparison, Living Wall types require much more investment and maintenance costs which are hardly economically sustainable. However, their social and environmental benefits should not be disregarded since they could increase the property value, possibly countering their high initial costs. So, more research is required to understand their effects fully.

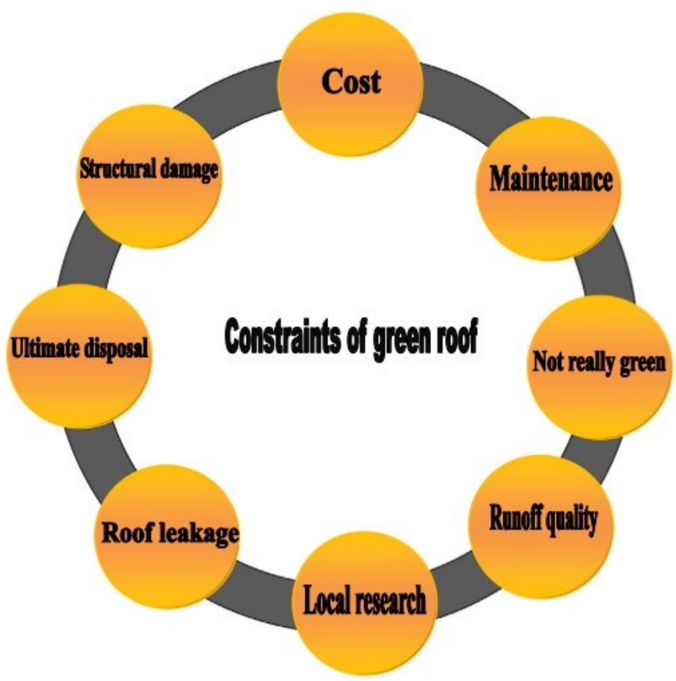


*Figure 3.4 General constraints of greenery system according to public perspective*[9].

Depending on the system's complexity, regular maintenance should be scheduled appropriately. It is unnecessary to irrigate or fertilize green roofs regularly; however, watering and fertilizing are required to maximize benefits from green roofs in drought conditions and rooftop farming systems. There should be a regular check on the green roof's plant, drainage, and substrate to extend the green roof's life [148]. Maintaining green facades involves simple trimming and pruning of climbers in order to prevent the plant from interfering with openings and windows. Whereas for living walls, maintenance is more complex due to the more extensive care required for the vegetation. In addition to trimming and pruning, plants might need replacement, and irrigation systems might require to be checked, ensuring an adequate supply of water [130]. Moreover, whenever frost damage is a possibility in winter conditions, the irrigation system must be emptied and replaced with a suitable system to provide the plants with the necessary nutrients [152]. After construction, the management of the system is essential due to the lack of cooperation and collaboration between different fields (architectural, Civil, Environmental Engineers, and Residents). Much effort is needed to cooperate and collaborate between different fields to apply and manage greenery systems construction costs and maintenance costs [30].

During the construction phase, the green envelope should be placed appropriately to avoid leakage and structural failure of the buildings. Generally, the greenery system can increase the chance of moisture problems in a building's enclosure. Additional vegetation and substrate layers must be insulated to prevent water and moisture from reaching the façade and roof, extending assembly life [151]. For example, in the green facade, due to a wind speed reduction behind the vegetation close to the façade and a minimum amount of solar radiation coming through, it is hard to remove moisture introduced into the cavity between a vertical greenery system and a building. On the other hand, the vegetation layer constantly releases moisture through evapotranspiration, raising the moisture content of the façade. It can be avoided with proper façade design and adequate water and moisture barriers when retrofitting a façade takes place[130]. Besides that, the possibility of rooting the vegetation layer into the green façade and impacting the wall's integrity can threaten the building. If the envelope has numerous cracks, roots can dig into the cracks, furthering the material's deterioration[153]. Since green envelopes can cause deterioration due to plant growth and water leakage, proper system design can prevent these damages, allowing the building to take full advantage of their benefits.

## 3.3 Greenery Classification

The most common places for using green structures on a building are roof greening, vertical greening, green balconies, outdoor and indoor rooftop gardens. The following sections go further in detail about the different types of building-integrated vegetation.

## 3.3.1 Green Roof

Approximately Roofs make up about 20–25% of overall urban surface areas. Green roofs are the most commonly used greenery system and have mainly been implemented in European, North American, and tropical Asian countries [11]. Every year, Green Roofs for Healthy Cities, a non-profit industry association in North America, conducts an annual survey on the green roof industry across North America. Green Roofs for Healthy Cities' mission is to develop and protect the market by increasing the awareness of the economic, social, and environmental benefits of green roofs, green walls, and other forms of living architecture through education, advocacy, professional development, and celebrations of excellence[154]. According to the latest survey in 2019, 763 projects in 34 U.S. states and three Canadian provinces across North America were recorded, installing 3,112,818 square feet of green roofing [10]. Fig.3.5 demonstrates the total Planted Square Footage green roofs in the top ten U.S. and Canadian cities.

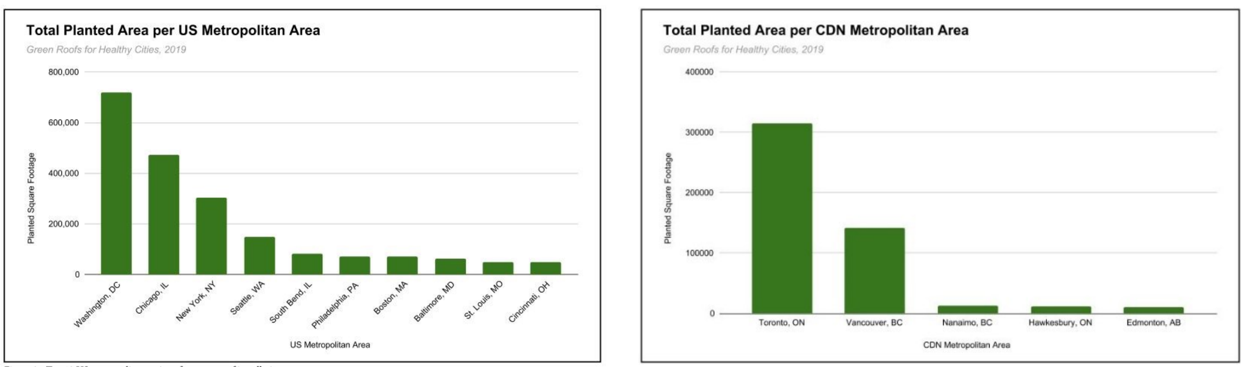


*Figure 3.5 Top 10 U.S. and Canadian metropolitan regions for green roof installations*[10].

Green roofs provide significant benefits to the performance of the building, environmental and aesthetical aspects. Regarding the Green Roofs for Healthy Cities survey, the 3,112,818 square feet of installed green roofs will yield the following approximate benefits [10]:

- 36.9 million gallons of stormwater retained per year;
- 120 tons of carbon sequestered every two years;
- 5.06 million kWh (equivalent) of energy saved per year;
- 1,199 full-time equivalent (FTE) construction jobs;
- 45 full-time equivalents (FTE) maintenance jobs annually.

There are further benefits like lasting roof service life by diminishing the deteriorating effects of U.V. light and temperature fluctuations, minimizing the risks of flooding by excessive water retention, improving the urban life and wildlife habitat, reducing local noise pollution within urban areas [127]. However, it has several disadvantages illustrated in Table 1 by ASHRAE GreenGuide [22].

*Table 3.5. potential benefits and drawbacks of Green Roofs* [22]

| **Advantages** | **Disadvantages** |
|---|---|
| Stormwater runoff reduction | Additional structural load |
| Reduced heat gains (in summer) and heat loss (in winter) to building structure | Cost |
| Longer life for the base roofing system (may not apply to an intensive green roof) | Additional maintenance, ranging from limited for an extensive green roof with low-maintenance plants too high for a manicured landscape intensive roof |
| Reduced noise transmission from outside | Optimal roof type, plant materials, and soil depths will vary depending on climate |
| Aesthetic benefits to people in or around the building with the additional green space | Documentation of benefits such as reduction in heat island effect has not been proven |
| Other general environmental benefits, such as reduced nitrogen runoff (source: bird droppings), air pollutant absorption, potential carbon sink, bird habitat | _ |

The green roof design includes several layers from top to bottom; vegetation, growing medium (substrate), filter, drainage, root barrier, waterproofing membrane, insulation layer, and structural layer, as shown in Fig.3.6 [9]. Besides that, depending on the climatic conditions, some additional components like irrigation systems are required for hot and arid regions, whereas they are useless for humid and temperate climates[34]. Green roofs can be classified as extensive, semi-intensive, and intensive depending on their weight, substrate layer, maintenance, cost, plant community, and irrigation, as shown in Fig.3.7 [127].


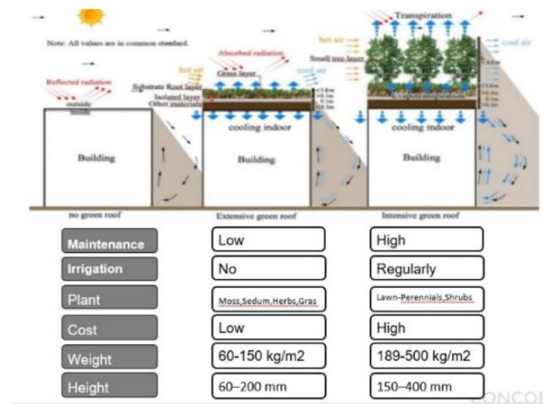


*Figure 3.6 Schematics of different green roof components*[9]

*Figure 3.7 Classification of green roofs* [11]

Extensive green roofs are characterized by a thin soil substrate, low maintenance, and a limited selection of plant species. In contrast, intensive green roofs provide more plant choices, resulting in higher maintenance costs due to a deeper substrate layer and irrigation system requirements[9]. However, By using suitable vegetation and a growing medium for the local climate conditions, the requirement of irrigation and maintenance costs can be decreased [155].

Green roofs can be considered a suitable retrofitting alternative for energy savings in buildings. Although it needs additional consideration, such as measuring the existing structural capacity, Castleton et al. found that the additional loads associated with extensive green roofs generally do not require additional structural support [123]. Fig.3.8 illustrates the distribution by building and project type that refers to the new versus retrofit green roof installations by Green roof for healthy cities. The right pie chart shows that most green roof installations took place in previous years on new construction projects. Speaking of construction and retrofitting, the following section goes further to the requirements and TORONTO municipal building codes and benchmarks.

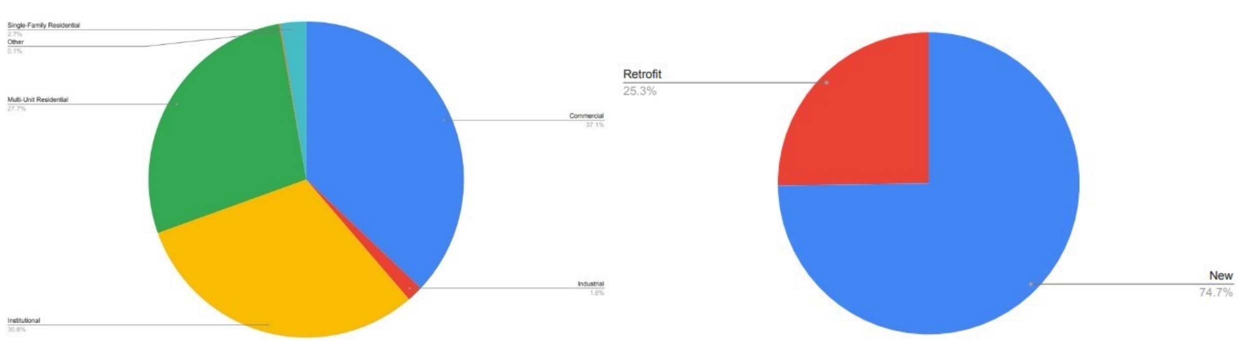


*Figure 3.8- 2018 reported installations by building and project type.*[10]

### 3.3.1.1 Green roof by law in Canada

Green roofs must cover a certain percentage of the roof area in new construction. According to the Toronto building codes, "Every building or building addition constructed with a gross floor area of 2,000 square meters or greater shall include a green roof with coverage of available roof space in accordance with the following chart" [156]:

| **Gross Floor Area (Size of Building)** | **Coverage of Available Roof Space (Size of Green Roof)** |
|---|---|
| 2,000 - 4,999 square metres | 20 percent |
| 5,000 - 9,999 square metres | 30 percent |
| 10,000 - 14,999 square metres | 40 percent |
| 15,000 - 19,999 square metres | 50 percent |
| 20,000 square metres or greater | 60 percent |

Toronto Green Roof Construction Standard aims to define minimum requirements for the construction and maintenance of green roofs. The design and construction of a green roof need to follow both the City's minimum green roof construction and the Ontario Building Code (OBC) requirements. Standards relating to the Green roof assembly, Gravity loads (Dead Loads and Live Loads), Slope stability, Wind uplift, Fire safety, Occupancy and safety, Waterproofing, Drainage, Water retention, Vegetation performance, Plant selection, irrigation, and Maintenance plan shall be met in the design and construction of a green roof [156]. In addition, The Green Roof Bylaw function, in conjunction with the Toronto Green Standard(TGS), complements the Leadership in Energy and Environmental Design (LEED) rating system, providing additional credit and score to the LEED certification[157]. The installation of green roofs potentially helps earn up to 11 LEED building credits in Canada by meeting performance goals, including stormwater management, heat island effect reduction, energy-saving, wildlife habitat, and other environmental benefits [158]. Therefore, finical incentives or water or property fee reduction policies are adopted to encourage owners to apply green roofs to the buildings. In 2020 Liberalesso et al. investigated 143 different incentive policies from 113 cities. According to the results, most green infrastructure incentive policies are concentrated in Europe and North America. In South America, incentive policies are mainly focused on property tax reduction (31 %) and obligations by law (23 %), while in North America, focusing on subsidies (23 %), obligations by law (18 %), stormwater fee discount (15 %) and sustainability certifications (15 %). In Europe, 85 % of incentives are financial subsidies. In the Asian continent, incentive policies mainly focus on financial subsidies (37 %) and obligations by law (37 %). For example, in Basal, Switzerland, the owner is repaid 20% of the total cost of the green roof [159]. In Canada, Three municipalities in Ontario, Kitchener, Waterloo, and Mississauga, offer financial incentives to property owners to compensate for stormwater management benefits. In Quebec, the money is paid to the user per square meter green roofs implementation . Many U.S. municipalities have their policies for the application of green roofs. For instance, In Portland, to reduce the pressure on the sewer system, a 100% discount was offered while property owners in the City of New York received a one-year property tax abatement of $4.50 (USD) per square foot and also Floor Area Ratio Bonus is introduced to the user. Nashville is promoting the green roofs with a $10 reduction in a property's sewer fee for every square foot of green roof. In Singapore, a Gross Floor Incentive Scheme for green roofs is introduced that will give financial benefits to the user for the application of green roofs. A density and a Floor Area Ratio (FAR) bonus are additional benefits associated with green roofs. Followed by the policies of the above countries, several countries like China, Hong Kong, Malaysia, and South Korea are also promoting green roofs adaptation in urban areas[159][160].

### 3.3.2 Rooftop Farming

Due to the rapidly growing interest in urban agriculture projects cultivating organic and locally grown produce in cities, a new form of green roofs called rooftop farms is emerging [161]. The same features as intensive green roofs apply to urban rooftop farming, including substrate thickness and maintenance requirements [162]. Many governments have begun to realize that local food production can be essential to urban food systems[163]. According to Liz Brumer, food travels 1,000 to 2,000 miles before reaching supermarket shelves, leading to about 20 to 30 percent of food loss during the transportation process. Urban farms [164]:

- “Increase food production
- Minimize air, water, and climate pollution.
- Generate more nutritional food.
- Use less water compared to industrial agricultural practices.
- Reduce food loss by cutting out excessive transportation timelines.
- Decrease the cost of food because it is grown and distributed locally.”

The urban farming movement has increased over 30% in the past 30 years around the world. The City of Detroit has the most over 1,400 urban farms, following cities like Boston, Cincinnati, New York City, and Chicago[164]. In 2014 Orsini et al. focused on the potential of rooftop farming production on the 10th-floor rooftops of two public housing buildings in Bologna (Italy). The result indicated that the Rooftop garden could provide more than 12,000 t/ year vegetables to Bologna, satisfying 77 % of the inhabitants’ requirements, and 624 t $CO_2$ are captured annually over three years [12]. Fig.3.9 shows the seasonal variation in daily productivity in this case study.

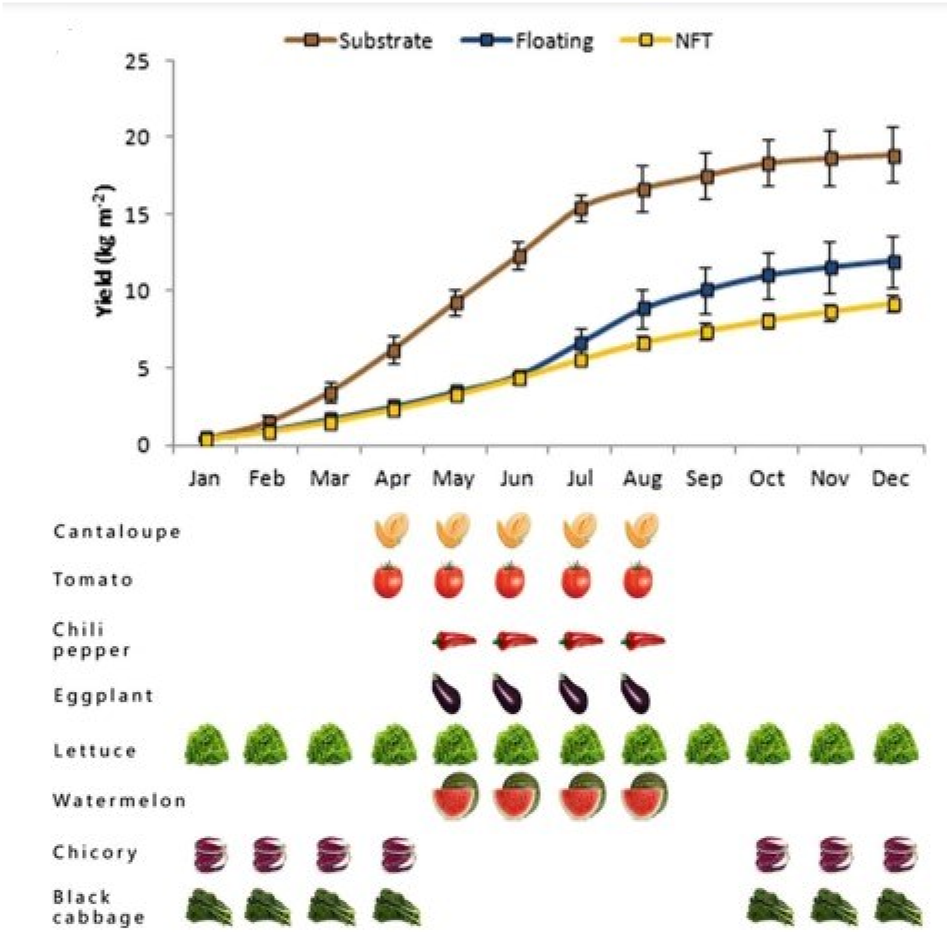


*Figure 3.9 Cumulated (kg/m² ) yield of the simplified soilless systems in the experiments according to crops grown in each season.*[12]

Below two major rooftop farms in Canada areintroduced.

IGA extra Famille Duchemin in Montreal's Saint-Laurent is the first supermarket to sell the products grown on its rooftop garden. The 242 square meters green roofs grow Over 30 different organic products certified by Ecocert Canada, including lettuce, peppers, herbs, tomatoes, and so much more. It uses an irrigation system with water recovered from its dehumidification system. The project demonstrates how planting roofs can improve urban environments by reducing heat island's effects, decreasing noise pollution, boosting energy efficiency, and purifying air and water.

In 2014 the Ryerson Urban Farm intended to introduce rooftop farming, a research lab on Ryerson University's campus in downtown Toronto. Fig.3.10 shows the different layers of the rooftop farm to illustrate the layout of what is beneath the soil[165]. The original growing media was 15.3 cm, so Ryerson Urban Farming (RUF) dug 46 cm-wide paths (5 cm deep) and used the soil to create 76 cm-wide permanent raised beds (25.5 cm deep).

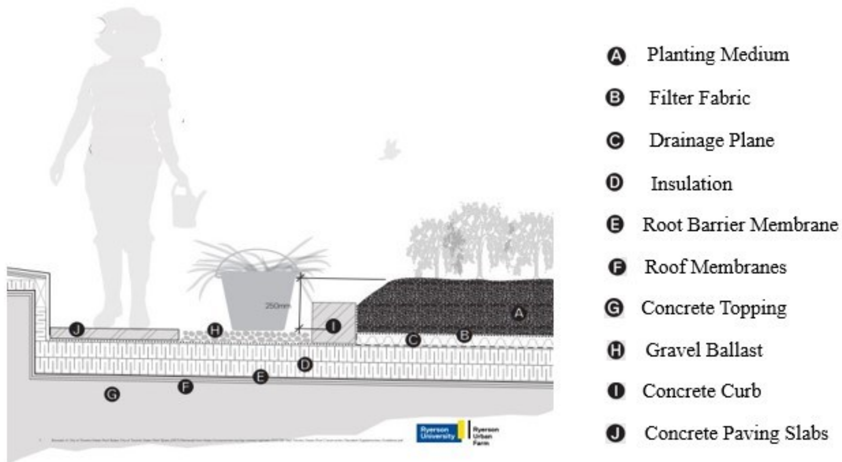


*Figure 3.10 Ryerson Urban Farm construction layers*

They used an ecological technique called "sheet mulching," the weeds were allowed to grow knee-high in spring, then mown down and covered with a black tarp (the "sheet") for three weeks to accelerate the decomposition process. It supports the soil food web (composed of bacteria, mycorrhizal fungi, and microorganisms) that keeps the soil rich, alive, and suitable for growing in Minimal labor that can plant various vegetables.

In 2016, the second green roof space for food production was designated on the new Daphne Cockwell Health Sciences Complex (DCC), initiating the first purpose-built rooftop farm established under the City of Toronto Green Roof Bylaw. A second rooftop farm is scheduled to be occupied by RUF in 2020 and is currently working to amend the engineered soil blend provided by Zinco Canada and plan to build a greenhouse for an entire year of food production on this rooftop[165].

### Harvest Plants

They have grown just about everything on the rooftop farm. The annual crop plan is roughly 30 different crops and 70 cultivars, resulting in 4082 kg of produce on their quarter-acre main production space atop, around 929$m^2$ of growing space. Also, in partnership with local beekeepers, Alvéole, two beehives contributed to a 35 kg honey harvest. According to their crops, there is no limit to what they can grow on a rooftop farm[85]. Fig.3.11 shows 2017 Produce Distribution.

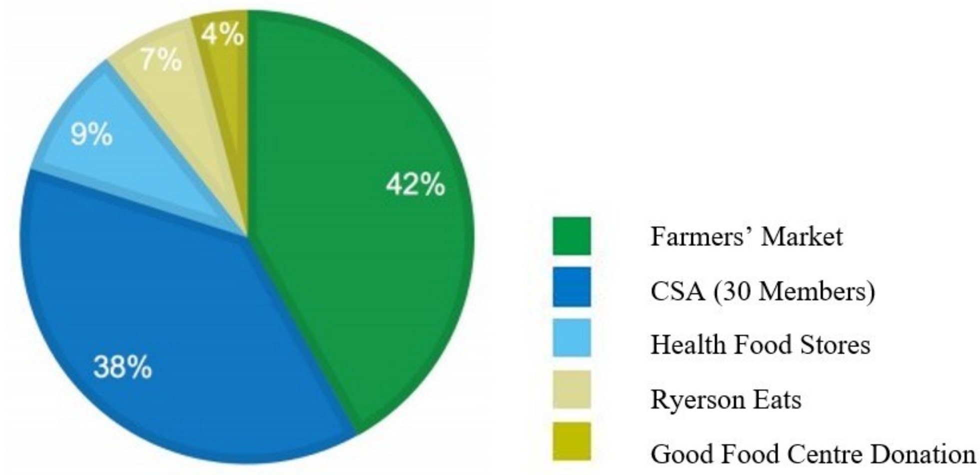


*Figure 3.11 RUF 2017 Produce Distribution*

Their Bed dimensions: 76 cm-wide beds with 46cm-wide paths; beds are on average 18m long and about 25.5 cm deep. For winter preparation to put the farm to bed, they plant cover crops to protect the soil, such as winter rye and clover and cover some beds with straw mulch. In terms of water management, they rely on rainwater as much as possible for Irrigation to maximize the benefits of green roof technology. Whenever rainwater is insufficient, they use water-efficient drip tape, which waters directly to roots, minimizes evaporation, and deters weeds. After harvest, they also reuse their wash station water by filling it into watering cans and spot-watering crops as needed.

Their main issue with the new rooftop farm is the soil health of the blend provided by green roof companies, which contain aggregate to help with water drainage but can be a challenge for growing food. Soil health is undoubtedly the biggest challenge in urban agriculture which the engineered soil blend is also low in organic matter. Green roof companies want the mixture to be lightweight and drain as quickly as possible. In contrast, rooftop farmers like RUF want the most organic matter for plants, which can get heavy when saturated with water during rain events. The water is preferred to stay around in the growing media long enough to benefit the plants rather than drain quickly[165]. Therefore, this is an excellent opportunity for researchers to continue their work in this field since it is trending due to its numerous benefits to cities.

### 3.3.3 Greenery system and photovoltaic panels

Integrating a PV system and a green roof is an effective strategy for producing green energy in urban areas. Due to the evapotranspiration feature of vegetation [166],[30], roof temperature and the surrounding area can be reduced [167],[168],[30], resulting in cooling down the PV surface, enhancing the PV system's energy performance, and maximizing the power output [169]. Fig.3.12 shows an example of the PV-green roof recently called Biosolar by expertise in this field [170]. Using solar photovoltaic panels and a green roof on one roof is the ultimate combination of having "double green" on one roof.

*Figure 3.12 An example of Biosolar Roof*

In 2014 Chemisana and Lamnato investigated the energy performance of PV- green roofs (Biosolar) in Spain and indicated that the PV-green roof reduced the surface temperature of PVs and increased the power output by 1–3% as compared to PV-gravel roof[171]. A study by Alshayeb and Chang (2018) found that the PV-green roof energy production was 1.4% greater than that of the PV-black roof at the University of Kansas in Lawrence, USA [172]. Jahanfar and his colleagues researched a probabilistic analysis about installing a PV- green roof all over Toronto that could supply 16% of the electricity needed and decrease around 12% of energy demand [173]. Plant species significantly impact the overall performance of the PV-green roof system. An experimental study showed that the PV power output with *sedum* species is 2.24% higher than the PV-*Gazania rigens* plant[171]. The PV-green roof has various additional benefits such as Long-term benefits, $CO_2$ emission reduction, removing dust, and cleaning the PV surface[8].

Regarding the green façade and PV panels synergy, In 2019, Tablada et al. did a web survey in Singapore among expertise and building professionals. This study analyses the developed multifunctional facade concept, which integrates green facades, vertical farming, and PV panels. The results indicate an overall acceptance of the new concept of façade and reveal a need for synergetic collaboration between architects/designers and other building professionals [8]. Penaranda Moren and Korjenic investigated through an experimental study from July 2015 to November 2016 a reduction in the building facade up to 30 ◦C and an average of 21.4 ◦C for the maximum temperatures. Whereas In winter, it limits the cooling down effect of the wall by about 3 ◦C on average[174]. Although all the benefits mentioned before for the green roof can apply to the green façade, there is a need for further research and investigation on the integration of green façade and PV panels.

### 3.3.4 Green Walls

Vertical greenery systems (VGS) can provide the same benefits as all the other building-integrated vegetation systems described in the previous section considering the macro and micro scales. Typically, they can create a more considerable impact because the vertical skin of buildings is larger than the roof area[11]. Consequently, they are receiving more attention to resolve the buildings' environmental impact, especially in high-density urban areas.

Green façades (GF) and living wall systems (LWS) are two main groups of VGS, as shown in Fig.3.13. The main differences between the two categories are their rooting systems, plant species, Irrigation system, and the cavity between the vegetation and the façade[127].

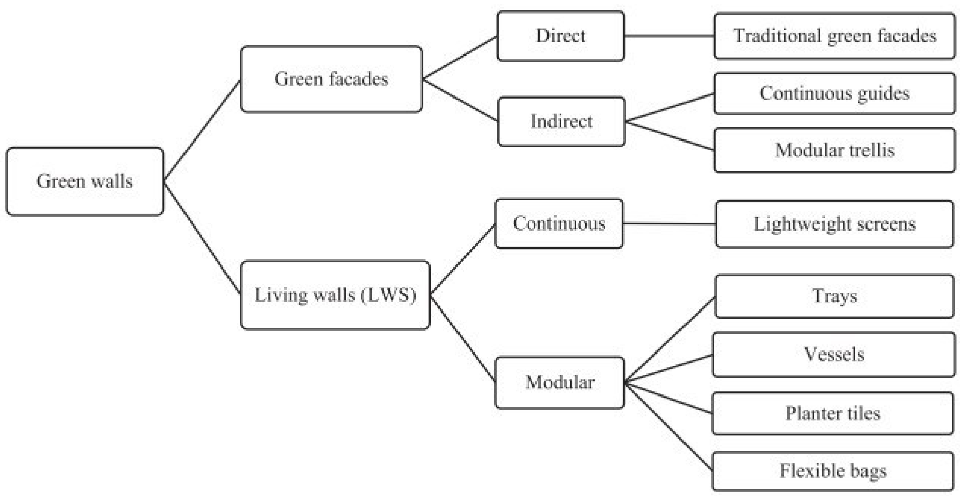


*Figure 3.13 Classification of green walls, according to their construction characteristics.*[13]

There are two categories of green façades, direct or indirect greening. In direct façades, plants are attached to the wall, adhering to the surface through aerial roots, suction, or adhesive root structures [175]. In contrast, indirect façades use a supporting structure to facilitate the vegetation layer's growth. This structure consists of cables, meshes, or nets made from stainless, coated, or galvanized steel, hardwood, aluminum, or plastic. Therefore, climber plant species are more suited for this application. The air gap between the vegetation layer and the façade in indirect greening systems changes their performance as an additional layer, improving the thermal resistance of the façade. Furthermore, the air gap allows air to flow freely, resulting in a natural ventilation system that removes moisture from the environment or the vegetation layer[176]. Both direct and indirect systems have advantages and disadvantages regarding their construction, maintenance, and performance. In summary, the benefits include no additional supporting structure (direct green façade), irrigation system, low water consumption and cost, high accessibility for maintenance, and easy and accessible plant replacement. On the other hand, the drawbacks are limited plant selection, slow growth rate, surface coverage, and the possibility of plant detachment from façade or supporting structures[13].

There are design considerations for green façades, referring to systems with direct ground rooting. For example, one restriction is selecting suitable plant species for this system, which is quite limited as they have to reach high elevations. Therefore, climbing plants are usually used in these systems, although they are limited to a maximum height of 25 meters [13]. Unlike green façades, living wall systems are not rooted into the ground, so they are not constrained by height restrictions. Indeed an artificial growing medium and substrate layer is required to allow proper plant growth. Common substrates planter boxes are foams, laminar layers of felt sheets, or mineral wool. There are benefits and merits compared with green façades, such as more efficient growth due to their pre-cultivation potential[11] and stormwater management due to the water retention capacity of the substrate layer[176]. Despite the advantages, it has penetration like Higher installation and maintenance cost, Complex implementation, a Heavy system which is limited to the structure's load-bearing capacity, and Limited space for root growth [13].

Fig.3.14 demonstrates the schematic of vertical greening systems[127].

Direct Facade Greenery

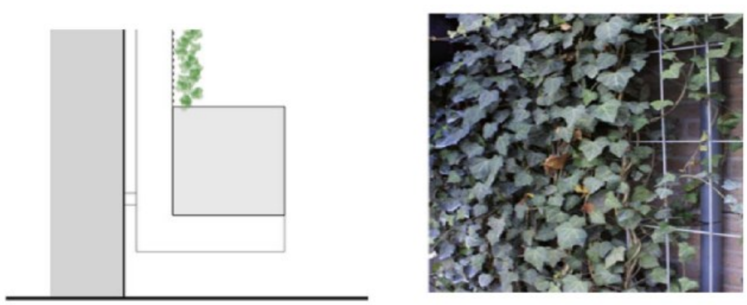

Indirect Facade Greenery

Living Wall (planter boxes)

*Figure 3.14 Types of green facades[65]*

These vertical greening systems can also affect the energy demand of buildings both in summer and winter by employing the following mechanisms:

- the shading impact of the vegetation;
- the evapotranspiration from the plants and the substrate decrease the environment temperature;
- the vegetation and substrate provide insulation and affect the wind circulation [74].

However, features like high investment and maintenance costs, unavailability of a shared constructive standard, challenging interpretation of inconsistent experimental data, and lack of certified simulation models should be considered gaps for these systems [176].

## 3.3.4.1 Green wall thermal model

One way to model the Green Wall is to adopt the Green Roof model from the EnergyPlus software. The built-in Green Roof module of EnergyPlus is developed for low-sloped exterior surfaces like roofs, and it is not recommended for high-sloped exterior surfaces like walls[23]. There is a possibility to ignore the differences between horizontal and vertical surfaces, especially the effect of gravity and irrigation requirements[177]. Malys et al. developed an evapotranspiration model, which accounts for the irrigation of GWs. This evapotranspiration model is integrated into the Green Roof mathematical model based on the heat balance principle of the plant and substrate layers in EnergyPlus [177]. The evaluation of these models is seen in Fig.3.15, which provides a better insight into their behavior.

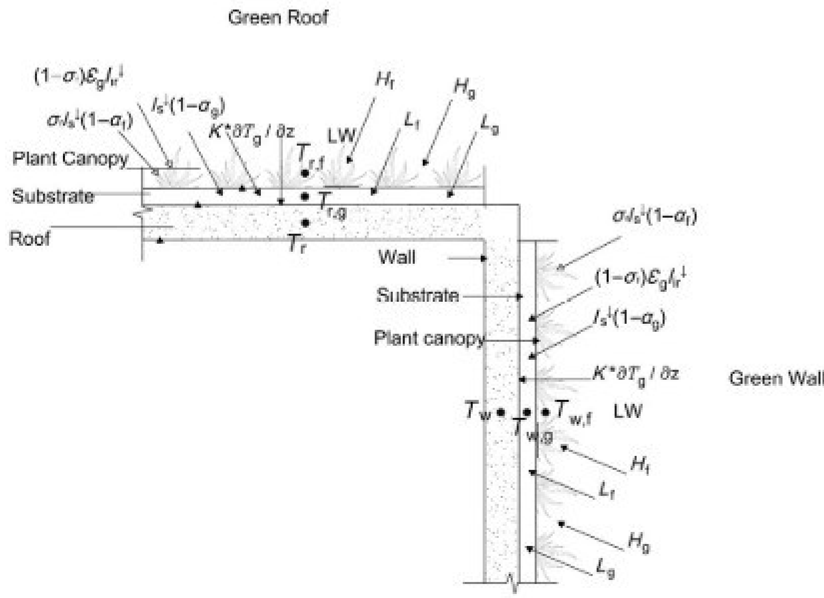


*Figure 3.15 Heat fluxes in green roof and green wall based on the EnergyPlus mathematical model*[14].

Table 3.6 referred to papers that conducted their research based on a green roof thermal model in Energyplus for green wall and validated the result with an empirical experiment.

*Table 3.6. The papers that consider the same Green Roof thermal model in Energyplus for the Green Wall*

| **Paper** | **Authors** | **Year of publishing** | **Main Findings** |
|---|---|---|---|
| Investigating the thermal performance of green wall: Experimental analysis, deep learning model, and simulation studies in a humid climate. | Abdollah BaghaeiDaemei et al. | 2021 | This study reports an investigation on the green wall thermal performance compared to the bare wall on the northern facade of a 2-story residential building in the humid climate of Rasht during summertime. For experimental measurements, temperature and humidity data loggers were used for real-time data collection, validated by EnergyPlus. According to the results, a decrease in indoor temperature by 9% and relative humidity by 32% was seen in the building with a green wall[178]. |
| Comparing reduction of building cooling load through green roofs and green walls by EnergyPlus simulations. | Kalani C. Dahanayake et al. | 2018 | This study uses EnergyPlus simulations to model both GRs and GWs. A self-developed green roof thermal model has been integrated with EnergyPlus, considering the irrigation schedule for the green wall. This model was validated in their previous study.[14] |
| An experimental method to quantitatively analyze the effect of thermal insulation thickness on the summer | F.Olivieri et al. | 2017 | This paper investigates a new methodology to simulate the thermal performance of green walls in the Energyplus using Green Roof properties. The model that was developed was experimentally |

| | | | |
|---|---|---|---|
| performance of vertical green wall. | | | validated[179] |
| Simulation assessment of living wall thermal performance in winter in the climate of Portugal | .Jorge S. Carlos et al. | 2015 | In this study, the simulations included a green roof surface that was vertical, covering 100% of the wall to simulate the greenery system with the same characteristics. For validation, they compared their result to the previous studies[180] |
| Simulation Analysis of Building Green Facade Eco-Effect | Xinchen Pan et al. | 2014 | This paper uses the facade renovation project of Wismar University in Germany, which uses Energy-Plus energy simulation software that validated the result with the other software [181] |

In 2017 Kalani et al. modeled the experimental setup in EnergyPlus with appropriate building materials information, thermal properties, and configurations. Boundary conditions of the simulation model were compatible with the experimental studies for validation[15]. Fig.3.16 illustrates the simulation workflow using Energy Management System (EMS) in EnergyPlus can develop custom control and modeling routines. EMS consists of a programming language called EnergyPlus Runtime Language (Erl) and enables customized EnergyPlus simulations with a high level of supervisory control to override selected aspects of EnergyPlus modeling[182].

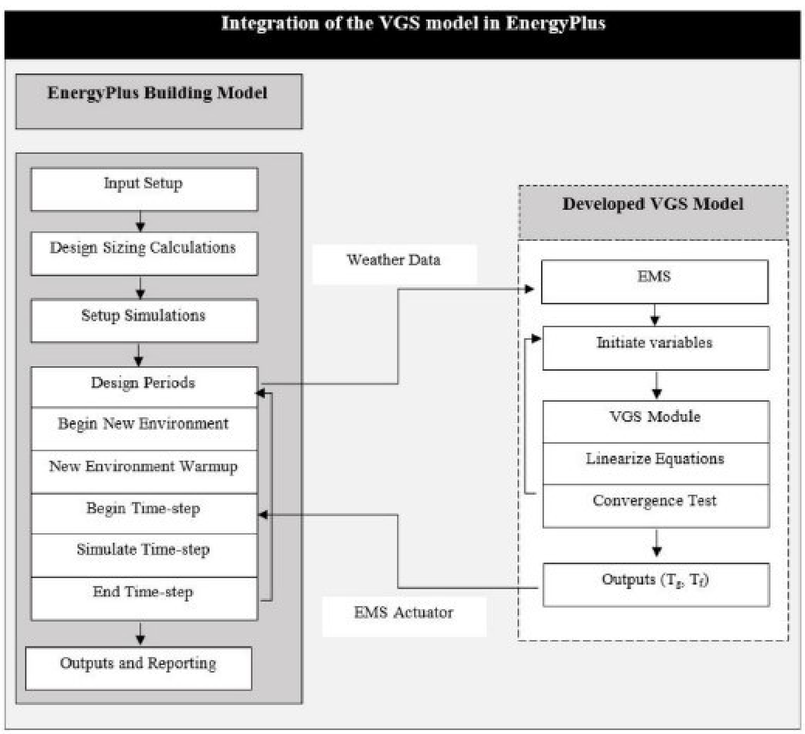


*Figure 3.16. Integration of VGS Module with EnergyPlus using features of EMS*[15].

The following chapter explains more about the green roof/wall thermal and physical model and relating equations.

## 3.4 Summary

This chapter contains a literature review on all aspects of greenery systems in the built environment, including the origins, use, benefits, and risks during the last ten years. It details the potential of these systems to improve the environmental conditions and gives an overview of the different types that one of them, which is rooftop farming, will be analyzed in this research project. They provide a significant amount of benefits, for example, aesthetic appearance, sound absorption and insulation, biodiversity, psychological benefits, external sun-shading, thermal insulation, mitigation of the UHI effect, and stormwater management. Besides, although they can cause damage to existing buildings, proper design, proper care, and regular maintenance can eliminate all the risks associated with using vegetation in the built environment. Furthermore, the literature review showed a gap in structuring information on the greenery system, which lacks a standardized data model and a comprehensive database of the plant and soil types and their properties. The following chapters introduce the development of a greenery system data model and catalog for urban simulation purposes.

# 4. Heat and mass transfer modeling of greenery systems

This chapter will analyze the mathematical models **for heat and mass transfer** involved in the energy balance of the greenery systems. It describes the characteristics of the greenery system regarding the mathematical modeling of the behavior of vegetation as a construction element for the built environment.

As discussed previously, new and better solutions such as Net Zero Energy Building (NZEB) design are needed to counter the effects of manmade climate change, enhance the energy efficiency of the built environment, and meet climate policy targets [183]. The current building industry includes old buildings with low insulation, which results in low thermal comfort and energy efficiency. Bio-climatic designs inspired by nature might reduce energy consumption and $CO_2$ emissions from the construction sector[184]. These strategies intend to minimize the environmental effects by using passive design techniques that take advantage of local weather conditions.

Moreover, in the NZEB design, one of the main constraints is the indoor thermal comfort requirements. According to Perini et al. [185], 0.5∘C change in the internal ambient air temperature can reduce air conditioning demands by up to 8%. Although the influence of external vegetation on internal comfort will not be analyzed as the topic is outside the scope of this thesis, Fig.4.1 indicates the acceptable comfort zones in the Psychrometric chart based on the application of bioclimatic strategies. As illustrated, the NZEB consideration can increase thermal comfort and limit the need for mechanical support and equipment under certain conditions. One of these conditions and strategies can be obtained with the proper integration of a greenery system. For a more detailed review of bioclimatic strategies and principles see [186], [184],[187],[188],[189].

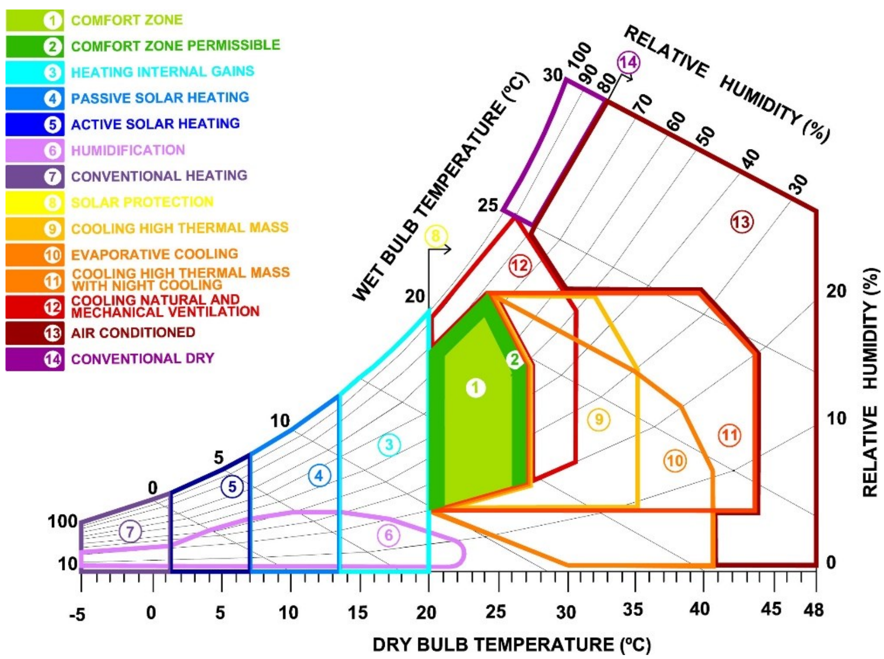


*Figure 4.1 Psychrometric chart adapted from Givoni* [16]

Building energy performance is a complex topic that involves a broad range of aspects such as lighting, ventilation, internal heat gains, thermal insulation, etc., in the early design phases. For example, proper building orientation or ventilation systems can lead to many benefits in the later stages [190]. Further research made by Sanaieian et al.[191] identified that the plan shape, depth, orientation, window-to-wall ratio, and envelope design are essential for minimizing energy demands. Chapter 3 of this thesis developed the benefits of building-integrated vegetation, suggesting greenery systems can reduce energy consumption. However, the uncertainty associated with their performance raises their complexity and can even limit their application as construction materials. Furthermore, there is a limitation in available design tools to assist developers and architects in heat and mass flux analyses, as both the plants and the substrate are necessary to explore the thermal performance[192]. Consequently, there is a significant need for a quantitative and physically-based building energy simulation tool that represents the effects of green envelope constructions. By using such simulation tools, greenery systems can be better integrated and benefit from energy codes and related standards such as LEED [17].In order to understand its behavior fully, the following sections will explain the heat balance of the vegetation layer and the influence of moisture content and density on the thermal properties of the soil substrate in both green roofs and green walls.

## 4.1 Green roof energy balance

The Energy plus simulation software contains a computational model for green roofs called RoofVegetation. EnergyPlus is a widely accepted open-source energy simulation package based on the fundamental heat balance principle [14]. It can simulate indoor thermal environments with mechanical and electrical systems incorporating building descriptions. EnergyPlus has a built-in module for simulating Green Roofs. This model accounts for heat transfer processes like[17] :

- long wave and short-wave radiative exchange within the plant canopy,
- plant canopy effects on convective heat transfer,
- evapotranspiration from the soil and plants,
- heat conduction (and storage) in the soil layer.

The energy budget analysis includes soil and plant canopy energy balance based on the Army Corps of Engineers' FASST vegetation models considering the thick soil layer [193], drawing heavily from BATS and SiB[194]. It accounts for a simplified moisture balance that allows precipitation, irrigation, and moisture transport between two soil layers (top and root zone)[17]. Fig.4.2 illustrates the energy exchange from solar radiation, including latent (L) and sensible (H) heat flux from soil (convection and evaporative) and plant surfaces combined with heat conduction into the soil substrate.

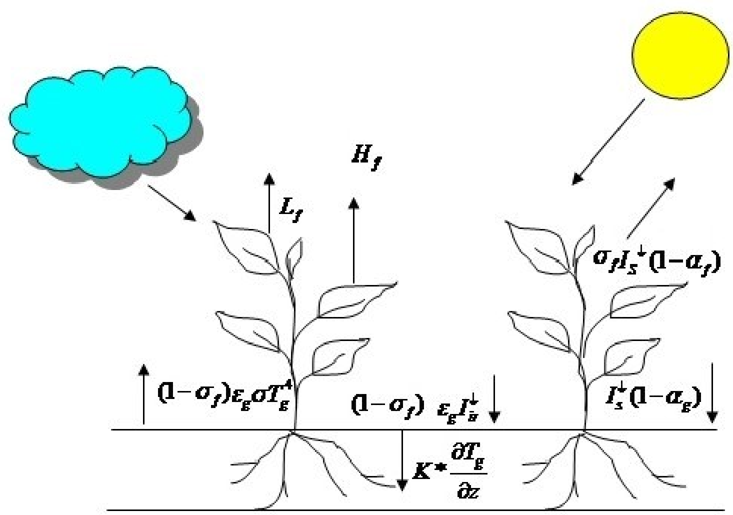


*Figure 4.2 The Energy Balance for a Green Roof* [17]

Longwave radiation represents the infrared part of the spectrum, which depends on the surface properties and their temperature. The amount of longwave radiation emitted from buildings is directly related to the surface's emission coefficient and temperature. The surface's albedo represents the fraction of incident shortwave irradiance that the surface can reflect and is an intrinsic material property that plays a pivotal role in maintaining the earth-atmosphere energy balance [195]. In general, the higher the surface albedo, the larger the amount of sunlight reflected on the surface. The albedo of different surfaces can vary significantly. The average albedo in an urban environment contributes to the UHI effect, and its influence on surface temperature is discussed in Chapter 6.

### 4.1.1 Energy model in the vegetation layer[196]

To simplify understanding the mathematical model, table 4.1 refers to the Nomenclatures.

*Table 4.1 list of the nomenclatures*

| $C^g_e$ | **latent heat flux bulk transfer coefficient at the ground layer** |
|---|---|
| $C_f$ | bulk heat transfer coefficient |
| $C^g_h$ | sensible heat flux bulk transfer coefficient at the ground layer |
| $C^f_{hn}$ | near-neutral transfer coefficient at foliage layer |
| $C^g_{hn}$ | near-neutral transfer coefficient at the ground layer |
| $C_{p,a}$ | specific heat of air at constant pressure (1005.6 J/kg K) |
| $C_{1,f/g}$, $C_{2,f/g}$, $C_{3,f/g}$ | coefficients in linearized temperature equations for foliage/ground |
| $e^*$ | saturation vapor pressure (Pa) |
| $f_1$ | multiplying factor for radiation effect on stomatal resistance |
| $f_2$ | multiplying factor for moisture effect on stomatal resistance |
| $f_3$ | additional multiplying factor for stomatal resistance |
| $F_f$ | net heat flux to foliage layer (W/m$^2$) |
| $F_g$ | net heat flux to ground surface (W/m$^2$) |
| $g_d$ | plant specific characteristic related to stomatal resistance |
| $H_f$ | foliage sensible heat flux (W/m$^2$) |
| $H_g$ | ground sensible heat flux (W/m$^2$) |
| $I^{\downarrow}_s$ | total incoming short-wave radiation (W/m$^2$) |
| $I^{\downarrow}_{ir}$ | total incoming long-wave radiation (W/m$^2$) |
| $K_v$ | von Karmen constant (0.4) |
| $l_f$ | latent heat of vaporization at foliage temperature (J/kg) |
| $l_g$ | latent heat of vaporization at ground temperature (J/kg) |
| $L_f$ | foliage latent heat flux (W/m$^2$) |
| $L_g$ | ground latent heat flux (W/m$^2$) |
| **LAI** | leaf area index (m$^2$/m$^2$) |
| $M_g$ | moisture saturation factor |
| $q_a$ | mixing ratio for air |
| $q_{af}$ | mixing ratio for air within foliage canopy |
| $q_{f,sat}$ | saturation mixing ratio at foliage temperature |
| $q_{g,sat}$ | saturation mixing ratio at ground temperature |
| $r_a$ | aerodynamic resistance to transpiration (s/m) |
| $r_s$ | foliage leaf stomatal resistance (s/m) |
| $r_{s,min}$ | minimum stomatal resistance to vapor diffusion (s/m) |
| **r"** | surface wetness factor |
| $R_{ib}$ | bulk Richardson number |
| $R_v$ | gas constant for water vapor (461.53 J/kgK) |
| $T_a$ | the air temperature at the instrument height (Kelvin) |
| $T_{af}$ | air temperature within the canopy (Kelvin) |
| $T_f$ | leaf temperature (Kelvin) |
| $T_g$ | ground surface temperature (Kelvin) |
| **W** | wind speed above canopy (m/s) |
| $W_{af}$ | wind speed with in the canopy (m/s) |

| | |
|---|---|
| **z** | height or depth (m) |
| $\mathbf{Z_a}$ | instrument height (m) |
| $\mathbf{Z_d}$ | displacement height (m) |
| $\mathbf{Z_o^f}$ | foliage roughness length scale (m) |
| $\alpha_f$ | albedo (short wave reflectivity) of the canopy |
| $\alpha_g$ | albedo (short wave reflectivity) of ground surface |
| $\varepsilon_1$ | $\varepsilon_g + \varepsilon_f - \varepsilon_g \varepsilon_f$ |
| $\varepsilon_f$ | emissivity of canopy |
| $\varepsilon_g$ | emissivity of the ground surface |
| $\Gamma_h$ | stability factor |
| $\rho_a$ | density of air at instrument height (kg/m$^3$) |
| $\rho_f$ | density of air at foliage temperature (kg/m$^3$) |
| $\rho_{af}$ | density of air at foliage temperature (kg/m$^3$) |
| $\rho_{ag}$ | density of air at ground surface temperature (kg/m$^3$) |
| $\sigma$ | the Stefan-Boltzmann constant (5.699*10$^{-8}$ W/m$^2$ $^o$K$^4$) |
| $\sigma_f$ | fractional vegetation coverage |
| **a** | air |
| **af** | air within the foliage layer |
| **e** | latent heat flux term |
| **f** | foliage surface |
| **g** | ground surface |
| **h** | sensible heat flux term |
| **n** | current time step |
| **n+1** | future time step |
| **ir** | infrared (or long-wave) |
| **sat** | saturation value |
| **S** | short-wave |

## 4.1.2 The Leaf energy balance

The foliage energy balance is given by:

$$F_f = 0 = \sigma_f \left[ I_s^{\downarrow}(1-\alpha_f) + \varepsilon_f I_{ir}^{\downarrow} - \varepsilon_f \sigma T_f^4 - P_f \right] + \frac{\sigma_f \varepsilon_f \varepsilon_g \sigma}{\varepsilon_1}(T_g^4 - T_f^4) + H_f + L_f$$

Where $\sigma_f$ is the fractional vegetation coverage, $I^{\downarrow}_s$, and $I^{\downarrow}_{ir}$ are the incoming short wave and longwave radiation in w/m2. $\alpha_f$ and $\varepsilon_f$ refer to the canopy's albedo (short wave reflectivity) and emissivity. The $\sigma$ is the Stefan-Boltzmann constant (5.699*10$^{-8}$ W/m$^2$ $^o$K$^4$). The temperature difference between $T_f$ (leaf temperature) and $T_g$ (ground surface temperature) in kelvin is considered in this equation.

The equation includes convective, sensible heat transfer and the short and longwave radiation absorbed and reflected by the vegetation. Below, the sensible and latent heat flux terms ($H_f$ and $L_f$) are discussed in more detail as they are complicated.

**Sensible heat flux in the foliage layer**

The sensible heat flux is given by:

$$H_f = (1.1\ LAI \rho_{af} C_{p,a} C_f W_{af})\ (T_{af} - T_f)$$

The temperature difference between $T_{af}$ (air temperature within the canopy ) and $T_f$, wind speed above the canopy ($W_{af}$ ) and Leaf Area Index (LAI) impact the sensible heat transfer between the near-canopy air and leaf surface ($H_f$). The Leaf Area Index (LAI) is an indirect measurement of the foliage density of a vegetation layer. It is defined as the ratio between the leaf area and the square meters of a surface below it which is dimensionless. It will be explained more in the following chapter. The constant 1.1 accounts for heat transfer from the stems, twigs, and limbs[(Deardorff)]. $C_{p,a}$ is the specific heat of air at constant pressure (1005.6 J/kg K), and $C_f$ is the bulk heat transfer coefficient, which explains later.

The air density near the foliage $\rho_{af}$ (kg/m$^3$) is given as:

$$\rho_{af} = \frac{\rho_a + \rho_f}{2}$$

Where $\rho_a$ is the air density at the instrument height and $\rho_f$ is the air density at the leaf temperature. The air temperature in the foliage is modeled as :

$$T_{af} = (1 - \sigma_f)(T_a) + \sigma_f\ (0.3T_a + 0.6T_f + 0.1T_g)$$

Where $T_a$ (k) is the air temperature at the instrument height, $T_f$(k), leaf temperature, and $T_g$ (k) is the ground surface temperature. The foliage wind speed is estimated as:

$$W_{af} = 0.83\sigma_f W' \sqrt{C^f_{hn}} + (1 - \sigma_f)W'$$

Here *W'* is the larger of 2.0 m/s or the actual wind speed above the canopy[197], and $C^f_{hn}$ is the heat transfer coefficient at near-neutral atmospheric stability conditions:

$$C^f_{hn} = \left[ k / \ln\left( \frac{Z_a - Z_d}{z^f_0} \right) \right]^2$$

Where $K_v$, is von Karmen's constant (0.4), $Z_a$ is the shelter height, $Z_d$ is the zero displacement height in meters (height above soil within which the wind speed is effectively zero), and $Z^f_0$ is the foliage roughness length scale (m). The zero displacement height and roughness length is calculated by [198]:

$$Z_d = 0.701 Z_f^{0.975}$$

$$Z_0^f = 0.131 Z_f^{0.997}$$

Finally, the bulk transfer coefficient defined by [199]:

$$C_f = 0.01(1+0.3/W_{af})$$

**Latent heat flux in the foliage layer**

The process of water loss through plant respiration is known as transpiration. The closing and opening of stomata control it - the intercellular openings between epidermal (guard) cells (Gates). The resistance to the diffusion of water vapor from these spaces into the atmosphere is called stomatal resistance. It depends on the light intensity, soil moisture content, and vapor pressure difference between the inside leaf and the outside atmosphere. It is measured in units of s/m and is formulated as:

$$r_s = \frac{r_{s,min}}{LAI} f_1 f_2 f_3$$

Here, $r_{s,min}$ is the minimum stomatal resistance. The actual stomatal resistance at any time is proportional to this minimum resistance and inversely proportional to LAI. The stomatal resistance is further modified by fractional multiplying factors related to incoming solar radiation and atmospheric moisture. As found in Frankenstein and Koenig, the inverses of the $f_1$, $f_2$, and $f_3$ , which are multiplying factors for radiation effect, moisture effect, and additional on stomatal resistance, are given by:

$$\frac{1}{f_1} = \min\left[1, \frac{0.004 I_s^{\downarrow} + 0.005}{0.81\left(0.004 I_s^{\downarrow} + 1\right)}\right]$$

$$\frac{1}{f_2} = \begin{cases} 0 & \theta_r > \bar{\theta} \; or \; \bar{\theta} > \theta_{max} \\ \dfrac{\bar{\theta} - \theta_r}{\theta_{max} - \theta_r} & \theta_r \le \bar{\theta} \le \theta_{max} \end{cases}$$

$$\frac{1}{f_3} = \exp\left(-g_D \left[e_{f,\,sat} - e_a\right]\right)$$

Here, $\Theta_r$, is the residual moisture content (defined as the amount of moisture in the soil when plants begin to wilt), $\Theta_{max}$ is the maximum moisture content (defined as the maximum amount of moisture a particular type of soil can hold, and above which runoff occurs), and $\bar{\Theta}$ is the average soil moisture in the root zone. The residual moisture content is typically around 0.01 $m^3/m^3$ [193]. The maximum moisture content depends upon the soil but generally varies from 0.3

to 0.6 $m^3/m^3$ [200]. In the expression for $f_3$, $g_d$ is a plant-specific characteristic that is only non-zero for trees, $e_{f,sat}$ is the saturated vapor pressure at the leaf temperature, and $e_a$ is the air vapor pressure.

Resistance to moisture exchange offered by the boundary layer formed on the leaf surface is known as aerodynamic resistance. It is measured in units of (s/m) and is influenced by wind speed, surface roughness, and atmospheric stability. It is formulated as:

$$r_a = 1/C_f W_{af}$$

The combined effect of aerodynamic and stomatal resistances to vapor diffusion is integrated into a foliage surface wetness factor:

$$r'' = \frac{r_a}{r_a + r_s}$$

This surface wetness factor is simply a ratio of the aerodynamic resistance to the total resistance. The wetness factor approaches zero (leaf surfaces remain dry as surface moisture is readily evaporated). As the aerodynamic resistance increases in importance relative to stomatal resistance, the wetness factor approaches 1.0 (moisture readily travels to the leaf surfaces but is not quickly evaporated).

The latent heat flux is then given by:

$$L_f = l_f \, LAI \rho_{af} \, C_f \, W_{af} \, r'' \, (q_{af} - q_{f,sat})$$

Here $l_f$, is the latent heat of vaporization (J/kg), $q_{f,sat}$ is the saturation mixing ratio at the leaf surface temperature, and $q_{af}$ is the mixing ratio of the air within the canopy. As developed in [193] the mixing ratio within the canopy can be determined from:

$$q_{af} = \frac{[(1-\sigma_f)q_a + \sigma_f(0.3q_a + 0.6q_{f,\,sat}r'' + 0.1q_{g,\,sat}M_g)]}{1-\sigma_f[0.6(1-r'') + 0.1(1-M_g)]}$$

where the factor $M_g$ (ranging from 0 to 1) is the ratio of volumetric moisture content to the porosity of the soil .

The latent heat of vaporization ($l_f$) is the amount of energy required to convert a unit mass of water to vapor. It is measured in units of J/kg and is inversely proportional to the temperature. From Henderson-Sellers it is estimated as:

$$l_f = 1.91846 * 10^6 \left[\frac{T_f}{T_f - 33.91}\right]^2$$

### 4.1.3 Soil Energy budget

The soil thermal properties mainly influence the energy budget at the soil surface, the amount of foliage coverage ($\sigma_f$), and the soil moisture. If the soil surface is densely covered, the diurnal range of surface temperature is small. In the soil energy budget, the heat released or gained due to phase changes of soil water, precipitation heat flux, and heat flux due to vertical transport of water in the soil are ignored. Future refinements to this model will incorporate these phenomena. The sign convention followed here is the same as above (heat flux into the soil is positive). The overall energy balance at the soil surface (as given in [193]) is:

$$F_g = (1-\sigma_f)\,[\,I^{\downarrow}_{s}(1-\alpha_g) + \varepsilon_g I^{\downarrow}_{ir} - \varepsilon_g T_g^4\,] -$$

$$\frac{\sigma_f \varepsilon_f \varepsilon_g \sigma}{\varepsilon_1}(T_g^4 - T_f^4)$$

$$+ H_g + L_g + \kappa \frac{\partial T_g}{\partial z}$$

As with the foliage's energy equation, this equation represents sensible heat flux (Hg), latent heat flux (Lg), and the multiple reflections associated with long and short wave radiation. The final term on the right side gives the conduction of heat into the soil substrate.

**Sensible heat flux in the soil layer**

Sensible heat flux between the soil surface and air in its vicinity is dependent on the temperature difference between the $T_{af}$ and $T_f$ and the wind speed within the canopy. It is given as:

$$H_g = \rho_{ag}\, C_{p,a}\, C_h^g\, W_{af}\,(T_{af} - T_g)$$

where $C_h^g$ is the bulk transfer coefficient and $\rho_{ag}$ is the density of air near the soil surface (kg/m$^3$) given by:

$$p_{ag} = \frac{p_a + p_g}{2}$$

Here $\rho_g$ is the density of air at the ground surface temperature.

The bulk transfer coefficient is given as the linear combination of bulk transfer coefficient near the ground ($C^f_{hn}$) and near foliage-atmosphere interface ($C^g_{hn}$) multiplied by the stability factor ($\Gamma_h$) and is formulated as:

$$C_h^g = \Gamma_h[(1-\sigma_f)C_{hn}^g + \sigma_f C_{hn}^f]$$

The ground and foliage bulk transfer coefficients, in turn, are given by:

$$C_{hn}^{g} = \frac{\left[\frac{k}{\ln\left(Z_a / z_o^g\right)}\right]^2}{r_{ch}}$$

And

$$C_{hn}^{f} = \left[k / \ln\left(\frac{Z_a - Z_d}{z_0^f}\right)\right]^2$$

Where $Z_0^g$ and $Z_0^f$ are the ground and foliage roughness lengths, $r_{ch}$ is turbulent Schmidt number (0.63), and $K_v$ is the von Karman constant (0.4).

The condition of the atmosphere ($\Gamma_h$) is determined as stable or unstable based on the sign of the bulk Richardson number:

$$R_{ib} = \frac{2gZ_a\left(T_{af} - T_g\right)}{\left(T_{af} + T_g\right)W_{af}^2}$$

Businger and Lumley and Panofsky [201] then give the atmospheric stability factor as:

$$\Gamma_h = \begin{cases} \frac{1.0}{1.0 - 16.0R_{ib}^{\;0.5}} & for \quad R_{ib} < 0 \\ \frac{1.0}{1.0 - 5.0R_{ib}} & for \quad R_{ib} > 0 \end{cases}$$

**Latent heat flux in the soil layer**

Removal of water vapor from the soil surface depends on the difference between the mixing ratio of the soil surface and air and the wind speed within the canopy. The resulting latent heat flux is then given by:

$$L_R = C_e^g \, l_g \, W_{af} \, \rho_{ag} \, ( q_{af} - q_g)$$

Here $C_e^g$ is the bulk transfer coefficient, $l_g$ is the latent heat of vaporization at the ground surface temperature, $q_{af}$ is the mixing ratio at the foliage-atmosphere interface, and $q_f$ is the mixing ratio at the ground surface, given by:

$$q_g = M_g \, q_{g,sat} + 1\text{-}M_g \, q_{af}$$

The bulk transfer coefficient for latent heat exchange is analogous to that for sensible heat exchange and is given by:

$$C_e^g = \Gamma_e[(1-\sigma_f)C_{en}^g + \sigma_f C_{hn}^f]$$

$C_{en}^g$ is the near ground bulk transfer coefficient for Latent heat flux, and $\Gamma_e$ is the latent heat exchange stability correction factor (assumed to be the same as $\Gamma_h$).

**Linearization**

In order to solve the foliage and soil heat budget equations, the 4th order terms $T_f^4$ and $T_g^4$ and mixing ratio terms $q_{g,sat}$ and $q_{f,sat}$ are linearized as given by :

$$[T_f^{n+1}]^4 = [T_f^n]^4 + 4[T_f^n]^3\ [T_f^{n+1} - T_f^n]$$

$$[T_g^{n+1}]^4 = [T_g^n]^4 + 4[T_g^n]^3\ [T_g^{n+1} - T_g^n]$$

Here $T_f^{n+1}$ and $T_g^{n+1}$ are the current time step leaf and ground surface temperatures in Kelvin. $T_f^n$ and $T_g^n$ are the corresponding temperatures at the previous time step.

The saturation mixing ratio at the ground and leaf surface temperatures are given as:

$$q_{g,sat}\ T_g^{n+1} = q_{sat}\ T_g^n + [\frac{\partial q\ sat}{\partial T}]_{Tg^n}\ T_g^{n+1} - T_g^n$$

$$q_{f,sat}\ T_f^{n+1} = q_{sat}\ T_f^n + [\frac{\partial q\ sat}{\partial T}]_{Tf^n}\ T_f^{n+1} - T_f^n$$

where $q_{sat}(T_g^n)$ is the saturation mixing ratio at the previous time step and is formulated as given by:

$$q_{sat}\ T_g^n = \frac{0.622e^*\ T_g^n}{P - e^*\ T_g^n}$$

Here the saturation vapor pressure e* (Pa) is evaluated at the ground temperature from the previous time step ($T_g^n$) as:

$$e^* = 611.2\exp\left[17.67\left(\frac{T_g^n - 273.15}{T_g^n - 29.65}\right)\right]$$

The derivative of saturation mixing ratio at the previous time step is given by:

$$\frac{dq^*}{dT_g^n} = \left[ \frac{0.622 * P}{P - 0.378 * e^{*\,2}} \right] \left( \frac{de^*}{dT_g^n} \right)$$

Here, the derivative of the saturation vapor pressure can be calculated from the Clausius-Clapeyron equation:

$$\frac{de^*}{dT_g^n} = \frac{l_g * e^* \; T_g^n}{R_v * \; T_g^{n\;2}}$$

Where $R_v$ is the gas constant for water vapor, and $l_g$ is the latent heat of vaporization at the soil surface temperature.

The corresponding saturation mixing ratio relations for the leaf surfaces can be obtained by replacing Tg with Tf in the above relations.

### 4.1.4 Final Equations

After linearization, the final equations are of the form:

$$c_1^{\mathrm{f}} + c_2^{\mathrm{f}} T_{\mathrm{g}} + c_3^{\mathrm{f}} T_{\mathrm{f}} = 0$$
$$c_1^{\mathrm{g}} + c_2^{\mathrm{g}} T_{\mathrm{g}} + c_3^{\mathrm{g}} T_{\mathrm{f}} = 0$$

The coefficients in these equations result from the direct combination of the equations from the above development. This final set of equations is then solved simultaneously to obtain $T_g$ and $T_f$. One key difference in implementing the FASST algorithm is that the conduction terms in the equations for $C_1^g$ and $C_2^g$ are solved by inverting the Conduction Transfer Functions (CTF) within the EnergyPlus solution scheme.[17]

## 4.2 Green wall energy balance

An independent analysis of green wall systems needs to be taken to determine their most optimal configuration in various climate conditions. Even though the benefits of greenery systems in warm climates have been proven, their effects on cold weather conditions require further research [202]. Several papers worked on the Green wall thermal model and validated the model through the field study [14],[203],[99],[95],[204]. As mentioned in chapter 3, in this research, the Green Wall thermal model was adopted from the Green Roof model from the EnergyPlus software. The built-in Green Roof module of EnergyPlus is developed for low-sloped exterior surfaces like roofs, and it is not recommended for high-sloped exterior surfaces like walls[23]. However, by adding an irrigation schedule, the evapotranspiration model is integrated into the Green Roof mathematical model based on the heat balance principle of the plant and substrate layers in EnergyPlus. The evaluation of these models is seen in Fig.4.3, which provides a better insight into their behavior.

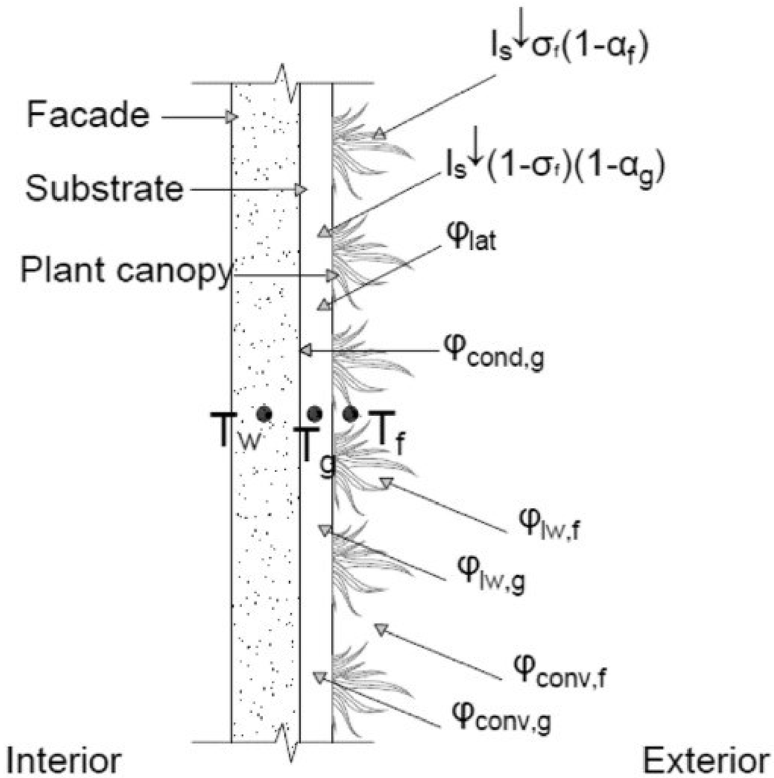


*Figure4.3 Heat Fluxes account in the proposed Green wall model*[15].

Where $\varphi_{sw,f} = I_s{\downarrow}\, \sigma_f\,(1 - \alpha_f)$ and $\varphi_{sw,g} = I_s{\downarrow}\,(1- \sigma_f)(1- \alpha_g)$ refer to the shortwave radiation absorption by foliage and by soil layer. $\Phi_{lw,f}$, and $\varphi_{lw,g}$ are the longwave radiation exchange within the plant canopy. The latent heat flux by evapotranspiration in foliage and substrate is illustrated by $\varphi_{lat}$ . Symbols $\varphi_{cond,g}$, $\varphi_{conv,f,}$ and $\varphi_{conv,g}$ show the soil layer heat conduction and sensible heat transfer from the vegetation and substrate, respectively.

Since the model is reliable and complete compared to other simulation software, the Energyplus material properties are chosen in this proposal. The following section describes the development a data model based on the Green Roof and wall properties and the outputs[205].

## 4.3 Evapotranspiration

Evapotranspiration plays a considerable role in the behavior of a plant layer in urban heat island mitigation. However, it relies on climatological parameters like solar radiation, wind speed, air temperature, relative humidity, and soil and vegetation characteristics such as LAI, stomatal resistance, and plant height [206]. It is defined as the combination of the water transpired by plants during their growth and retained in the plant tissue (transpiration) plus the moisture evaporated from the soil surface and vegetation (evaporation). When plants are small, water is mainly lost by evaporation from the soil; later, once the vegetation is well developed and completely covers the soil surface, transpiration becomes the primary process[207]. The concept was first developed by Howard Penmann in 1948 and defined the latent heat flux from vegetation [27], which led to the development of the Penmann-Monteith equation in 1965 [208].

$$\lambda ET = \frac{\Delta(R_n - G) + \rho_a * C_{p_a} * \frac{(e_s - e_a)}{r_a}}{\Delta + \gamma\left(1 + \frac{r_s}{r_e}\right)}$$

"Where $R_n$ is the net radiation, G is the soil energy flux, ($e_s$ - $e_a$) represents the vapor pressure deficit of the air, $\rho_a$ is the mean air density at constant pressure, $c_p$ is the specific heat of the air, $\Delta$ represents the slope of the saturation vapor pressure temperature relationship, g is the psychrometric constant, and $r_s$ and $r_a$ are the (bulk) surface and aerodynamic resistances" [208]. As both soil evaporation and plant transpiration coincide, it is complicated to make a clear distinction.

Identifying the water requirements for proper plant growth is particularly relevant for the agricultural sector. These requirements can be obtained by estimating the evapotranspiration rate, which allows an accurate prediction of water use [209]. As these requirements are specific to each plant species, the Food and Agricultural Organization of the United Nations (FAO) developed a simplified method to determine the evapotranspiration rate of any plant based on a reference crop.

Evapotranspiration can be measured with the Lysimeter equipment made of a soil volume covered by plants placed in a container hydrologically separated by the surrounding soil. Lysimeters can be classified as non-weighing and weighing types. The weighing lysimeter is based on the principle of mass continuity. The evapotranspiration (ET), expressed in mm, is calculated by the bellow equation as the difference among precipitation (P), drainage (D), superficial runoff (O), and the variations in soil water storage ($\Delta$S). Fig.22 refers to the lysimeter schematic[207]. Furthermore, through the EnergyPlus simulation software, the dynamic evapotranspiration rate can be calculated.

$$ET = P - D - O \pm \Delta S$$

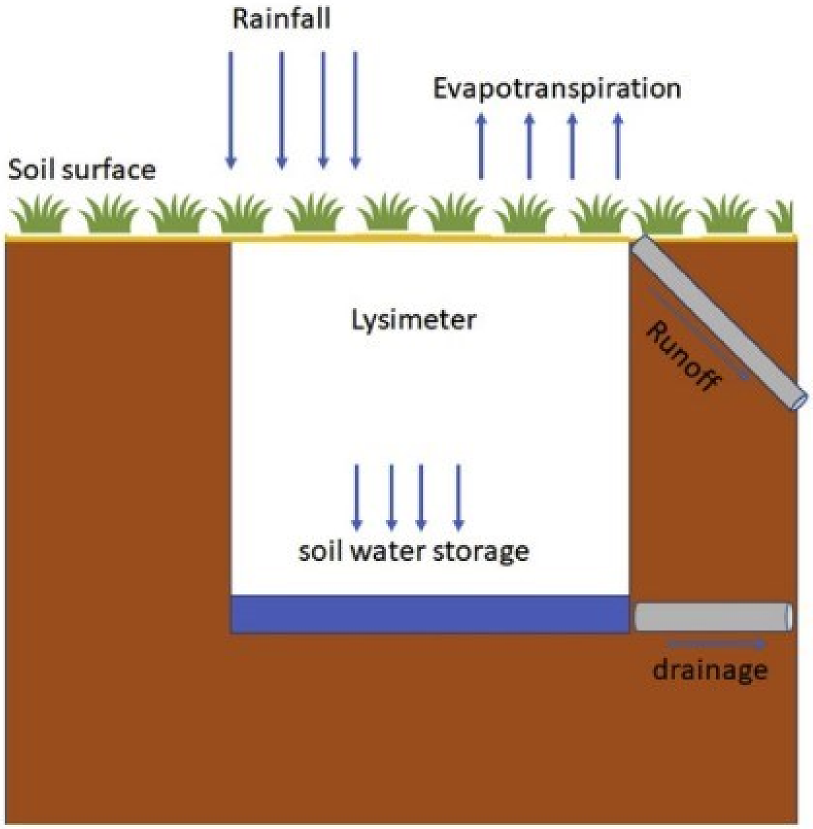


*Figure 4.4 Schematic representation of the soil water balance in weighing lysimeter.*

## 4.4 Summary

This chapter analyzes the greenery system's different physical phenomena that determine thermal behavior. Furthermore, the energy balance of greenery systems was broken down, and each component was analyzed individually to create a parametric approach to the problem, which allows the creation of a quantifiable mathematical model. The effects of short wave radiation, longwave radiation, convective heat transfer, evapotranspiration, and substrate insulation were identified as the main variables responsible for the system's behavior. They showed the potentially significant effects that changes in the composition of Green Envelop can have on their thermal performance.

# 5. Creating Greenery system Parameter Catalogs for Simulation

The energy performance of the Green Envelope could be investigated with both experimental and modeling procedures. The experimental studies are more reliable, but they are time-consuming and expensive. On the other hand, a detailed model is needed to evaluate the complicated feature of vegetation and soil layers in the modeling studies, like heat and moisture flows in the plant, air canopy, and soil layers[210]. This requires inputs and developed databases that include relating parameters and attributes. However, there is a lack of standardized and categorized data models and databases to represent the collected data for interoperability and ease of applications in Green Envelope. This chapter refers to creating a data model for the greenery system.

## 5.1 Data Modeling Approach

The computational model for building energy demand and consumption simulation requires elaborated algorithms and the design of model structure and parameters. Structural aspects like building geometry and building arrangement that determine shadowing and heat transfer must be defined more by many numeric, ordinal, or nominal parameters. Since the validated and accurate simulation output is highly correlated with the input parameters' availability and level of detail, an organized database is essential. A database is a place where a user is able to store, manipulate and retrieve the data [211]. **A data model** is a visual representation that describes how data elements organize data and standardizes how the data elements relate to one another[212].

Even though data models and the software that create, maintain and deploy them should be independent of any particular simulation software, the content and structure need to be compatible with simulation models in order to convey information to them. [213]. To create data from or to XML files, domain specialists encode their knowledge into a graphical design describing components, relations, attributes, features, and characteristics. It can be employed by Object-oriented software embodied in programming languages like Java, C++, Python, and graphical notations like the Unified Modeling Language (UML)[214]. UML class diagrams are the basis of object-oriented design and analysis that show the classes of the system, their interrelationships, including inheritance, aggregation, and association, and the relations and attributes of the classes, which will be discussed further below [215].

## 5.2 Development of a data model in an integrated development environment

The data model was developed and implemented in the Eclipse application. Eclipse was initially developed by IBM and became Open Source in 2001. It is best known for its Integrated Development Environments (IDEs) for Java and C++, Python, and many other programming languages[216]. The Eclipse application framework offers "Industry-proven domain specific languages (DSLs) and code generators for data models and UIs based on the *Eclipse Modeling Framework"*[213][217] (EMF), which consists of:

- *Ecore* [218] for model-driven development of Java classes and storage layers for databases or extensible markup language (XML)
- *Eclipse* Sirius [219] supports the design and creation of graphical and form-based User Interfaces (UIs).
- Modifying and customizing technics to meet specific needs in data models and forms. For example, adding quantities (numbers with units) to Ecore is a significant feature for parameter catalogs.

This thesis thoroughly discusses several types of greenery systems in chapter 3 that integrate into the data model. The greenery data model consists of the green roof /façade, rooftop farming, urban greening, and the categorized plant and soil types. Fig.5.1 illustrates a Greenery System UML diagram edited in the *Eclipse* application. The data model was developed with the support of the software engineer Kai-Holger Brassel, Hamburg, using his tutorial licensed under CC BY-NC-ND 4.0 [213]. Also, he supported the whole process to complete the catalog.

In the *GreeneryCatalog* on the top, we have the *GreeneryCatalog* composed of *VegetationCategory*, *PlantCategory*, and *Soil*. *VegetationCategory* refers to the types of the greenery systems like urban greening, green roof/façade, and rooftop farming linked to the *Vegetation,* which shows the act of planting that needs to define the thickness of soil and defines the type of greenery system based on the management tab. Management represents the different types of Green roofs, which can be extensive, semi-intensive, and intensive. Regarding the green façade, the air gap defines whether the greenery system is a green façade and has an air gap or not. And then, the *Vegetation* connects to the *PlantPercentage,* referring to the percentage of different plants making up the vegetation and *Soil* class with several types of soils and their properties. The *PlantPercentage* itself lined to the *Plant* class.

Back to the top of the diagram, the *PlantCategory* is about the family type of plant that can be Flower, Grass, and Vegetable. Each *PlantCategory* class is composed of the *Plant* that belongs to the *PlantCategory* and each *Plant* has the *Soil* object associated to it on which it can grow. Therefore, there is no need to specify the soil type for the *Vegetation* class. The Roughness data type refers to the different levels of roughness in the soil attributes. Fig.5.2 illustrates the Eclipse Modeling Framework(EMF) Preview, which shows the different greenery systems described here and the relating plant and soil types. The following sections describe in detail the relation between the classes and the plant and soil attributes.

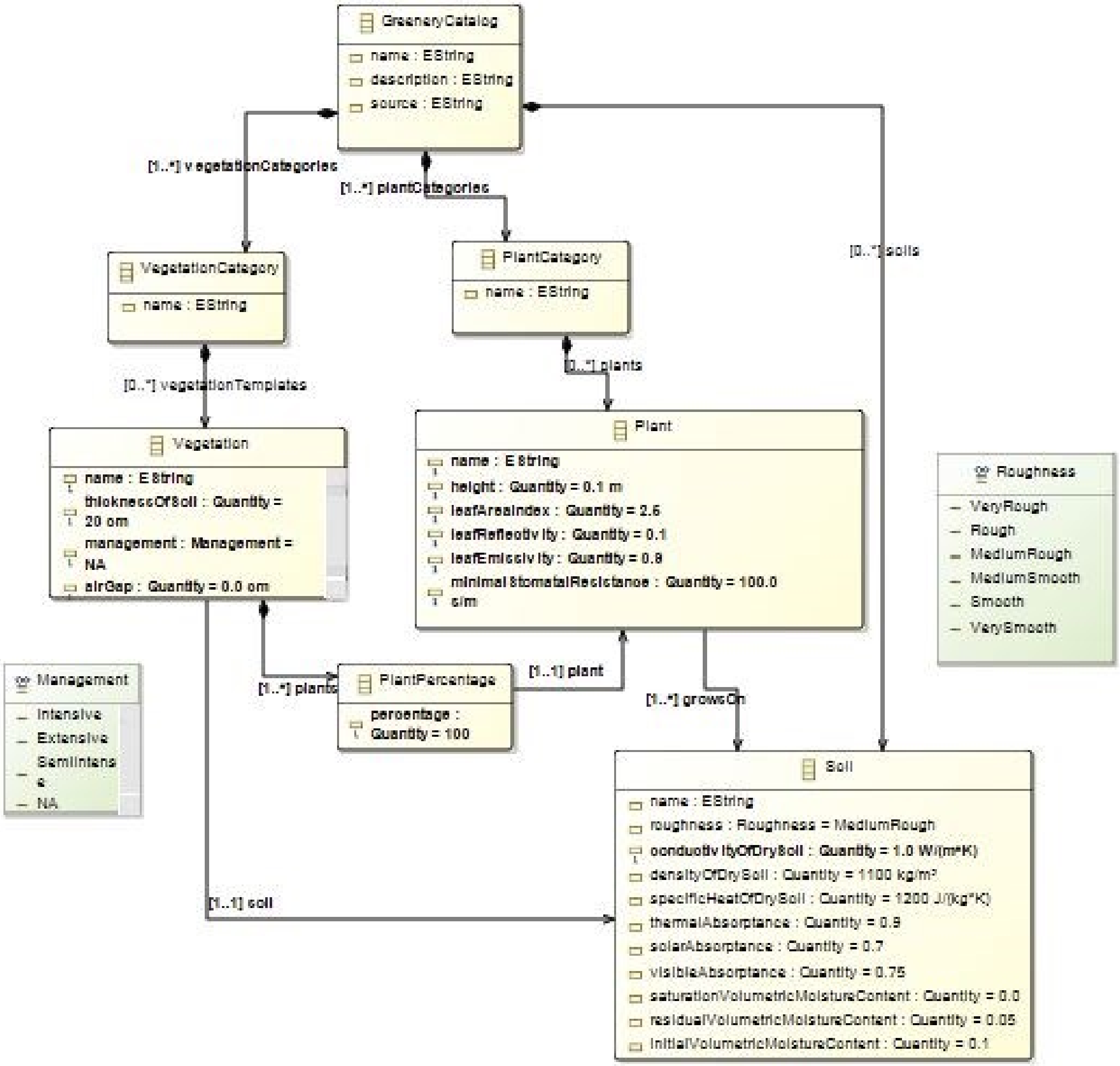


*Figure 5.1 Greenery System UML diagram*

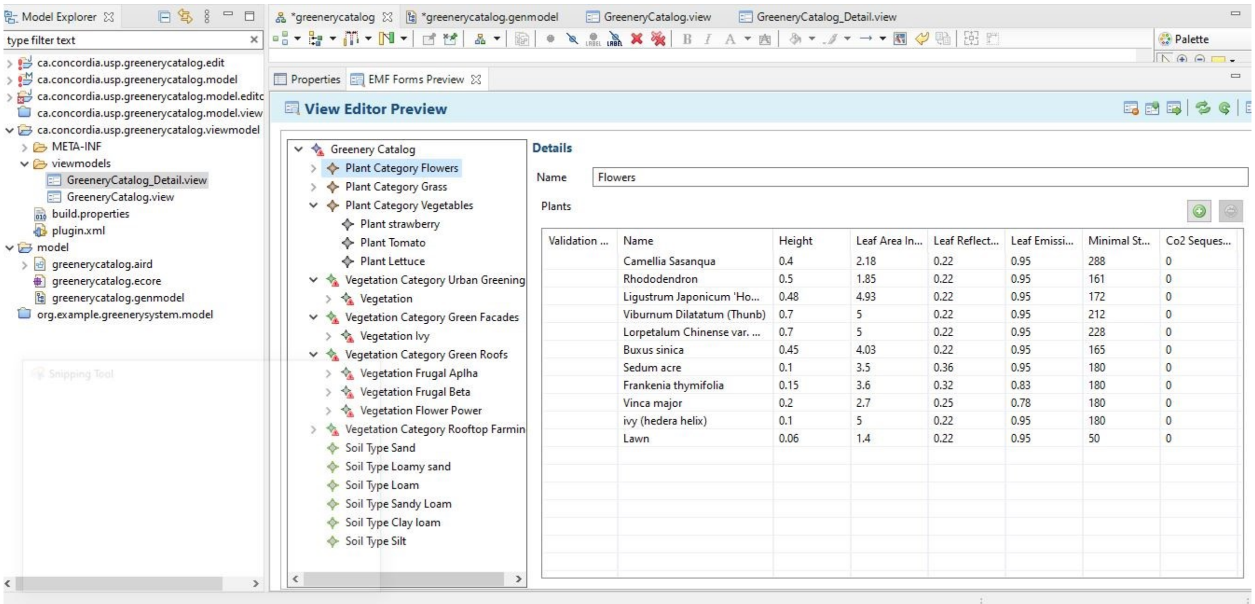

*Figure 5.2 EMF with newly developed Greenery System catalog*

### 5.2.1 Greenery System model data with UML Class Diagrams

To build data models and parameter catalogs from scratch, some basics about Eclipse are needed. Then we can model our data with Ecore, a graphical diagram editor for Eclipse, followed by the generation of Java classes and user interface (UI). Finally, we will install some plug-ins in Eclipse installation to add units and quantities to the mix. Ecore diagrams are simplified UML class diagrams that should be understood to begin modeling the data. Here the central object-oriented concepts Class, Object, Attribute, Association, Composition, and Multiplicity is briefly explained.

Class diagrams show classes and their relationships. Class diagrams are used for a wide variety of purposes, including both conceptual/domain modeling and detailed design modeling [220]. A class describes a group of objects with similar properties (attributes), behavior (operations), common relationships to other objects, and semantic meaning[220]. Classes are typically modeled as rectangles with two sections: the top section for the name of the class and the middle section for the class's attributes. Attributes are the information stored and at least temporarily maintained about an object[215]. Fig.5.3 shows an example of a Plant class in the Greenery System catalog. Plant refers to the name of the class, which has the attributes like name, height, leaf area index, etc., that are explained in the following section.

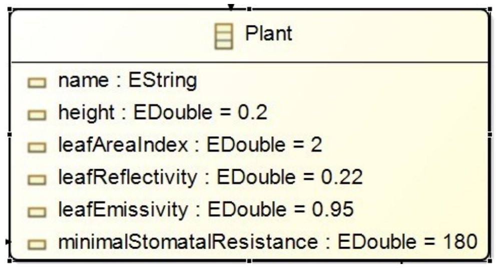


*Figure 5.3 Class with Attribute*

The UML diagram with the catalog itself is represented by the class *GreeneryCatalog* . Unlike dozens or hundreds of objects to be cataloged —plant, soil types etc. — there will be just precisely one catalog object in the data representing the catalog itself. Its "singularity" is not visible in the class diagram, but an Ecore convention requires that all objects need to form a composition hierarchy with only one root object[213].

**Associations**

Objects are often associated with or related to other objects. Association models in UML class diagrams can be illustrated by a thin line connecting two classes, as shown in Fig.5.4 Associations can become quite complex. The optional label, which is highly recommended, is typically one or two words describing the association. For example, plants need soils to grow.

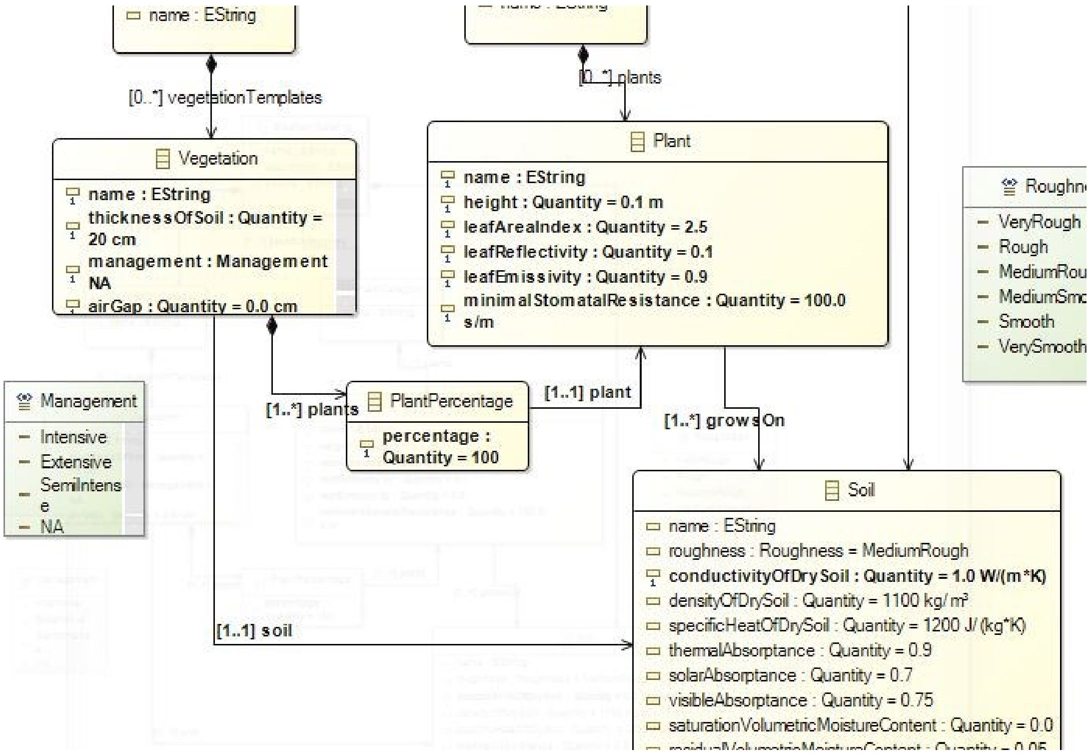


*Figure 5.4 Greenery data model*

Referring to the Greenery data model, plant type produced By *Plant* class to *SoilType* makes it a uni-directional reference. One can grow on soil, but not the other way around. With a bi-directional reference, both queries would be available. Observe also the annotations 0..* and 1..1 near soil class, which refers to the multiplicities of associations: a *GreeneryCatalog* contains zero, one, or many objects of class *Soil*, and *Vegetation* must reference exactly one *Soil* — not less, not more.

**Composition**

"If one object is composed of others in the domain, this is expressed by a special kind of association called composition. Compositions are depicted as a link with a diamond shape attached to the containing object"[213]. For instance, the link in the *VegetationCategory* of the *GreeneryCatalog* contains — or is composed of — zero or more (0..*) vegetation objects stored in a list named *VegetationCategory.*

Ecore's types of relations are represented in The Greenery catalog. Fig.5.5 refers to creating a relationship between a subclass and a superclass using the tool SuperType that can be found in the Ecore editor's palette. It is possible to use the other tools to associate classes, uni-directional reference, a bi-directional reference, or a composition[213].

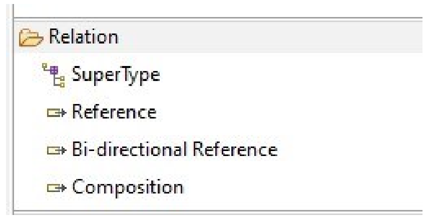


*Figure 5.5 Ecore Relations*

### 5.2.2 Attributes

Considering soil and vegetation layers as building materials need to have related attributes and properties to calculate the thermal performance, as shown in the previous section. The modeling of the greenery system needs to consider the study of the transfer of mass and heat between its layers and elements of plant physiology[221]. This data model considered various aspects of the green roof and wall construction, including growing media depth, thermal properties, plant canopy density, height, stomatal conductance (ability to transpire moisture), and soil moisture conditions (including irrigation). Table 5.1 refers to all the input data needed to simulate the thermal behavior of the greenery system, followed by a brief description.

*Table 5.1 Input data for the green component* [23]

| Classification | Input parameter | Range | Default value |
|---|---|---|---|
| **Plant morphology** | Height of Plants [m] | 0.005 to 1.00 m | 0.2 m |
| | Leaf Area Index (LAI) | 0.001 to 5.0 | 1 |
| **Plant moisture** | minimum stomata resistance [s/m] | 50.0 to 300.0 | 180 s/m |
| **Soil texture class and related thermal moisture properties** | Roughness | "VeryRough" to "VerySmooth" | MediumRough |
| | Thickness [m] | 0.05 to 0.7 m | 0.1 |
| | Conductivity of Dry Soil W/(m-K) | 0.2 to 1.5 | 0.35 W/(m-K) |
| | Density of Dry Soil kg/m3 | 300 to 2000 | 1100 kg/m3 |
| | Specific Heat of Dry Soil J/(kg-K) | | |
| | Saturation Volumetric Moisture Content of the Soil Layer | 0.1 to 0.5 | 0.3 |
| | Residual Volumetric Moisture Content of the Soil Layer | 0.01 to 0.1 | 0.01 |
| | Initial Volumetric Moisture Content of the Soil Layer | 0.05 to 0.5 | 0.1 |
| **Radiation related** | Leaf Reflectivity | 0.05 to 0.5 | 0.22 |

| | | | |
|---|---|---|---|
| | Leaf Emissivity | 0.8 t0 1 | 0.95 |
| | Soil layer Thermal Absorptance | 0 to 1 | 0.9 |
| | Soil layer Solar Absorptance | 0 to 1 | 0.7 |
| | Soil layer Visible Absorptance | 0.5 to 1 | 0.75 |
| **weather file: precipitation data** | EnergyPlus Weather Data (EPW) | | |
| **General/site related** | location | | |
| | Irrigation schedule | | |

**Plant layer**

**Height of Plants**

Defines the height of plants in meters.

**Leaf Area Index**

The protection against solar radiation by vegetation is a consequence of leaf density and vegetation cover, represented by the LAI. The leaf area index (LAI) is an indirect measurement of the foliage density of a vegetation layer. It is defined as the ratio between the leaf area and the square meters of façade or roof besides or below it. Although it has a defining role in a plant's behavior, there is no defined relationship between it and its potential for energy savings [104]. The LAI can be determined either directly or indirectly. The direct approach measures the area of each leaf in a square meter. At the same time, the indirect one evaluates the amount of light transmitted or reflected by the plant's canopy by measuring total photosynthetically active radiation (PAR) above the canopy and comparing it with the measured PAR below the canopy[210].Fig.25 shows an example of various values of LAI, and their associated foliage density in the green façade, while Fig.5.5 refers to the LAI of lettuce in a 49-day crop cycle in autumn and winter.

LAI : 0.25 LAI: 0.5 LAI :0.75

*Figure 5.5 Varying levels of leaf area index in a vegetation layer* [31]

The LAI varies significantly over the plant growth cycle, as shown in Fig.5.6. The LAI growth rate tends to be higher at the beginning of the crop development due to the less plant self-shading and reduced crop mutual shading[162].

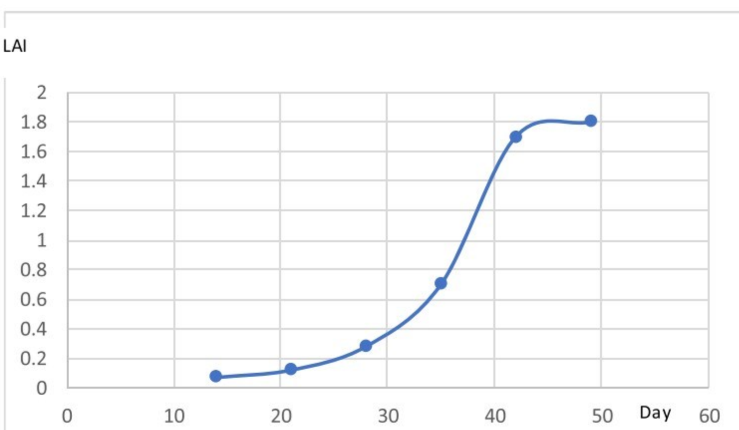


*Figure 5.6 Variation of LAI during lettuce growth* [18]

**Minimum Stomatal Resistance**

In plants, stomatal resistance is the resistance to water vapor and carbon dioxide transport to and from the stomata on the leaves. The dimension is time over distance (s/m); plants with low values of stomatal resistance will result in higher evapotranspiration rates than plants with high resistance[207].

**Leaf Reflectivity**

Represents the fraction of incident solar radiation that is reflected by the individual leaf surfaces (albedo). Solar radiation includes the visible spectrum as well as infrared and ultraviolet wavelengths.

**Leaf Emissivity**

The ratio of thermal radiation emitted from leaf surfaces to that emitted by an ideal black body at the same temperature. This parameter is used when calculating the long wavelength radiant exchange at the leaf surfaces.

## Soil Layer

**Roughness**

Defines the relative roughness of a particular material layer. This parameter only influences the convection coefficients, more specifically the exterior convection coefficient. A keyword is expected in this field with the options being "VeryRough", "Rough", "MediumRough", "MediumSmooth", "Smooth", and "VerySmooth" in order of roughest to smoothest options.

**Thickness**

This field characterizes the thickness of the material layer in meters.

**Conductivity of Dry Soil**

The thermal conductivity W/(m-K).

**Density of Dry Soil**

The density in kg/m3.

**Specific Heat of Dry Soil**

Represents the specific heat in units of J/(kg-K).

**Thermal Absorptance**

The fraction of incident long-wavelength (>2.5 microns) radiation that is absorbed by the material. This parameter is used when calculating the long-wavelength radiant exchange between various surfaces and affects the surface heat balances (both inside and outside as appropriate). For long wavelength radiant exchange, thermal emissivity and thermal emittance are equal to thermal absorptance.

**Solar Absorptance**

The fraction of incident solar radiation that is absorbed by the material. Solar radiation (0.3 to 2.537 microns) includes the visible spectrum as well as infrared and ultraviolet wavelengths. This parameter is used when calculating the amount of incident solar radiation absorbed by various surfaces and affects the surface heat balances (both inside and outside as appropriate). If solar reflectance (or reflectivity) data is available, absorptance equals 1.0 minus reflectance (for opaque materials).

**Visible Absorptance**

The visible absorptance field in the Material input syntax represents the fraction of incident visible wavelength radiation absorbed by the material. Visible wavelength radiation ( 0.37 to 0.78 microns weighted by photopic response) is a part of solar radiation. The visible band of wavelengths is narrow, while solar radiation includes the visible spectrum and infrared ultraviolet wavelengths. This parameter is used when calculating the amount of incident visible radiation absorbed by various surfaces and affects the surface heat balances (both inside and outside as appropriate) as well as the daylighting calculations. If visible reflectance (or reflectivity) data is available, absorptance equals 1.0 minus reflectance (for opaque materials).

**Saturation Volumetric Moisture Content of the Soil Layer**

Input of the saturation moisture content of the soil layer.

**Residual Volumetric Moisture Content of the Soil Layer**

Input of the residual moisture content of the soil layer.

After defining attributes in data modeling, the next step is creating a catalog by adding various vegetation and substrate layer types and their attributes from the available bibliographic review. Tables 5.2 and 5.3-4 present the characteristics of the substrates. For the first version of the Greenery Catalog, nine soils types were added to the data model like sand, loamy sand loam, sandy loam, clay loam, and slit. Moreover, through the literature review, three types of soil composition contained organic compost at 50%; the other 50% varies in: carbonized rice husk, crushed pine bark, or coconut fiber. Table 5 shows the data gathered through the literature on input parameters needed for the plant attributes in three categories: flower, grass, and vegetable. It should be mentioned that whenever it was challenging to find the data, the default mentioned in energy plus documentation was used [205].

*Table 5.2 Main characteristics of the plant layers*

| | Plant Type | Height (m) | LAI | Leaf Reflectivity | Leaf Emissivity | Minimal Stomatal Resistance(s/m) |
|---|---|---|---|---|---|---|
| Plant Layer | | | | | | |
| | Camellia | **0.4** [210] | **2.18** [210] | **0.22** [222] | **0.95** [222] | **288** [210] |
| | Rhododendron | **0.5** [210] | **1.85** [210] | **0.22** [222] | **0.95** [222] | **161** [210] |
| | Ligustrum | **0.48** [210] | **4.93** [210] | **0.22** [222] | **0.95** [222] | **172** [210] |
| | Viburnum | **0.7** [210] | **5** [210] | **0.22** [222] | **0.95** [222] | **212** [210] |
| | Lorpetalum | **0.7** [210] | **5** [210] | **0.22** [222] | **0.95** [222] | **228** [210] |
| | Buxus | **0.45** [210] | **4.03** [210] | **0.22** [222] | **0.95** [222] | **165** [210] |
| | Sedum acre | **0.1** [131] | **3.5** [131] | **0.36** [131] | **0.95** [131] | **180** [222] |
| | Frankenia thymifolia | **0.15** [131] | **3.6** [131] | **0.32** [131] | **0.83** [131] | **180** [222] |
| | Vinca major | **0.2** [131] | **2.7** [131] | **0.25** [131] | **0.78** [131] | **180** [222] |
| | Hedera ivy | **0.2** [223] | **4** [223] | **0.22** [222] | **0.95** [222] | **180** [222] |
| | | | | | | |
| | Lawn | **0.06** [224] | **1.4** [224] | **0.22** [131] | **0.95** [131] | **50** [225] |
| | | | | | | |
| | strawberry | **0.2** | **2** [226] | **0.22** [131] | **0.95** [131] | **180** [222] |
| | Tomato | **1** [222] | **4.12** [222] | **0.31** [227] | [1]**0.95** [228] | [1]**100-200** [227] |
| | Lettuce | **0.25** [222] | **2.03** [222] | **0.566** [229] | **0.95** [230] | [1]**180** [230] |
| | Cucumber | **0.6** | **3.5** [231] | **0.22** [131] | **0.95** [131] | **180** [222] |

1= approximated value (data obtained by similarity)

*Table 5.3 Main characteristics of the substrate layers_first part*

| | Soil Type | Roughness | Thickness (m) | Conductivity of Dry Soil (W/(m-K)) | Density of Dry Soil (kg/m3) | Specific Heat of Dry Soil (J/(kg-K)) |
|---|---|---|---|---|---|---|
| Substrate Layer | Sand | Medium Rough[205] | **0.1** [205] | **1.26** | **1100** [205] | **1200** [205] |

| | | | | | | |
|---|---|---|---|---|---|---|
| | Loamy sand | Medium Rough[205] | **0.1** [205] | **0.35** | **1100** [205] | **1200** [205] |
| | Loam | Medium Rough[205] | **0.1** [205] | **0.67** | **1100** [205] | **1200** [205] |
| | Sandy Loam | Medium Rough[205] | **0.1** [205] | **1.06** | **1100** [205] | **1200** [205] |
| | Clay loam | Medium Rough[205] | **0.1** [205] | **0.7** | **1100** [205] | **1200** [205] |
| | Silt | Medium Rough[205] | **0.1** [205] | **0.35** | **1100** [205] | **1200** [205] |
| | 50% CRH +50% OC | Very Rough [222] | **0.1-0.15** [222] | **0.048** (CRH) [232] **0.25** (OC) [233] | **100** (CRH) [232] [1]**300** (OC) [222] | **4812**(CRH) [232] **1925.9**(OC) [233] |
| | 50% CPB +50% OC | Few Rough [222] | **0.1** [222] | **0.14**(CPB) [222] **0.25** (OC) [233] | **336.36**(CPB) [222] [1]**300** (OC) [222] | **877**(CPB) [228] **1925.9**(OC) [233] |
| | 50% CF+50% OC | Rough [222] | **0.15** [222] | **0.041**(CF) [222] **0.25**(OC) [233] | **89.34** (CF) [222] [1]**300** (OC) [222] | **1736** (CF) [222] **1925.9**(OC) [233] |

OC: Organic Compost. CRH: Carbonized Rice Husk CPB: Crush Pines Bark CF: Coconut Fibre

1= approximated value (data obtained by similarity)

*Table 5.4 Main characteristics of the substrate layers_second part*

| Substrate Layer | Soil Type | Thermal Absorptance | Solar Absorptance | Visible Absorptance | Volumetric Saturation Rate | Residual Saturation Rate | Initial Saturation Rate |
|---|---|---|---|---|---|---|---|
| | Sand | **0.9** [205] | **0.7** [205] | **0.75** [205] | **0.43** [210] | **0.045** [210] | **0.1** [205] |
| | Loamy sand | **0.9** [205] | **0.7** [205] | **0.75** [205] | **0.41** [210] | **0.057** [210] | **0.1** [205] |
| | Loam | **0.9** [205] | **0.7** [205] | **0.75** [205] | **0.43** [210] | **0.087** | **0.1** [205] |

| | | | | | | | |
|---|---|---|---|---|---|---|---|
| | | | | | | [210] | |
| | Sandy Loam | **0.9** [205] | **0.7** [205] | **0.75** [205] | **0.41** [210] | **0.065** [210] | **0.1** [205] |
| | Clay loam | **0.9** [205] | **0.7** [205] | **0.75** [205] | **0.41** [210] | **0.095** [210] | **0.1** [205] |
| | Silt | **0.9** [205] | **0.7** [205] | **0.75** [205] | **0.46** [210] | **0.034** [210] | **0.1** [205] |
| | 50% CRH +50% OC | **0.9** [228] | **0.9** [228] | **0.7** [229] | [1]**0.5** [234] | [1]**0.01** [234] | [1]**0.1** [228] |
| | 50% CPB +50% OC | **0.9** [230] | **0.6** [230] | **0.7** [228] | [1]**0.7** [230] | [1]**0.01** [230] | [1]**0.5** [230] |
| | 50% CF+50% OC | **0.9** [228] | **0.9** [228] | **0.7** [228] | [1]**0.5** [228] | [1]**0.01** [228] | [1]**0.15** [228] |

OC: Organic Compost. CRH: Carbonized Rice Husk CPB: Crush Pines Bark CF: Coconut Fibre

1= approximated value (data obtained by similarity)

## Outputs

According to the energy plus software, the following outputs are available for the Roof Vegetation surface with the above attributes, which are needed as parameters in the EnergyPlus IDF editor[205].

Average Zone Green Roof Soil Temperature [C]

Average Zone Green Roof Vegetation Temperature [C]

Average Zone Green Roof Soil Root Moisture Ratio

Average Zone Green Roof Soil Near Surface Moisture Ratio

Average Zone Green Roof Soil Sensible Heat Transfer Rate per Area [W/m2]

Average Zone Green Roof Vegetation Sensible Heat Transfer Rate per Area [W/m2]

Average Zone Green Roof Vegetation Moisture Transfer Rate [m/s]

Average Zone Green Roof Soil Moisture Transfer Rate [m/s]

Average Zone Green Roof Vegetation Latent Heat Transfer Rate per Area [W/m2]

Average Zone Green Roof Soil Latent Heat Transfer Rate per Area [W/m2]

Sum of Zone Green Roof Cumulative Precipitation Depth [m]

Sum of Zone Green Roof Cumulative Irrigation Depth [m]

Sum of Zone Green Roof Cumulative Runoff Depth [m]

Sum of Zone Green Roof Cumulative Evapotranspiration Depth [m]

Sum of Zone Green Roof Current Precipitation Depth [m]

Sum of Zone Green Roof Current Irrigation Depth [m]

Sum of Zone Green Roof Current Runoff Depth [m]

Sum of Zone Green Roof Current Evapotranspiration Depth [m] [23]

## 5.3 Summary

This chapter shows the results of one of this thesis's main objectives: developing a data model for greenery systems that could integrate into an energy simulation software workflow. It discussed how to creat a UML class diagram and develop a database that includes data inputs used within building simulation programs for green roof/facade energy performance appraisals. All the relevant attributes are taken from the EnergyPlus simulation software. This data model could be used in an energy simulation workflow based on the EnergyPlus simulation as the dynamic building energy modeling engine. Input data are used from the literature and, where not available, from the default values of the EnergyPlus software. First, the user needs to define their properties to add a green roof/wall in the material and construction module. The user can then specify various aspects of the green roof construction, including growing media depth, thermal properties, plant canopy density, plant height, stomatal conductance (ability to transpire moisture), and soil moisture conditions (including irrigation). In addition, such databases help organize and store data to analyze and optimize the green infrastructure with higher quality. Furthermore, an urban energy simulation platform can incorporate such a data model and facilitate the appraisals of the green envelope within whole buildings and city integrated greenery system.

# 6. Simulation

This chapter will detail the definition of the parametrized mathematical model, its conception, software formulation, and boundary conditions used to evaluate the urban roof farming energy consumption and surface temperature reduction. One of the most challenging parts of the simulation process is the accuracy and the validation of the result. According to Polly et al.[235] the accuracy of the simulation model depends on multiple factors like the simulation engine and software used and the input data. This study uses the Ladybug tools and Design_Builder software that both works with the Energy plus engine. Energy consumption and surface temperature were modeled in Ladybug tools, Cost and Carbon were computed by Design-Builder as shown in Fig.6.1. The following section explains more about the simulation software and how to model a green roof with them. The case study for this thesis is a heritage industrial buildings project located in Montreal, Canada.

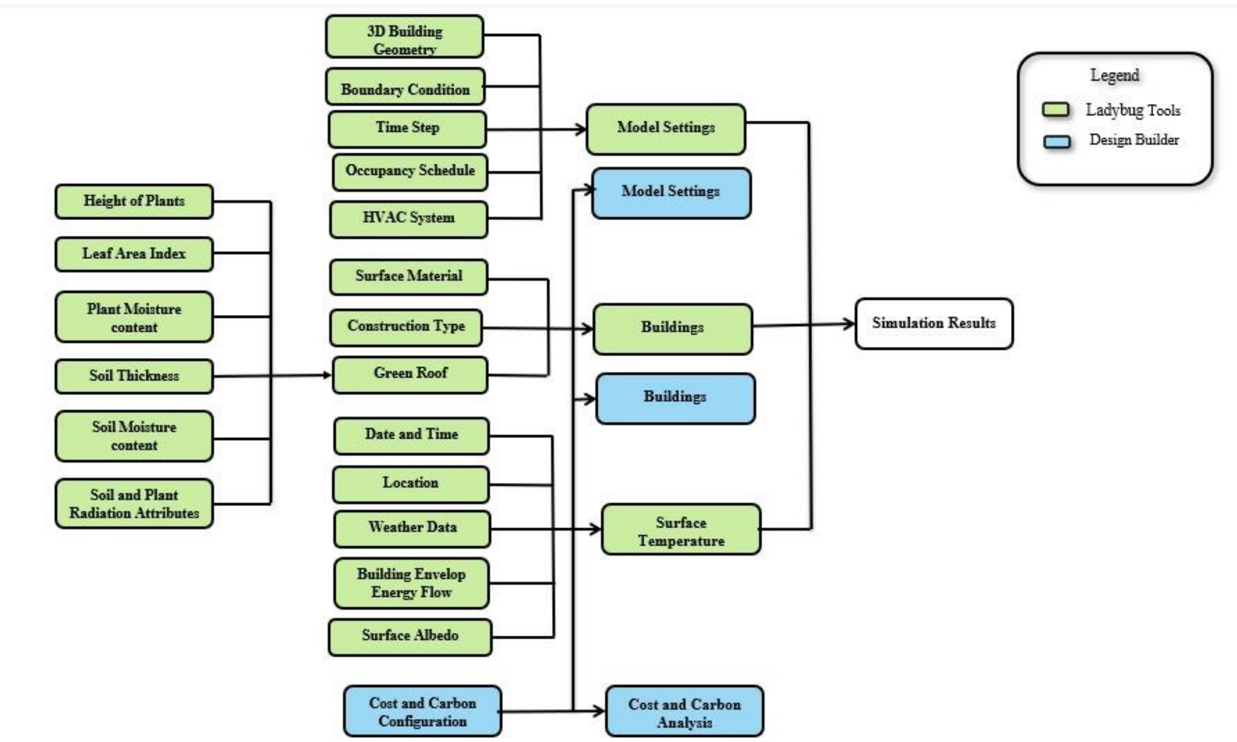


*Figure 6.1 Energy modeling workflow*

## 6.1 Parametric Design

Parametric design is a form of modeling based on algorithms that combines parameters and rules to create a design [236]. It provides a geometrical representation of entities with editable attributes and relationships. Attributes, or design variables, can be expressed as independent values serving as inputs for the model that lead to different solutions. Every solution obtained from a parametric definition is generated respecting the previously defined relationships between the design variables. A parametric approach can generate high flexibility in the design process, which allows an exploration of different configurations and geometries to perceive the result better. The design exploration process can significantly increase the efficiency of the design process as a multitude of solutions can be evaluated for a particular objective. Based on the specific constraints of the problem, the optimal solution can be found in the design landscape that fits the objective function while respecting the boundary conditions. In the case of architectural or engineering design processes, parametrization is highly beneficial as it is suited for integrating different disciplines. For the optimization problem tackled in this research, parametrization allows the creation of a continuous workflow meant to test and evaluate several configurations of rooftop farming systems through the mathematical relationships that represent the physical processes governing their behavior. Parametric modeling's potential to break down complex problems and analyze the relationship between its building blocks can be applied to an endless number of projects. As detailed in Chapter 4, the performance of a vegetation layer depends on several individual variables. Although many aspects influence the performance of a Greenery Component under a particular set of boundary conditions, the dominant variables were studied to better understand the system's behavior. This led to the development of design considerations or rules of thumb, which can be used for large-scale implementation of Rooftop Farming in urban areas. Parametric design tools are used to define the basis for the computational workflow of this research, which has shown its potential for the definition of complex problems and to increase efficiency by reducing computational time and resources.

## 6.2 Simulation platform

### 6.2.1 Ladybug Tools

Ladybug Tools[237] is a collection of free computer applications that support environmental design and education. Ladybug Tools are among the most comprehensive available environmental design software packages, connecting 3D Computer-Aided Design (CAD) interfaces to a host of validated simulation engines. However, it must first be referred to as visual programming languages (VPLs), such as Grasshopper or Dynamo. Since this work was done with Grasshopper, Dynamo is not discussed here. Fig. 6.2 shows the Ladybug analysis tools.


*Figure 6.2 Ladybug Tools*[19]

### 6.2.2 Grasshopper and Rhino 3D

According to Davidson [238], Grasshopper is "for designers who are exploring new shapes using generative algorithms. Grasshopper is a graphical algorithm editor tightly integrated with Rhino's 3-D modeling tools. Unlike RhinoScript, Grasshopper requires no knowledge of programming or scripting but still allows designers to build form generators from the simple to the awe-inspiring." Since Rhino 6 Grasshopper is included in Rhino, this makes Grasshopper appear as a VPL plug-in for use with Rhino 3D. Rhinoceros 3D (also Rhino) is a commercial, CAD-based 3D modeler software developed in 1980 by Robert McNeel and Associates[239]. Fig6.3 refers to the Rhino 3D model for the thesis case study.

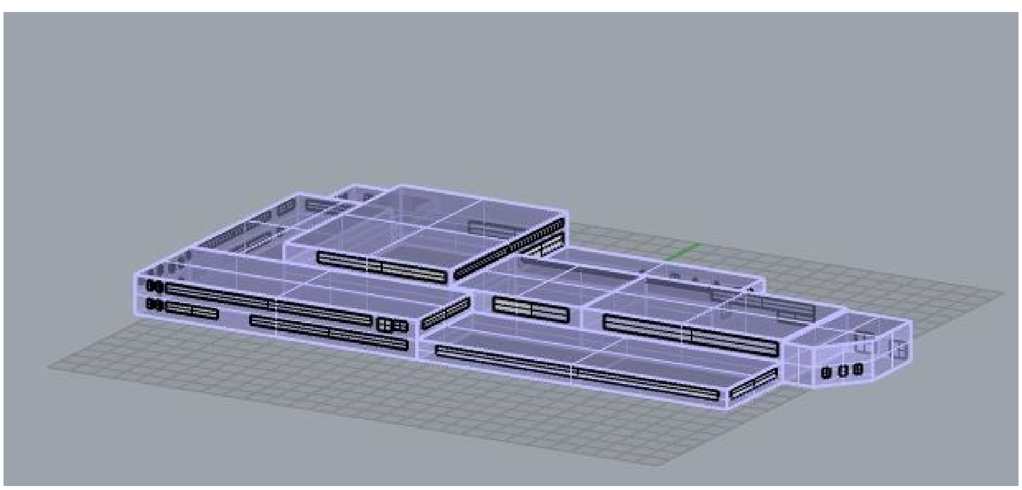

*Figure 6.3 3D model geometry*

Mostapha Sadeghipour Roudasri originally developed the Ladybug Tools in 2012. At first, only Ladybug was released as a plug-in for Grasshopper, and around one year later, in 2014 Honeybee was released as a Grasshopper plug-in. After that, Chris Mackey joined and helped to improve Ladybug. Both now act as co-founders of Ladybug Tools LLC [237].

Ladybug and Honeybee are two open-source plug-ins for Grasshopper/Rhino developed to help research and assess environmental performance. Ladybug imports standard EnergyPlus Weather files (EPW) into Grasshopper and offers a variety of interactive 2D and 3D graphics. It supports the evaluation and decision-making of initial design phases through solar radiation studies, view analysis, sunshine hour modeling, and more, as shown in Fig.6.2. It is evident that the integration in the visual programming environment allows for flexible working and immediate feedback on changes[240].

On the other hand, Honeybee deals with daylight and thermodynamic models, which are usually most relevant in the later design phases. To achieve this, it combines Grasshopper's visual programming environment with four simulation engines (EnergyPlus, Radiance, Daysim, and OpenStudio), which evaluate the energy consumption, comfort, and daylighting of buildings, as illustrated in Fig.6.4. It also serves as an object-oriented application programming interface (API) for these engines. As it is a free and open-source development, users can adapt the tool to their needs and contribute to the source code [240].

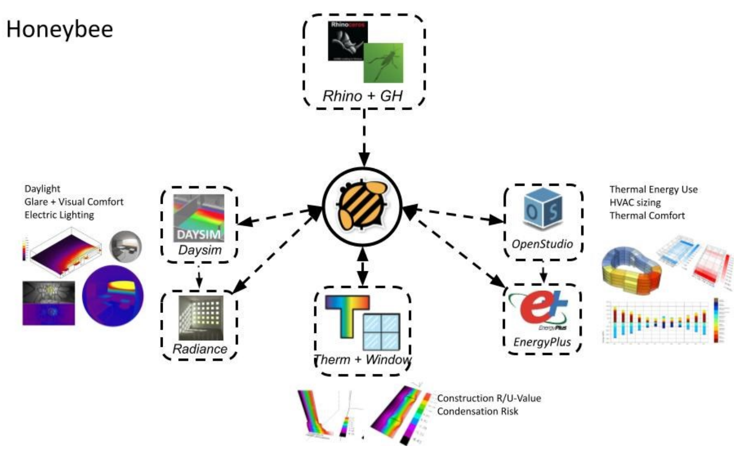


*Figure 6.4 Honeybee workflow* [19]

### 6.2.4 EnergyPlus

EnergyPlus is a building energy simulation program[241]. It can model the building energy consumption for heating, cooling, ventilation, lighting. When RoofVegetation is added to the model, all related attributes like LAI, soil thickness, plant and soil moisture content, and radiation properties must be defined. Fig 6.5 refers to all the attributes that should be characterized.

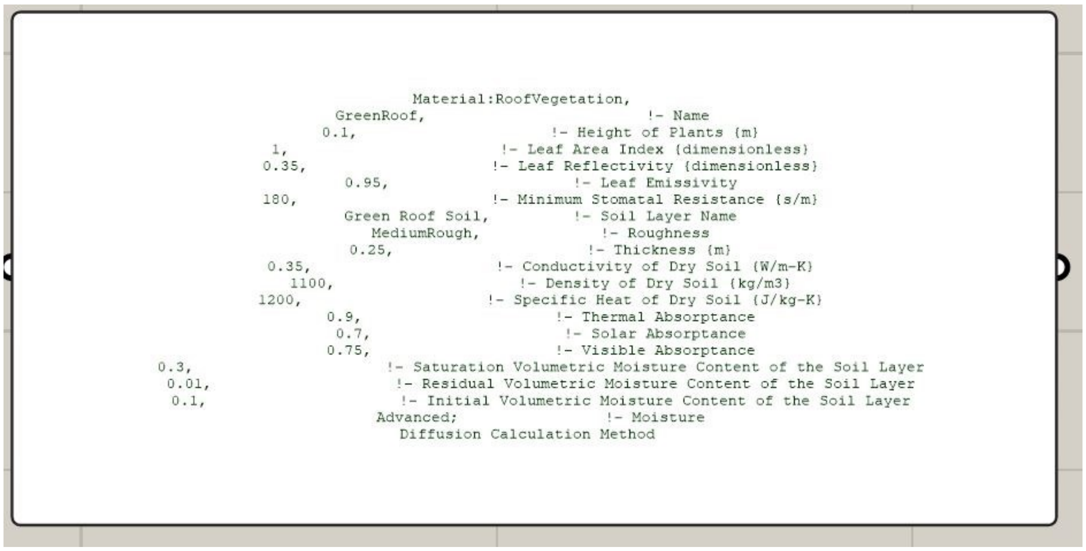

```
Material:RoofVegetation,
GreenRoof,                 !- Name
0.1,                       !- Height of Plants {m}
1,                         !- Leaf Area Index {dimensionless}
0.35,                      !- Leaf Reflectivity {dimensionless}
0.95,                      !- Leaf Emissivity
180,                       !- Minimum Stomatal Resistance {s/m}
Green Roof Soil,           !- Soil Layer Name
MediumRough,               !- Roughness
0.25,                      !- Thickness {m}
0.35,                      !- Conductivity of Dry Soil {W/m-K}
1100,                      !- Density of Dry Soil {kg/m3}
1200,                      !- Specific Heat of Dry Soil {J/kg-K}
0.9,                       !- Thermal Absorptance
0.7,                       !- Solar Absorptance
0.75,                      !- Visible Absorptance
0.3,                       !- Saturation Volumetric Moisture Content of the Soil Layer
0.01,                      !- Residual Volumetric Moisture Content of the Soil Layer
0.1,                       !- Initial Volumetric Moisture Content of the Soil Layer
Advanced;                  !- Moisture
Diffusion Calculation Method
```

*Figure 6.5 RoofVegetation input attributes*

### 6.2.5 Open Studio

OpenStudio is a collection of software tools to support energy modeling of entire buildings with EnergyPlus and advanced daylight analysis with Radiance. OpenStudio is an open-source project that includes graphical user interfaces and a Software Development Kit (SDK) [242].

Fortunately, in ladybug tools, there is a possibility to add green roof material to the building component. The simulation model based on the energy balance of a green roof, developed and integrated with the energy of the building, for the EnergyPlus software, developed by [17] named "RoofVegetation," which is entirely explained in chapter 4. The program adopts a series of variables that involve the thermal balance of a green roof, such as the characteristics of the vegetation, the substrate under the vegetation, and solar radiation.

### 6.2.6 Design Builder

DesignBuilder is the well-known user interface to EnergyPlus, which provides fully-integrated performance analysis including energy and comfort, HVAC, daylighting, cost, Life Cycle Assessment (LCA), design optimization, CFD, and LEED credits. DB integrates all these multiple perspectives using a simplified method. In this study, the cost and embodied carbon analysis were simulated by Design-Builder[243].

## 6.3 Case Study

### 6.3.1 Location

The project is a historical building located at 4000 St.Patrick Street in Montreal, Canada, used for shipbuilding during World War II. Based on Köppen's climate classification Montreal is classified as a warm-summer humid continental climate. Summers are warm to hot and humid with a maximum daily average of 26 to 27 °C (79 to 81 °F) in July; Winter brings cold, snowy, windy, and, at times, icy weather, with a daily average ranging from −10.5 to −9 °C (13.1 to 15.8 °F) in January[244]. Fig.6.6 and 6.7 refer to the yearly wind speed and direction (Wind rose) and sun path created in the Rhino Grasshopper. The influence of sunlight orientation has a considerable effect when bio-climatic strategies are in use, as they significantly reduce heating and cooling demands, daylight, and visual comfort in buildings.

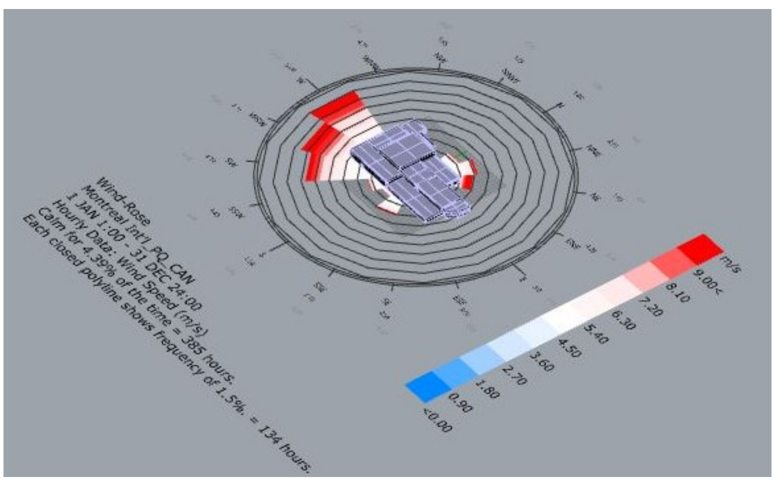


Figure 6.6 Annual wind rose

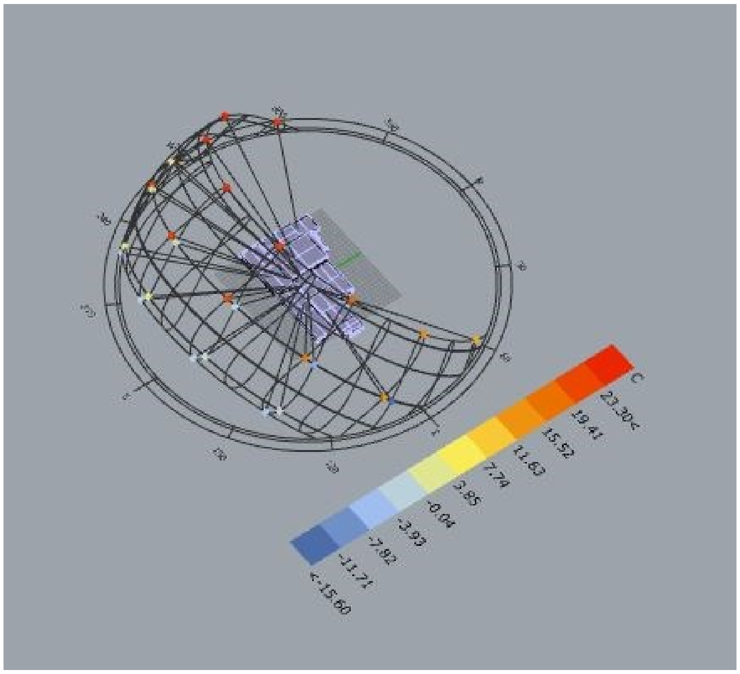


*Figure 6.7 Annual Sun path*

The building selected for the study is an old building located in the Lachine Area of downtown Montreal, an industrial building of the pre-1920 era. Most of the spaces in the building are double-height spaces with high volumes to be conditioned. The purpose of choosing this case study is that this location has been selected for a redevelopment and rehabilitation competition named C40 re-inventing cities competition in 2021.


*Figure 6.8 Field study site*

### 6.3.2 Building Energy Model Setup

This study investigates the impact of rooftop farming compared to a common type of green roof that is extensive on the building energy demand and surface temperature for both base and retrofitted conditions. It is assumed that the building has nine zones with a warehouse schedule for the base case and office schedules for the retrofitted case. The detailed input data used for the building model characteristics are summarized in Table 6.1 based on Quebec Construction Code from the National Energy Code of Canada for Buildings (NECB)[245]. Missing data regarding the building material and construction and the occupancy schedule were identified using the Energy Plus library based on the Ashrae 189.1.

*Table 6.1 Energy model Inputs and Results*

| **Building Input data for energy modeling** | | |
|---|---|---|
| | **Base case** | **Retrofitted** |
| Total Floor Area(m2) | 9650 | 9650 |
| No of floor | 1 | 1 |
| Roof Material | 8 IN Concrete HW | 8 IN Concrete HW+Insulation |
| Roof R-Value | 0.3 ($m^2K/W$) | 3.9 ($m^2K/W$) |
| Wall Material | 8 IN Concrete HW | 8 IN Concrete HW+Insulation |
| Wall R-Value | 0.25 ($m^2K/W$) | 5.8 ($m^2K/W$) |
| WWR | 30% | 30% |
| Window Type | Single Pane | Double Pane |
| Window U-Value | 5.7 | 1.4 ($W/m^2K$) |
| Solar heat gain coefficient (SHGC) | 0.81 | 0.35 |
| Visible light transmission (VLT) | 0.88 | 0.55 |
| Shading | No Shading | No Shading |
| Building program | Wearhouse | Closed Office |
| HVAC System | Ideal Air Load | Ideal Air Load |
| Construction | Ashrae 189.1 | Ashrae 189.1 |
| **Results** | | |
| | **Base case** | **Retrofitted** |
| Energy Use Intensity (EUI) | 284.37 ($kWh/m^2$) | 148.46 ($kWh/m^2$) |
| Energy use | 2744222.8 (kWh) | 1432640 (kWh) |
| Heating Load | 2616151.2 (kWh) | 1294003 (kWh) |
| Cooling load | 128071.65 | 138636.9 (kWh) |

| | | |
|---|---|---|
| Electric Lighting Energy | 328010.76 (kWh) | 375087.7 (kWh) |
| Electric Equipment Energy | 167196.43 (kWh) | 320027.2 (kWh) |

Regarding the cost and carbon analysis, Design-Builder reported the Basic model construction cost of the building design and the embodied carbon in the building material, referring to he inventory of carbon and energy (ICE) datasets that the University of Bath initially created [246]. Table 6.2 Refers to the input data from the Design-Builder library and the Cost and Carbon analysis results for the retrofitted case. The estimated building construction cost data shown in Table 6.2 is based on 'per gross internal floor area' costs of services, structure, and frame construction. The cost of constructions and glazing is based on the 'per surface area' cost data from the constructions and glazing database. Surface finish costs are calculated from actual building surface areas and entered surface finish per area costing data.

*Table 6.2 Cost model Inputs and Results*

| **Input for Retrofitted Cost Analysis** | | | |
|---|---|---|---|
| **Tariffs** | **Source** | **Season** | **Cost per Unit(CAD/kWh)** |
| Flat Electricity Charge | Total Energy | Annual | 0.070 |
| Flat Gas Charge | Total Energy | Annual | 0.055 |
| **Construction Cost** | **CAD/m$^2$** | | |
| Structure | 173 | | |
| Exterior Wall | 113 | | |
| Ground_Floor | 471 | | |
| Roof | 581 | | |
| **Retrofitted model Results** | | | |
| | **Area (m$^2$)** | **Cost (CAD)** | |
| Structure Costs | 9542.9 | 4,834,735.35 | |
| Exterior Wall | 3415.1 | 385,839.46 | |
| Roof | 9791.6 | 5,684,901.83 | |
| Ground Floor | 9791.6 | 4,609,379.86 | |
| Double pane Window | 1096.3 | 285,046 | |

The estimated embodied and equivalent carbon data are shown below in table 6.3, which is based on bulk carbon data obtained from the Bath ICE (The Bath university inventory of carbon and energy (ICE)) and other data sources. The embodied carbon associated with building services such as lighting and HVAC equipment is not covered in these results.

Equivalent carbon is similar to embodied carbon but also includes the effects of other greenhouse gases to provide an equal amount of $CO_2$ that would cause the same amount of global warming as the actual greenhouse gases (which may include sulfur dioxide, methane.) emitted by the processes involved in the production of the material. Fig 6.9 illustrates the material and construction embodied carbon in the retrofitted building.

*Table 6.3 Embodied Carbon Retrofitted model Inputs and Results*

| **Input for Retrofitted Embodied Carbon Analysis** | | | | |
|---|---|---|---|---|
| **Material** | **Embodied Carbon ($kgCO_2/kg$)** | **Source** | **Assumption/Factor boundary** | |
| Plasterboard | 0.38 | ICE v1.6 | Cradle to gate | |
| EPS Expanded Polystyrene | 2.5 | ICE v1.6 | Cradle to gate | |
| Cast Concrete | 0.08 | ICE v1.6 | Average of BATH ICE BLOCKS | |
| **Retrofitted model Results** | | | | |
| **Materials Embodied Carbon and Inventory** | **Area (m2)** | **Embodied Carbon ($kgCO_2$)** | **Equivalent $CO_2$ ($kgCO_2e$)** | **Mass (kg)** |
| Plasterboard | 9791.6 | 135437.4 | 142565.7 | 356414.2 |
| EPS Expanded Polystyrene | 9791.6 | 152993.7 | 199503.8 | 61197.5 |
| Cast Concrete | 19583.2 | 469996.7 | 469996.7 | 85874959.1 |
| **Constructions Embodied Carbon and Inventory** | **Area ($m^2$)** | **Embodied Carbon ($kgCO_2$)** | **Equivalent $CO_2$ ($kgCO_2e$)** | |
| Exterior Wall | 3415.1 | 120270.4 | 127886.2 | |
| Roof | 9791.6 | 533710.6 | 587349.0 | |
| Ground_Floor | 9791.6 | 234998.4 | 234998.4 | |
| Double pane Window | 1096.3 | 19733.8 | 19733.8 | |

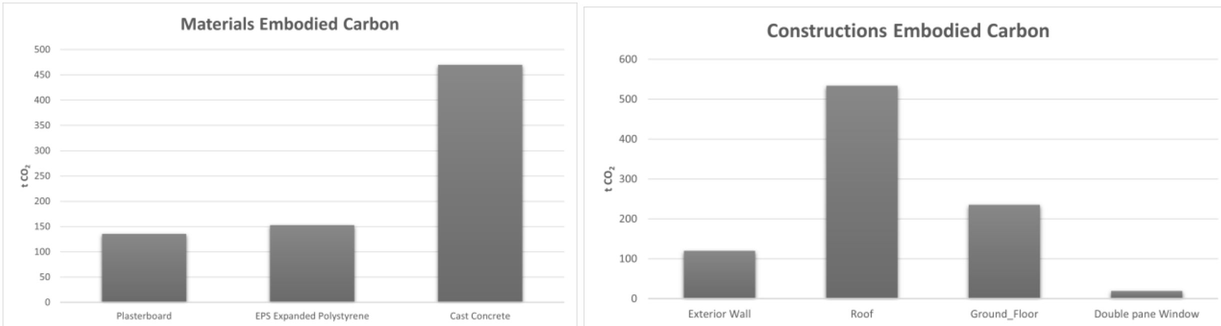


*Figure 6.9 Materials and construction embodied carbon*

## 6.3.3 Impact on the energy consumption

### 6.3.3.1 Green Roofs and Rooftop Farming Scenarios

The extensive Green Roof was considered with the Sedume and Lawn plants for the first scenario where both plants' relating attributes were averaged to add to the simulation model. A 0.1 m soil thickness for this scenario was assigned.

For the Rooftop farming scenario, strawberry, cucumber , tomato, and lettuce were chosen from the data model. Like the other scenario, the averaged characteristics were considered for simulation; however, there is another consideration regarding Rooftop farming. Since Montreal has an intensely cold winter, the input data differ in cold and warm seasons. The warm season includes April to October, and the Cold season is from November to March. Attributes were added for the warm and cold seasons separately, compared to other scenarios. Table 6.4 refers to the parameter configuration for the green roof and Rooftop farming scenarios.

*Table 6.4 Parameter configuration for the green roof scenarios*

| | **Extensive Green roof** | **Rooftop farming** | |
|---|---|---|---|
| **Attribute** | | Cold Season | Warm Season |
| **Height (m)** | 0.08 | 0.1 | 0.5 |
| **LAI** | 2 | 1 | 4 |
| **Leaf Reflectivity** | 0.29 | 0.35 | 0.35 |
| **Leaf Emissivity** | 0.95 | 0.95 | 0.95 |
| **Minimal Stomatal Resistance(s/m)** | 115 | 180 | 180 |

| | | | |
|---|---|---|---|
| **Soil Thickness(m)** | 0.15 | 0.25 | 0.25 |

According to the results, there is no significant energy saving in the Extensive Green Roof scenario due to the Montreal weather conditions compared to the retrofitted case. Despite this, when using Rooftop farming, since there is a higher soil thickness that contributes to increasing insulation and more vegetation coverage, resulting in more shading, the energy saving is about to double. Still, it is not notable compared to the less expensive roof assembly like white roofs. However, as mentioned before, all impacts should be considered in green roof studies.

Table 6.5 refers to the energy used and saving of base and retrofitted cases, and both scenarios following with Fig 6.10 and 6.11, illustrating the Heating and Cooling load comparison in the base and retrofitted cases and both scenarios. In terms of cooling load, the retrofitted case has increased due to the change in schedule, which was a warehouse in the base case and a closed office in the retrofitted case, leading to more lighting and equipment.

*Table 6.5 Energy consumption and saving for the green roof scenarios*

| | **Heating Load** (MWh) | **Cooling Load** (MWh) | **Energy use** (MWh) | **Energy Use Intensity** (kWh/m$^2$) | **Energy savings** (%) | **Roof R-Value** (m$^2$K/W) |
|---|---|---|---|---|---|---|
| **Base Case** | 2744 | 128 | 2616 | 284 | - | 0.3 |
| **Retrofitted** | 1294 | 138 | 1433 | 148 | 52 | 3.9 |
| **Extensive Green Roof** | 1150 | 114 | 1265 | 131 | 58 | 7.2 |
| **Rooftop Farm** | 968 | 90 | 1058 | 109 | 65 | 7.2 |

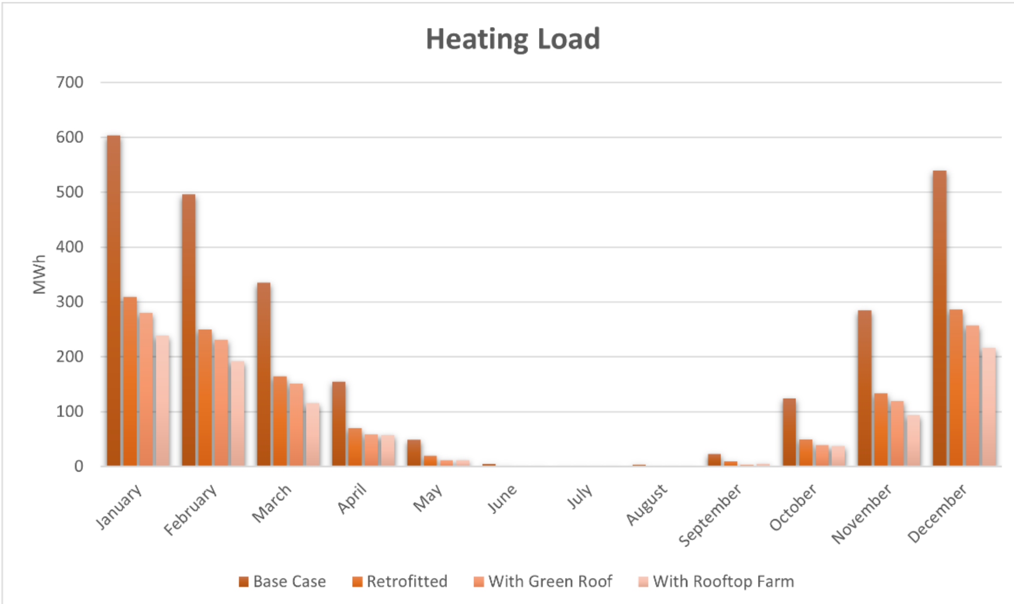


*Figure 6.10 Monthly Heating Load for Base, retrofitted case, and GR Scenarios.*

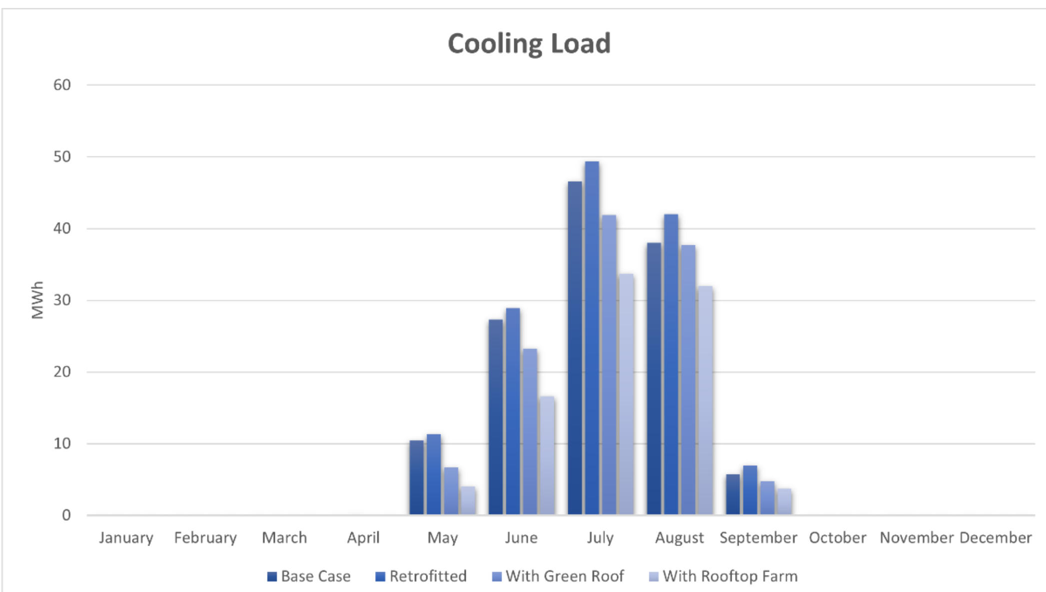


*Figure 6.11 Monthly Cooling Load for Base, retrofitted case, and GR Scenarios.*

In addition to the reductions of energy in both scenarios, the other benefits described in Chapter 3 should be taken into consideration. Also, Economic and Environmental analyses are required to evaluate their feasibility in different construction projects, as described in the following sections.

### 6.3.4 Economic and Embodied Carbon feasibility

A construction project's material selection depends significantly on its functionality, availability, accessibility, and in most cases, cost. A return on investment should be high enough to attract investors. Based on the literature review and the results of this project shown in Table 6.6, integrating a green roof and rooftop farm will increase costs and embodied carbon for the project. Still, this investment will produce energy savings and $CO_2$ sequestration, which might give a payback. The input data for the Green roof and Rooftop Farm cost scenarios were gathered from the literature review in chapter 3. Based on Table 3.4. When converting to the Canadian dollar, the average cost for applying an Extensive Green Roof is 100 CAD/m$^2$. The Rooftop farm is considered an intensive Green Roof, and it will cost around 240 CAD/m$^2$. Therefore, it would cost more for the project, like 979,160 CAD and 2,349,984 CAD for the Green roof and Rooftop Farm, respectively shown in Table 6.6.

*Table 6.6 Aditional cost for applying Green Roof Scenarios*

| **Input for GR Cost Analysis** | | |
|---|---|---|
| **Construction Cost** | **CAD/m$^2$** | |
| Green Roof | 100 | |
| Rooftop Farm | 240 | |
| **Results** | | |
| | **Area (m$^2$)** | **Cost(CAD)** |
| Green Roof | 9791.6 | 979,160 |
| Rooftop Farm | 9791.6 | 2,349,984 |

The cost-saving is based on the electricity and natural gas charge per cooling and heating consumption per CAD/kWh due to the reduction in energy consumption summarized in Table 6.7. Cost-saving is calculated according to the electricity and natural gas rates, which are 70 and 55 ₵/kWh in Quebec [247]. According to the results, rooftop farming investment takes 23 years to pay back while the extensive green roof needs 11 years.

*Table 6.7 Cost saving by energy reduction*

| **Scenario** | **Heating load saving** (kWh) | **Cooling load saving** (kWh) | **Annual electricity cost-saving**(CAD) | **Annual natural gas cost-saving** (CAD) | **Payback Year** |
|---|---|---|---|---|---|
| **Retrofitted** | 1450219 | -10565* | -739 | 79762 | _ |
| **Extensive green roof** | 1593915 | 13640 | 955 | 87665 | 11 |

| | | | | | |
|---|---|---|---|---|---|
| **Rooftop farm** | 1776016 | 38038 | 2663 | 97680 | 23 |

*as mentioned before, there is an increase in cooling demand in the retrofitted scenario, which shows by a negative amount.

Regarding calculating the embodied carbon input data, the green roof layers were decomposed, and the modular green roof embodied carbon was obtained from The inventory of carbon and energy (ICE) datasets. Table 6.8 illustrates the green roof layers: Soil, Insulation, waterproofing layer, embodied carbon 0.023,1.86, and 1.65 kg $CO_2$, respectively. The whole computed embodied carbon for the Extensive Green Roof and Rooftop Farm scenarios are 723.6 and 1575.76 t $CO_2$, as shown in Fig.6.12. The rooftop farm has emitted more because of more soil thickness and additional insulation material. Fig.6.12 refers to

*Table 6.8 Aditional embodied carbon for applying Green Roof Scenarios*

| **Input for GR Embodied Carbon Analysis** | | | |
|---|---|---|---|
| **Material** | **Embodied Carbon ($kgCO_2/kg$)** | **Source** | **Assumption/Factor boundary** |
| Soil | 0.023 | ICE v1.6 | - |
| Insulation | 1.86 | ICE v1.6 | - |
| Water Proofing Layer | 1.65 | ICE v1.6 | - |
| **Results** | | | |
| **Construction Embodied Carbon** | **Area ($m^2$)** | **Embodied Carbon (t $CO_2$)** | |
| Green Roof | 9791.6 | 723.6 | |
| Rooftop Farm | 9791.6 | 1575.76 | |

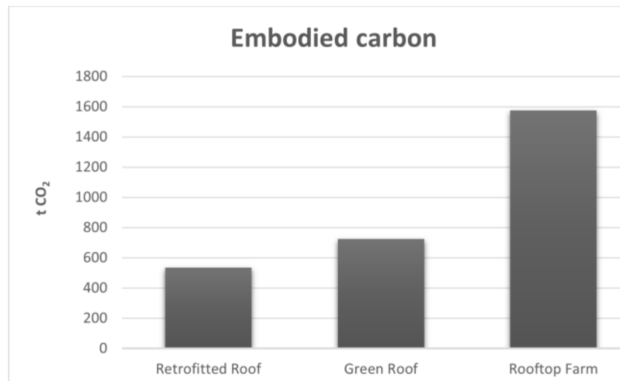


*Figure 6.12 Green roof and rooftop farm embodied carbon.*

Green roofs reduce $CO_2$ emissions in two ways: first by CO2 sequestration during the photosynthesis process and second by reducing the energy demand of buildings, which leads to lower fossil fuel consumption and $CO_2$ emission. According to the governmental data and literature review producing each kilowatt-hour of the non-renewable source produces 0.918 kg of $CO_2$ emission and as the project located in Montreal which is used hydro Quebec, the renewable source emission is considered too which is 0.13 kg per kWh. Fig.6.13 illustrates relating graphs showing the $CO_2$ emissions reduction due to the deduction of energy consumption and plant $CO_2$ sequestration by adding the green roof and rooftop farm. It is obvious due to the more energy consumption reduction we have lower $CO_2$ emissions for the rooftop farm scenario. $CO_2$ sequestration was calculated based on the amount averaged in the literature review which is 0.143 kg $CO_2$ for the green roof and 0.607 kg $CO_2$ for the rooftop farm. It is obvious due to the more energy consumption reduction we have lower $CO_2$ emissions for the rooftop farm scenario.

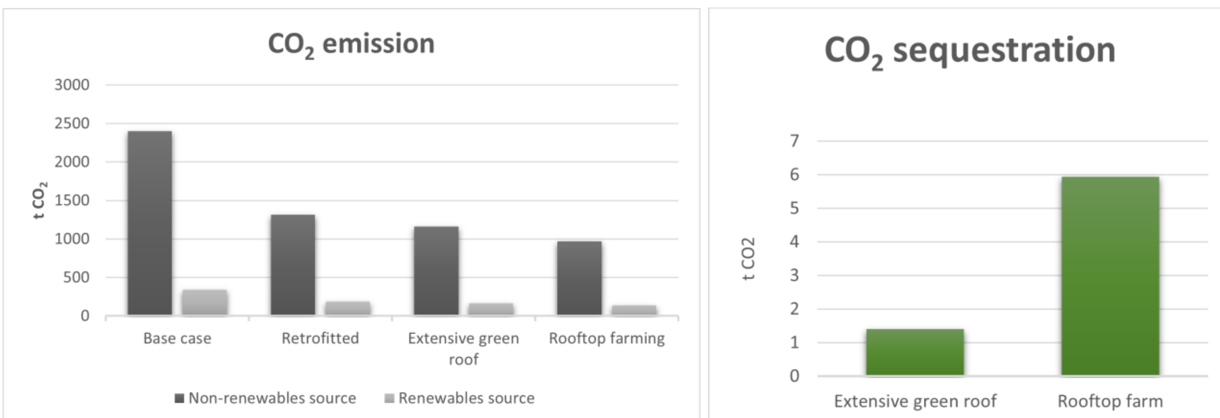


*Figure 6.13 $CO_2$ emission reduction by reducing energy consumption and $CO_2$ sequestration.*

Table 6.9 tries to show there is a possibility to pay back the additional embodied carbon in green roofs and rooftop farms which is between 4 to 6 years.

*Table 6.9 Aditional embodied carbon for applying Green Roof Scenarios*

| | Embodied Carbon ($t\ CO_2$) | Annual $CO_2$ reduction | | Payback year |
|---|---|---|---|---|
| | | $CO_2$ reduction by energy consumption reduction ($t\ CO_2$) | $CO_2$ sequestration ($t\ CO_2$) | |
| **Green roof** | 723.6 | 154.13 | 1.4 | 4-5 |
| **Rooftop farm** | 1575.76 | 343.7 | 5.95 | 5-6 |

### 6.3.5 Impact on the Surface Temperature

Green Envelopes offer many benefits beyond reducing heating and cooling demand in a building. As described in Chapter 3, they provide a wide range of environmental benefits, including aesthetics, biodiversity, air quality, and mitigation of the urban heat island effect. Therefore, integrating vegetation into an urban environment can directly mitigate the negative impacts of urbanization. Section 3.2.1 explores the ability of vegetation layers to mitigate the adverse effects associated with UHI.

Increasing temperatures have been observed in urban areas because of street canyons' configuration and material. This thesis analyzes the effects of building-integrated vegetation on the ambient temperature as a potential mitigation strategy for UHI. To simulate the building surface temperature, the ladybug tools were used for both scenarios: Rooftop Farm and Extensive Green Roof compared to the retrofitted building model conditions using concrete for the roof material. Fig6.12 refers to the workflow of the outdoor thermal comfort. Only the surface temperature was studied. Energy plus was used to model solar distribution, shading, and absorption by surfaces, Radiative heat transfer between surfaces, Conduction to the building interior, and Convective heat transfer using standard outdoor coefficients (not informed by CFD)[20].

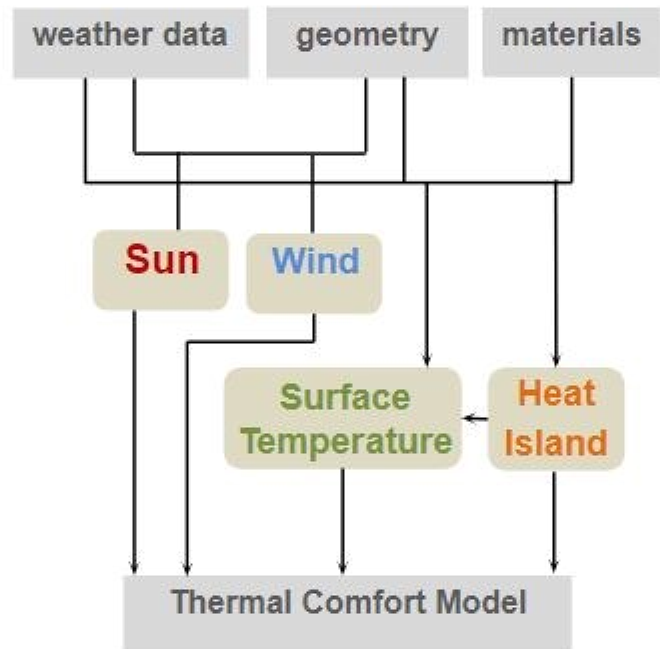


*Figure 6.12 Outdoor thermal comfort distributed model*[20]

Results indicate a reduction of around 6°C when applying the extensive green roof and about 9°C with the Rooftop farm. This reduction happens because green roofs provide shade, remove heat from the air, and reduce temperatures of the roof surface and surrounding air due to evapotranspiration. Vegetation provides shading to the roof, lowering the amount of short wave radiation incident in it and keeping the energy in the system. The surface temperature reduction in Rooftop Farm is more than Green roof because of more vegetation layer and higher shading and evapotranspiration. The analysis period was chosen on $16^{TH}$ of July between 15:00-16:00 for the summer. An error was received for investigating the surface temperature impact in winter, and the simulation was interrupted because of too cold months EPW weather datasets. Fig6.13 and 6.14 illustrate the surface temperature difference when applying the Green roof and Rooftop farm, respectively.

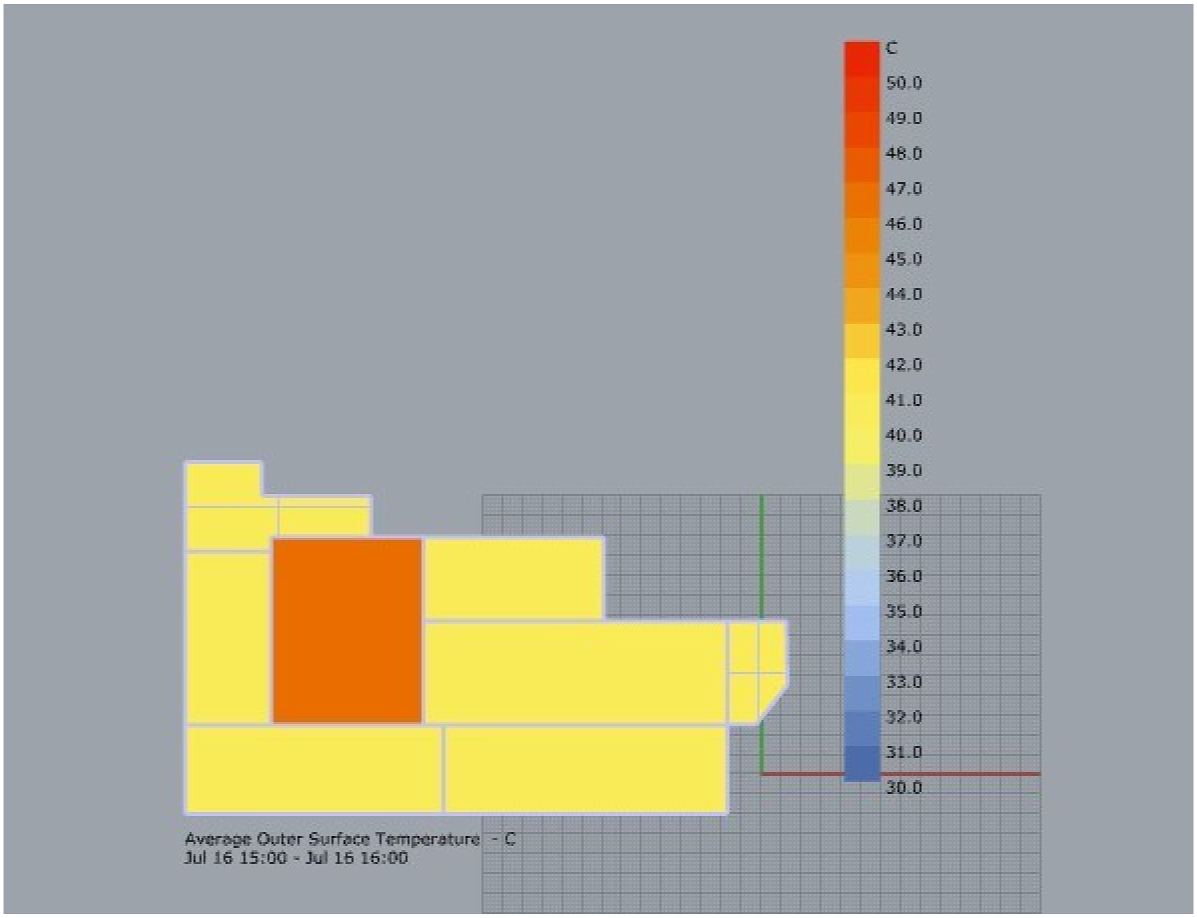


*Figure 6.13 Extensive Green Roof and concrete surface temperate comparison*

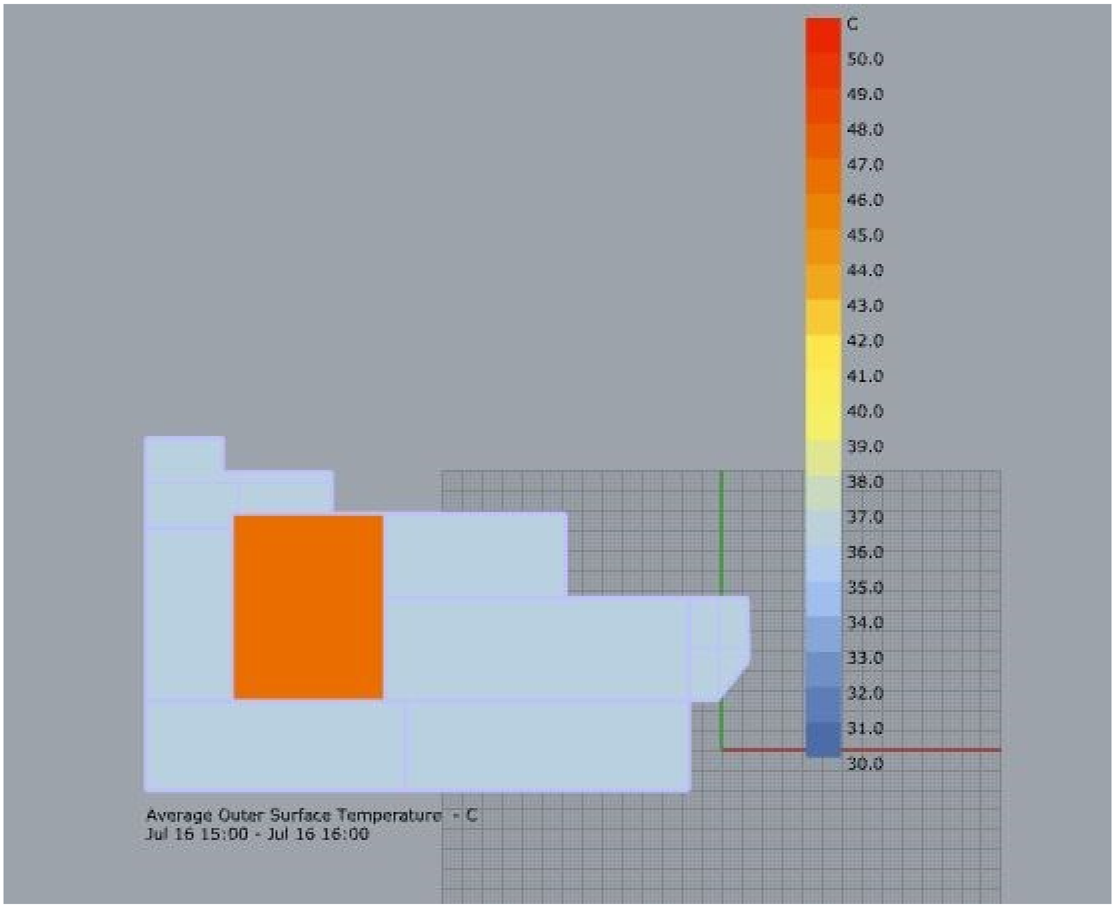


*Figure 6.14 Rooftop Farm and concrete surface temperate comparison*

## 6.4 Summary

The energy model results illustrate that the addition of a green roof and rooftop farm on the base case decreases the EUI by 153.3 kWh/m$^2$ and 174.7 kWh/m$^2$. However, if the retrofitted case is considered, the reductions are 17.4 kWh/m$^2$ and 38.8 kWh/m$^{2,}$ respectively. Total energy savings for extensive green roofs and rooftop farms are 12% and 26% compared with retrofitted buildings. Based on the higher energy savings for the non-insulated case, which is 58% and 65% for green roofs and rooftop farms, it indicates that the energy savings of green roofs are highly dependent on the existing roof insulation. Energy savings are greater when the roof has less insulation and a lower R-Value.

On the other hand, results indicate that by integrating green roofs and rooftop farms additional construction embodied carbon can be paid back by 4-6 years and their initial investment would be back by 11 and 23 years for the green roof and rooftop farm respectively.

Furthermore, extensive green roofs and rooftop farms, which differ in LAI and soil depth, demonstrate the importance of LAI and soil depth for energy savings; thus, rooftop farms have more significant savings due to the higher LAI and soil depth. Changing these characteristics of the green roof model also affected the surface temperature. On a warm day in summer with an extensive green roof, there is a reduction of about 6°C, while with the Rooftop farm there is a reduction of about 9°C. Green roofs reduce temperatures due to their ability to provide shade, remove heat from the air, and reduce surface temperatures and surrounding temperatures due to evaporation.

# 7. Conclusion and Discussion

During the literature review, a gap was identified in the lack of a comprehensive dataset, which could be used for modeling greenery systems in the built environment. This study aimed to develop a greenery system data model and use it in a case study. The developed data model was applied to the heritage building as retrofitting scenarios for the extensive green roof and rooftop farm to investigate the effect of the green roof retrofit plan on the building energy consumption, cost, carbon, and building surface temperature. Two software, Ladybug tools, and Design-Builder were used to analyze these impacts.

## 7.1 Conclusions

The goal of this research project is to include greenery systems in building energy modeling within an urban context. As a result, the research questions stated in Chapter 2 are answered using the results and discussion provided throughout this thesis:

*What is the procedure for creating a data model for the greenery system that can be combined with a larger urban data model?*

As part of this study, a data model for greenery systems based on a UML class diagram was developed using Eclipse to be integrated into an energy simulation workflow based on EnergyPlus as the dynamic building energy modeling engine. Such a data model facilitates the data storage and organization to analyze and optimize green infrastructure.
Moreover, an urban energy simulation platform can incorporate such a data model and facilitate the appraisals of the green envelope within whole buildings and city integrated greenery system. More explanations can be found in chapter 5 of this thesis.

*Are there possibilities of replacing green roofs with rooftop farming?*

Considering a rooftop farm as an intensive green roof, there are many benefits to developing the common form of a green roof to the rooftop farm ranging from an ecological to a social point of view. This study revealed that the rooftop farm scenario has less energy consumption and building surface temperature than the retrofitted and extensive green roof scenarios. A rooftop farm, however, has a longer payback period and emits more $CO_2$ during integration, so it is a trade-off decision based on several factors that should be weighed ahead of the integration.

*Which are the parameters with the most substantial influence on the performance of the greenery system?*

Evaluating the most critical parameters in the greenery systems depends on how they are integrated into the built environment and what benefit is considered. For example, building energy consumption was reduced more in this study with the higher plant height, LAI, and soil layer thickness. At the same time, the radiation properties should also be considered regarding the surface temperature levels.

*To what extent is the insulation, evapotranspiration, and shading effect capable of reducing a building's energy demand?*

The rate of the evapotranspiration process is controlled by the contribution of both aerodynamic resistance and surface bulk resistance of a green envelope. This resistance is directly related to the foliage density of the vegetation represented by the leaf area index. It also helped increase the vegetation layer's shading effect, resulting in a decrease in heat transmission.

In terms of the insulation impact, a direct effect is observed since a resistance to heat flux is introduced, which is due to the thickness and moisture content of the substrate layer. Indirectly, it serves as a growing medium for the vegetation layer allowing the cooling effect through the evapotranspiration process. Therefore, energy consumption was found to be more influenced by the soil depth than the LAI. On the whole, there is a higher energy consumption reduction in the rooftop farming scenario because of more LAI and soil thickness.

*How does a greenery system respond under the urban heat island effect and $CO_2$ sequestration in an urban environment?*

Greenery systems in urban environments lead to a reduction in ambient temperature. Due to the change in the surface albedo and the cooling effect caused by the evapotranspiration process, a measurable temperature drop depends on the amount of reflected short wave radiation, wind patterns, and vapor pressure deficit in the atmosphere. Furthermore, the surface albedo change can significantly alter the reflected short wave radiation, reducing the total amount of energy received and stored in the urban canopy. The purpose of this study was to investigate whether the integration of green roofs affects the surface temperature, which is not influenced by microclimatic conditions, such as wind patterns and vapor pressure deficit. The results showed a possibility of a temperature drops of 6°-9° C on a hot summer day.

Energy modeling indicates that heating and cooling demand savings can be achieved by adding a green roof retrofit to the case study. Total annual energy savings for the retrofitted, extensive green roof and rooftop farm scenarios in a case study building are 1183, 1351, and 1558 MWh, respectively. According to the Canada Energy Regulator(CER)[247], the equivalent carbon emission is1.3 grams of $CO_2e$ per kilowatt-hour for the current green hydroelectricity in Quebec. Therefore, the retrofitted, extensive green roof and rooftop farm energy-conserving equates to an annual equivalent carbon reduction of 138, 1756, and 2025 kg $CO_2e$.

Integrating a green roof and rooftop farm will increase costs and embodied carbon for the project, which might pay back by energy savings and $CO_2$ sequestration, which is explained more in the limitations sections.

## 7.2 Limitations

While this study aimed to reduce the uncertainty in modeling the integration of green envelopes into buildings, several limitations and drawbacks were identified during the research, including:

- The greenery system's potential effects on the ambient temperature are hard to simulate in software as it is difficult to know the moisture-related plant and soil characteristics. In this study, the substrate layer moisture was assumed constant during the analysis periods, keeping both the magnitude of the insulation provided by the substrate and the rate of evapotranspiration constant, which is not an accurate representation of reality. A decreased effect could be seen in a real setting due to decreased moisture over time.
- The result regarding the surface temperature effect was obtained only for the summer period due to receiving errors in the simulation software for the winter weather conditions in Montreal.
- In terms of carbon reduction, there is a lack of information on the selected plant carbon sequestrations in the scenarios, making it difficult to consider this effect on carbon reduction. Therefore the final calculation of the total carbon reduction by integrating green roofs is calculated based on the average from the literature review.
- During the plant species selection for simulation, it should be considered cold-tolerant plants that would be suitable to grow in a zone 5 hardiness region, such as Montreal

x

## 7.3 Recommendations and Future works

This project's scope was so broad that many topics were not fully considered. Therefore, more research regarding the following topics is needed to continue the learning process and quantify a greenery system's performance, including:

- develop an automated workflow to integrate the greenery system catalog into the CERC NextGenCities, urban building energy simulation platform.
- Propose green roof and rooftop farm scenarios retrofitted plan for the Concordia university deep retrofit proposal.
- Identifying the full extent of the cooling effects provided by the greenery systems regarding their distribution in space and their optimization potential on different urban configurations and climate conditions.
- A more accurate computational model for the soil moisture content and releasing process into the environment due to the cooling effect. Moreover, the amount of water required to maintain optimal moisture levels and prevent a decrease in the evapotranspiration rate.
- More research on the effect of building characteristics on greenery envelope integrated on energy savings needs to be done. For example, the envelope's shape, height, and temperature would need to be Investigated.
- Finally, larger flexibility of the Grasshopper model to interpret the weather data from the Energy Plus Weather file (EPW), especially for the extreme weather conditions.

## Bibliography


[1] "CER – Provincial and Territorial Energy Profiles - Quebec." https://www.cer-rec.gc.ca/en/data-analysis/energy-markets/provincial-territorial-energy-profiles/provincial-territorial-energy-profiles-quebec.html (accessed Aug. 14, 2021).

[2] "WSUD and Urban Heat Island Effect Mitigation - ScienceDirect." https://www-sciencedirect-com.lib-ezproxy.concordia.ca/science/article/pii/B9780128128435000198 (accessed Aug. 17, 2021).

[3] L. Kleerekoper, M. van Esch, and T. B. Salcedo, "How to Make a City Climate-Proof : Addressing the Urban Heat Island Effect," *Plan. Clim. Chang.*, pp. 250–262, Sep. 2018, doi: 10.4324/9781351201117-28.

[4] "Quebec - Air Quality Health Index (AQHI) - Environment Canada." https://weather.gc.ca/airquality/pages/provincial_summary/qc_e.html (accessed Jan. 12, 2022).

[5] "Harmful Noise Levels | HealthLink BC." https://www.healthlinkbc.ca/health-topics/tf4173 (accessed Sep. 09, 2021).

[6] "Living The Noom | Departamentos Wellness y Sustentables Cancún." https://www.livingthenoom.com/ (accessed Sep. 10, 2021).

[7] V. Anderson, "Deep Adaptation: A Framework for Climate Resilience, Decarbonization, and Planetary Health," *ProQuest Diss. Theses*, no. 10937535 PG–186, p. 186, 2018, [Online]. Available: http://ezproxy.library.dal.ca/login?url=https://www.proquest.com/dissertations-theses/deep-adaptation-framework-climate-resilience/docview/2150178410/se-2?accountid=10406 NS -.

[8] V. Sangiorgio, F. Fiorito, and M. Santamouris, "Development of a holistic urban heat island evaluation methodology," 2020, doi: 10.1038/s41598-020-75018-4.

[9] K. Vijayaraghavan, "Green roofs: A critical review on the role of components, benefits, limitations and trends," *Renew. Sustain. Energy Rev.*, vol. 57, pp. 740–752, 2016, doi: 10.1016/j.rser.2015.12.119.

[10] Green Roofs for Healthy Cities, "2019 Annual Green Roof," no. November, 2019, [Online]. Available: https://greenroofs.org/industry-surveys.

[11] B. Raji, M. J. Tenpierik, and A. Van Den Dobbelsteen, "The impact of greening systems on building energy performance: A literature review," 2015, doi: 10.1016/j.rser.2015.02.011.

[12] F. Orsini *et al.*, "Exploring the production capacity of rooftop gardens (RTGs) in urban agriculture: the potential impact on food and nutrition security, biodiversity and other ecosystem services in the city of Bologna," *Food Secur.*, vol. 6, no. 6, pp. 781–792, 2014, doi: 10.1007/s12571-014-0389-6.

[13] M. Manso and J. Castro-Gomes, “Green wall systems: A review of their characteristics,” 2014, doi: 10.1016/j.rser.2014.07.203.

[14] K. C. Dahanayake and C. Lun Chow, “Comparing reduction of building cooling load through green roofs and green walls by EnergyPlus simulations Article History,” doi: 10.1007/s12273-017-0415-7.

[15] K. W. D. K. C. Dahanayake and C. L. Chow, “Studying the potential of energy saving through vertical greenery systems: Using EnergyPlus simulation program,” *Energy Build.*, vol. 138, pp. 47–59, 2017, doi: 10.1016/j.enbuild.2016.12.002.

[16] B. Givoni, “Comfort, climate analysis and building design guidelines,” *Energy Build.*, vol. 18, no. 1, pp. 11–23, Jan. 1992, doi: 10.1016/0378-7788(92)90047-K.

[17] “Green Roof Model (EcoRoof): Engineering Reference — EnergyPlus 8.0.” https://bigladdersoftware.com/epx/docs/8-0/engineering-reference/page-029.html (accessed Oct. 20, 2021).

[18] B. Radin, C. Reisser Júnior, R. Matzenauer, and H. Bergamaschi, “Crescimento de cultivares de alface conduzidas em estufa e a campo,” *Hortic. Bras.*, vol. 22, no. 2, pp. 178–181, 2004, doi: 10.1590/s0102-05362004000200003.

[19] “Performance Newtwork Presentation1 - Google Slides.” https://docs.google.com/presentation/d/1_evNerddSTk3uGCSjdcwuyBwMoAK85e2Mlv46gcwIsc/edit#slide=id.g16cfefcfdb_0_21 (accessed Jan. 06, 2022).

[20] “20170802_Building_Simulation_Outdoor_Thermal_Comfort - Google Slides.” https://docs.google.com/presentation/d/1mKQByZxfwZSvdSvXUw7IRBzY2gRjIJq4iSN1ug5k00Q/edit#slide=id.p11 (accessed Feb. 13, 2022).

[21] M. Manso, I. Teotónio, C. M. Silva, and C. O. Cruz, “Green roof and green wall benefits and costs: A review of the quantitative evidence,” *Renew. Sustain. Energy Rev.*, vol. 135, no. July 2020, 2021, doi: 10.1016/j.rser.2020.110111.

[22] “ASHRAE GreenGuide: The Design, Construction, and Operation of Sustainable Buildings.” https://www.ashrae.org/technical-resources/bookstore/ashrae-greenguide-the-design-construction-and-operation-of-sustainable-buildings (accessed Sep. 22, 2021).

[23] “EnergyPlus Documentation Input Output Reference The Encyclopedic Reference to EnergyPlus Input and Output,” 1996.

[24] “Energy | UN-Habitat.” https://unhabitat.org/topic/energy (accessed Apr. 27, 2021).

[25] N. I. Report, “1990 – 2019 : GREENHOUSE GAS SOURCES AND SINKS IN CANADA CANADA ’ S SUBMISSION TO THE UNITED NATIONS FRAMEWORK,” 2019.

[26] N. Ahmad Ludin *et al.*, “Prospects of life cycle assessment of renewable energy from solar photovoltaic technologies: A review,” 2018, doi: 10.1016/j.rser.2018.07.048.

[27] T. A. M. Pugh, § A Robert Mackenzie, J. D. Whyatt, and C. Nicholas Hewitt, “Effectiveness of Green Infrastructure for Improvement of Air Quality in Urban Street

Canyons," 2012, doi: 10.1021/es300826w.

[28] M. Santamouris, "Cooling the cities - A review of reflective and green roof mitigation technologies to fight heat island and improve comfort in urban environments," *Sol. Energy*, vol. 103, pp. 682–703, 2014, doi: 10.1016/j.solener.2012.07.003.

[29] F. Balany, A. W. Ng, N. Muttil, S. Muthukumaran, and M. S. Wong, "Green Infrastructure as an Urban Heat Island Mitigation Strategy-A Review," doi: 10.3390/w12123577.

[30] M. Shafique, R. Kim, and M. Rafiq, "Green roof benefits, opportunities and challenges-A review," 2018, doi: 10.1016/j.rser.2018.04.006.

[31] T. Susca, S. R. Gaffin, and G. R. Dell'osso, "Positive effects of vegetation: Urban heat island and green roofs," doi: 10.1016/j.envpol.2011.03.007.

[32] V. Albino, U. Berardi, and R. M. Dangelico, "Smart cities: Definitions, dimensions, performance, and initiatives," *J. Urban Technol.*, vol. 22, no. 1, pp. 3–21, 2015, doi: 10.1080/10630732.2014.942092.

[33] B. Peuportier, S. Thiers, and A. Guiavarch, "Eco-design of buildings using thermal simulation and life cycle assessment," 2012, doi: 10.1016/j.jclepro.2012.08.041.

[34] S. Berry and K. Davidson, "Improving the economics of building energy code change: A review of the inputs and assumptions of economic models," 2016, doi: 10.1016/j.rser.2015.12.220.

[35] A. Martínez-Molina, I. Tort-Ausina, S. Cho, and J.-L. Vivancos, "Energy efficiency and thermal comfort in historic buildings: A review," 2016, doi: 10.1016/j.rser.2016.03.018.

[36] "Climate Change 2013: The Physical Science Basis: Working Group I ... - Intergovernmental Panel on Climate Change - Google Books." https://books.google.ca/books?hl=en&lr=&id=o4gaBQAAQBAJ&oi=fnd&pg=PR1&ots=WhlBcQFtLi&sig=60cnVRC2yEXpeyWLt2K0HMMgeSg&redir_esc=y#v=onepage&q&f=false (accessed Aug. 11, 2021).

[37] M. Hosseini, A. Bigtashi, and B. Lee, "Generating future weather files under climate change scenarios to support building energy simulation-A machine learning approach," 2020, doi: 10.1016/j.enbuild.2020.110543.

[38] B. Raji, M. J. Tenpierik, and A. Van Den Dobbelsteen, "An assessment of energy-saving solutions for the envelope design of high-rise buildings in temperate climates: A case study in the Netherlands," *Energy Build.*, vol. 124, pp. 210–221, 2016, doi: 10.1016/j.enbuild.2015.10.049.

[39] T. Hong, W. Zhang, Y. Xu, X. Luo, K. Sun, and X. 2019 Luo, "Visualizing Urban Microclimate and Quantifying its Impact on Building Energy Use in San Francisco," 2019, doi: 10.1145/3363459.3363536.

[40] N. H. Wong *et al.*, "Evaluation of the impact of the surrounding urban morphology on building energy consumption," *Sol. Energy*, vol. 85, no. 1, pp. 57–71, Jan. 2011, doi: 10.1016/j.solener.2010.11.002.

[41] A. Salvati, H. C. Roura, and C. Cecere, “Assessing the urban heat island and its energy impact on residential buildings in Mediterranean climate: Barcelona case study,” *Energy Build.*, vol. 146, pp. 38–54, 2017, doi: 10.1016/j.enbuild.2017.04.025.

[42] “Climate Change | National Geographic Society.” https://www.nationalgeographic.org/encyclopedia/climate-change/ (accessed Aug. 12, 2021).

[43] M. N. Assimakopoulos, G. Mihalakakou, and H. A. Flocas, “Simulating the thermal behaviour of a building during summer period in the urban environment,” *Renew. Energy*, vol. 32, pp. 1805–1816, 2007, doi: 10.1016/j.renene.2006.08.003.

[44] M. K. Theophilou and D. Serghides, “(No Title),” *Energy Build.*, vol. 108, pp. 137–144, 2015, doi: 10.1016/j.enbuild.2015.08.034.

[45] E. Jamei, Y. Jamei, P. Rajagopalan, R. Ossen, and S. Roushenas, “Effect of built-up ratio on the variation of air temperature in a heritage city,” *Sustain. Cities Soc.*, vol. 14, pp. 280–292, 2015, doi: 10.1016/j.scs.2014.10.001.

[46] E. Jamei and P. Rajagopalan, “Urban development and pedestrian thermal comfort in Melbourne,” 2017, doi: 10.1016/j.solener.2017.01.023.

[47] A. M. Coutts, J. Beringer, and N. J. Tapper, “Impact of increasing urban density on local climate: Spatial and temporal variations in the surface energy balance in Melbourne, Australia,” *J. Appl. Meteorol. Climatol.*, vol. 46, no. 4, pp. 477–493, 2007, doi: 10.1175/JAM2462.1.

[48] “A P P L I C AT I O N S A N D I M P L E M E N TAT I O N Multiscale Approach to Life Cycle Assessment Evaluation of the Effect of an Increase in New York City’s Rooftop Albedo on Human Health,” 2012, doi: 10.1111/j.1530-9290.2012.00560.x.

[49] T. Auer, M. Radi, and M. Brkovi, “Green Facades and Living Walls — A Review Establishing the Classification of Construction Types and Mapping the Benefits,” *Sustain.*, vol. 11, pp. 1–23, 2019.

[50] A. Baklanov, L. T. Molina, and M. Gauss, “Megacities, air quality and climate,” *Atmos. Environ.*, vol. 126, pp. 235–249, 2016, doi: 10.1016/j.atmosenv.2015.11.059.

[51] M. Z. Jacobson, “Review of Solutions to Global Warming, Air Pollution, and Energy Security.”

[52] M. Bruse, “Particle filtering capacity of urban vegetation: A microscale numerical approach,” *Berliner Geogr. Arb.*, vol. 109, no. January, pp. 61–70, 2007, [Online]. Available: https://www.researchgate.net/profile/Michael_Bruse/publication/265449484_Particle_filtering_capacity_of_urban_vegetation_A_microscale_numerical_approach/links/54b79c700cf2e68eb280300c.pdf.

[53] P. E. J. Vos, B. Maiheu, J. Vankerkom, and S. Janssen, “Improving local air quality in cities: To tree or not to tree?,” *Environ. Pollut.*, vol. 183, pp. 113–122, 2013, doi: 10.1016/j.envpol.2012.10.021.

[54] P. Kumar *et al.*, "New directions: From biofuels to wood stoves: The modern and ancient air quality challenges in the megacity of São Paulo," *Atmos. Environ.*, vol. 140, pp. 364–369, 2016, doi: 10.1016/j.atmosenv.2016.05.059.

[55] D. K. Heist, S. G. Perry, and L. A. Brixey, "A wind tunnel study of the effect of roadway configurations on the dispersion of traffic-related pollution," *Atmos. Environ.*, vol. 43, no. 32, pp. 5101–5111, 2009, doi: 10.1016/j.atmosenv.2009.06.034.

[56] A. Y. Bigazzi and M. A. Figliozzi, "Roadway determinants of bicyclist exposure to volatile organic compounds and carbon monoxide," *Transp. Res. Part D Transp. Environ.*, vol. 41, pp. 13–23, 2015, doi: 10.1016/j.trd.2015.09.008.

[57] J. Gallagher, L. W. Gill, and A. Mcnabola, "Optimizing the use of on-street car parking system as a passive control of air pollution exposure in street canyons by large eddy simulation," doi: 10.1016/j.atmosenv.2010.12.059.

[58] J. Gallagher, L. W. Gill, and A. McNabola, "Numerical modelling of the passive control of air pollution in asymmetrical urban street canyons using refined mesh discretization schemes," *Build. Environ.*, vol. 56, pp. 232–240, 2012, doi: 10.1016/j.buildenv.2012.03.013.

[59] J. Yang, J. McBride, J. Zhou, and Z. Sun, "The urban forest in Beijing and its role in air pollution reduction," *Urban For. Urban Green.*, vol. 3, no. 2, pp. 65–78, 2005, doi: 10.1016/j.ufug.2004.09.001.

[60] "Air quality: frequently asked questions - Canada.ca." https://www.canada.ca/en/environment-climate-change/services/air-quality-health-index/frequently-asked-questions.html (accessed Jan. 12, 2022).

[61] W. H. Organization, "Burden of Disease from Environmental Noise," p. 128, 2011.

[62] J. H. Ko, S. Il Chang, M. Kim, J. B. Holt, and J. C. Seong, "Transportation noise and exposed population of an urban area in the Republic of Korea," *Environ. Int.*, vol. 37, no. 2, pp. 328–334, 2011, doi: 10.1016/j.envint.2010.10.001.

[63] P. M. L. Anderson, C. Okereke, A. Rudd, and S. Parnell, *Regional assessment of Africa*. 2013.

[64] A. Rastandeh and M. Jarchow, "Urbanization and biodiversity loss in the post-COVID-19 era: complex challenges and possible solutions," 2020, doi: 10.1080/23748834.2020.1788322.

[65] K. C. Seto, B. Güneralp, and L. R. Hutyra, "Global forecasts of urban expansion to 2030 and direct impacts on biodiversity and carbon pools," doi: 10.1073/pnas.1211658109.

[66] F. Harkouss, F. Fardoun, and P. H. Biwole, "Passive design optimization of low energy buildings in different climates," *Energy*, vol. 165, pp. 591–613, 2018, doi: 10.1016/j.energy.2018.09.019.

[67] S. A. I. Global, F. Iso, and C. License, "Din En 15251 (2012)," *Eur. Stand.*, vol. 44, pp. 0–9, 2012.

[68] F. Harkouss, F. Fardoun, and P. H. Biwole, "Optimization approaches and climates investigations in NZEB-A review," doi: 10.1007/s12273-018-0448-6.

[69] "THE 17 GOALS | Sustainable Development." https://sdgs.un.org/goals (accessed Nov. 24, 2021).

[70] "BCL." https://bcl.nrel.gov/ (accessed Nov. 25, 2021).

[71] "TABULA WebTool." https://webtool.building-typology.eu/#bd (accessed Nov. 25, 2021).

[72] M. Du and X. Zhang, "Urban greening: A new paradox of economic or social sustainability?," *Land use policy*, vol. 92, no. April 2019, p. 104487, 2020, doi: 10.1016/j.landusepol.2020.104487.

[73] K. Yeang, L. Davies, Y. Tr, H. Yeang, S. Bhd, and R. Powell, "DESIGNING THE ECOSKYSCRAPER: PREMISES FOR TALL BUILDING DESIGN PART 1: THEORY AND PREMISES PART 2: EXEMPLARY PROJECTS PART 1: THEORY AND PREMISES," 2007, doi: 10.1002/tal.414.

[74] G. Pérez, J. Coma, I. Martorell, and L. F. Cabeza, "Vertical Greenery Systems (VGS) for energy saving in buildings: A review," *Renew. Sustain. Energy Rev.*, vol. 39, pp. 139–165, 2014, doi: 10.1016/j.rser.2014.07.055.

[75] C. Wang, S.-S. Er, and H. Abdul-Rahman, "I Indoor ndoor and and Built uilt Environment Indoor vertical greenery system in urban tropics," doi: 10.1177/1420326X14550508.

[76] C. Y. Jim, "Green roof evolution through exemplars: Germinal prototypes to modern variants," 2017, doi: 10.1016/j.scs.2017.08.001.

[77] B. Kotzen, "Green Roofs Social and Aesthetic Aspects," *Nat. Based Strateg. Urban Build. Sustain.*, pp. 273–281, Jan. 2018, doi: 10.1016/B978-0-12-812150-4.00025-2.

[78] "Sheppard Robson creates Europe's largest green wall for this mixed-use building in London." https://worldarchitecture.org/article-links/eepff/sheppard-robson-creates-europe-s-largest-green-wall-for-this-mixeduse-building-in-london.html (accessed Sep. 15, 2021).

[79] "IKEA reveals plans for car-free store wrapped in greenery." https://www.dezeen.com/2020/01/23/ikea-vienna-westbahnhof-car-free-store/ (accessed Sep. 15, 2021).

[80] "Tropical plants cover the balconies of Chicland hotel in Vietnam." https://www.dezeen.com/2020/01/13/chicland-co-trong-nghia-hotel-vietnam-architecture/ (accessed Sep. 15, 2021).

[81] "Liuzhou Forest City | Stefano Boeri Architetti." https://www.stefanoboeriarchitetti.net/en/project/liuzhou-forest-city/ (accessed Sep. 15, 2021).

[82] "Stylish, green and eco-friendly modern urban village to be built in the heart of Tokyo by 2023 | SoraNews24 -Japan News-." https://soranews24.com/2019/08/29/stylish-green-and-eco-friendly-modern-urban-village-to-be-built-in-the-heart-of-tokyo-by-2023/ (accessed

Sep. 15, 2021).

[83] "Bosco Verticale (Vertical Forest), Milan - Greenroofs.com." https://www.greenroofs.com/projects/bosco-verticale-vertical-forest-milan/ (accessed Sep. 15, 2021).

[84] "Thammasat University Urban Rooftop Farm (TURF) - Greenroofs.com." https://www.greenroofs.com/projects/thammasat-university-urban-rooftop-farm-turf/ (accessed Sep. 15, 2021).

[85] "Urban Farm - University Business Services - Ryerson University." https://www.ryerson.ca/university-business-services/urban-farm/ (accessed May 16, 2021).

[86] "Melbourne Car Park to be Turned Into a Rooftop Skyfarm - Greenroofs.com." https://www.greenroofs.com/2019/05/18/melbourne-car-park-to-be-turned-into-a-rooftop-skyfarm/ (accessed Nov. 25, 2021).

[87] S. M. Zaid, E. Perisamy, H. Hussein, N. E. Myeda, and N. Zainon, "Vertical Greenery System in urban tropical climate and its carbon sequestration potential: A review," *Ecol. Indic.*, vol. 91, no. March, pp. 57–70, 2018, doi: 10.1016/j.ecolind.2018.03.086.

[88] E. J. Gago, J. Roldan, R. Pacheco-Torres, and J. Ordóñez, "The city and urban heat islands: A review of strategies to mitigate adverse effects," *Renew. Sustain. Energy Rev.*, vol. 25, pp. 749–758, 2013, doi: 10.1016/j.rser.2013.05.057.

[89] R. Djedjig, R. Belarbi, and E. Bozonnet, "Green wall impacts inside and outside buildings: Experimental study," *Energy Procedia*, vol. 139, pp. 578–583, 2017, doi: 10.1016/j.egypro.2017.11.256.

[90] E. Ng, L. Chen, Y. Wang, and C. Yuan, "A study on the cooling effects of greening in a high-density city: An experience from Hong Kong," *Building and Environment*, vol. 47, no. 1. pp. 256–271, 2012, doi: 10.1016/j.buildenv.2011.07.014.

[91] L. L. H. Peng and C. Y. Jim, "Green-roof effects on neighborhood microclimate and human thermal sensation," *Energies*, vol. 6, no. 2, pp. 598–618, 2013, doi: 10.3390/en6020598.

[92] S. E. Ouldboukhitine, R. Belarbi, and D. J. Sailor, "Experimental and numerical investigation of urban street canyons to evaluate the impact of green roof inside and outside buildings," *Applied Energy*, vol. 114. pp. 273–282, 2014, doi: 10.1016/j.apenergy.2013.09.073.

[93] D. Li, E. Bou-Zeid, and M. Oppenheimer, "The effectiveness of cool and green roofs as urban heat island mitigation strategies," *Environmental Research Letters*, vol. 9, no. 5. 2014, doi: 10.1088/1748-9326/9/5/055002.

[94] D. Chen, X. Wang, M. Thatcher, G. Barnett, A. Kachenko, and R. Prince, "Urban vegetation for reducing heat related mortality," *Environmental Pollution*, vol. 192. pp. 275–284, 2014, doi: 10.1016/j.envpol.2014.05.002.

[95] R. Djedjig, E. Bozonnet, and R. Belarbi, "Analysis of thermal effects of vegetated

envelopes: Integration of a validated model in a building energy simulation program," *Energy Build.*, vol. 86, pp. 93–103, 2015, doi: 10.1016/j.enbuild.2014.09.057.

[96] G. Lobaccaro and J. A. Acero, "Comparative analysis of green actions to improve outdoor thermal comfort inside typical urban street canyons," *Urban Clim.*, vol. 14, pp. 251–267, 2015, doi: 10.1016/j.uclim.2015.10.002.

[97] A. Meek, N. Jayasuriya, E. Horan, and R. Adams, "Environmental Benefits of Retrofitting Green Roofs to a City Block," *J. Hydrol. Eng.*, vol. 20, no. 4, p. 05014020, 2015, doi: 10.1061/(asce)he.1943-5584.0001048.

[98] C. Gromke, B. Blocken, W. Janssen, B. Merema, T. van Hooff, and H. Timmermans, "CFD analysis of transpirational cooling by vegetation: Case study for specific meteorological conditions during a heat wave in Arnhem, Netherlands," *Building and Environment*, vol. 83. pp. 11–26, 2015, doi: 10.1016/j.buildenv.2014.04.022.

[99] S. Flores Larsen, C. Filippín, and G. Lesino, "Modeling double skin green façades with traditional thermal simulation software," *Sol. Energy*, vol. 121, pp. 56–67, 2015, doi: 10.1016/j.solener.2015.08.033.

[100] "Assessment of the effectiveness of cool and green roofs for the mitigation of the Heat Island effect _ Enhanced Reader.pdf." .

[101] J. S. MacIvor, L. Margolis, M. Perotto, and J. A. P. Drake, "Air temperature cooling by extensive green roofs in Toronto Canada," *Ecological Engineering*, vol. 95. pp. 36–42, 2016, doi: 10.1016/j.ecoleng.2016.06.050.

[102] T. Sun, C. S. B. Grimmond, and G. H. Ni, "How do green roofs mitigate urban thermal stress under heat waves?," *Journal of Geophysical Research*, vol. 121, no. 10. pp. 5320–5335, 2016, doi: 10.1002/2016JD024873.

[103] A. Sharma, P. Conry, H. J. S. Fernando, A. F. Hamlet, J. J. Hellmann, and F. Chen, "Green and cool roofs to mitigate urban heat island effects in the Chicago metropolitan area: Evaluation with a regional climate model," *Environ. Res. Lett.*, vol. 11, no. 6, 2016, doi: 10.1088/1748-9326/11/6/064004.

[104] G. Pérez, J. Coma, S. Sol, and L. F. Cabeza, "Green facade for energy savings in buildings: The influence of leaf area index and facade orientation on the shadow effect," *Appl. Energy*, vol. 187, pp. 424–437, 2017, doi: 10.1016/j.apenergy.2016.11.055.

[105] Y. He, H. Yu, N. Dong, and H. Ye, "Thermal and energy performance assessment of extensive green roof in summer: A case study of a lightweight building in Shanghai," *Energy Build.*, vol. 127, pp. 762–773, Sep. 2016, doi: 10.1016/J.ENBUILD.2016.06.016.

[106] S. S. Alcazar, F. Olivieri, and J. Neila, "Green roofs: Experimental and analytical study of its potential for urban microclimate regulation in Mediterranean–continental climates," *Urban Clim.*, vol. 17, pp. 304–317, Sep. 2016, doi: 10.1016/J.UCLIM.2016.02.004.

[107] T. Zölch, J. Maderspacher, C. Wamsler, and S. Pauleit, "Using green infrastructure for urban climate-proofing: An evaluation of heat mitigation measures at the micro-scale," *Urban For. Urban Green.*, vol. 20, pp. 305–316, Dec. 2016, doi: 10.1016/J.UFUG.2016.09.011.

[108] U. Berardi, "The outdoor microclimate benefits and energy saving resulting from green roofs retrofits," *Energy Build.*, vol. 121, pp. 217–229, Jun. 2016, doi: 10.1016/J.ENBUILD.2016.03.021.

[109] M. Taleghani, D. Sailor, and G. A. Ban-Weiss, "Micrometeorological simulations to predict the impacts of heat mitigation strategies on pedestrian thermal comfort in a Los Angeles neighborhood," *Environmental Research Letters*, vol. 11, no. 2. 2016, doi: 10.1088/1748-9326/11/2/024003.

[110] T. E. Morakinyo, K. W. D. Kalani, C. Dahanayake, E. Ng, and C. L. Chow, "Temperature and cooling demand reduction by green-roof types in different climates and urban densities: A co-simulation parametric study," *Energy Build.*, vol. 145, pp. 226–237, Jun. 2017, doi: 10.1016/J.ENBUILD.2017.03.066.

[111] S. Wilkinson, R. C. Feitosa, I. T. Kaga, and I. H. De Franceschi, "Evaluating the Thermal Performance of Retrofitted Lightweight Green Roofs and Walls in Sydney and Rio de Janeiro," *Procedia Eng.*, vol. 180, pp. 231–240, Jan. 2017, doi: 10.1016/J.PROENG.2017.04.182.

[112] L. S. H. Lee and C. Y. Jim, "Subtropical summer thermal effects of wirerope climber green walls with different air-gap depths," *Build. Environ.*, vol. 126, pp. 1–12, 2017, doi: 10.1016/j.buildenv.2017.09.021.

[113] A. Solcerova, F. van de Ven, M. Wang, M. Rijsdijk, and N. van de Giesen, "Do green roofs cool the air?," *Build. Environ.*, vol. 111, pp. 249–255, Jan. 2017, doi: 10.1016/J.BUILDENV.2016.10.021.

[114] M. Mirnezhad, A. M. R. Bin Aminudin, and K. S. Yeap, "Thermal performance & temperature mitigation towards application of green roof in tropical climate," *Chem. Eng. Trans.*, vol. 56, pp. 397–402, 2017, doi: 10.3303/CET1756067.

[115] S. Charoenkit and S. Yiemwattana, "Role of specific plant characteristics on thermal and carbon sequestration properties of living walls in tropical climate," *Build. Environ.*, vol. 115, pp. 67–79, 2017, doi: 10.1016/j.buildenv.2017.01.017.

[116] Y. He, H. Yu, A. Ozaki, N. Dong, and S. Zheng, "An investigation on the thermal and energy performance of living wall system in Shanghai area," *Energy and Buildings*, vol. 140. pp. 324–335, 2017, doi: 10.1016/j.enbuild.2016.12.083.

[117] Y. Y. Huang, C. T. Chen, and W. T. Liu, "Thermal performance of extensive green roofs in a subtropical metropolitan area," *Energy Build.*, vol. 159, pp. 39–53, Jan. 2018, doi: 10.1016/J.ENBUILD.2017.10.039.

[118] M. D. Lalošević, M. S. Komatina, M. V Miloš, and N. R. Rudonja, "Green Roofs and Cool Materials As Retrofitting Strategies for," vol. 22, no. 6, pp. 2309–2324, 2018.

[119] P. Piro, M. Carbone, M. De Simone, M. Maiolo, P. Bevilacqua, and N. Arcuri, "Energy and hydraulic performance of a vegetated roof in sub-mediterranean climate," *Sustainability (Switzerland)*, vol. 10, no. 10. 2018, doi: 10.3390/su10103473.

[120] R. Castiglia Feitosa and S. J. Wilkinson, "Attenuating heat stress through green roof and green wall retrofit," *Build. Environ.*, vol. 140, pp. 11–22, Aug. 2018, doi:

10.1016/J.BUILDENV.2018.05.034.

[121] Y. He, H. Yu, P. Chen, and M. Zhao, "Thermal performance evaluation of a new type of green roof system," *Energy Procedia*, vol. 152, pp. 384–389, Oct. 2018, doi: 10.1016/J.EGYPRO.2018.09.161.

[122] JEAN-F. TOMB *et al.*, "Enhanced Reader.pdf," *Nature*, vol. 388. pp. 539–547, 1997.

[123] H. F. Castleton, V. Stovin, S. B. M. Beck, and J. B. Davison, "Green roofs; Building energy savings and the potential for retrofit," *Energy Build.*, vol. 42, no. 10, pp. 1582–1591, 2010, doi: 10.1016/j.enbuild.2010.05.004.

[124] M. Anwar, M. G. Rasul, and M. M. K. Khan, "Performance Analysis of rooftop greenery systems in Australian subtropical climate," *Energy Reports*, vol. 6, pp. 50–56, 2020, doi: 10.1016/j.egyr.2019.08.017.

[125] X. Hao, Q. Xing, P. Long, Y. Lin, J. Hu, and H. Tan, "Influence of vertical greenery systems and green roofs on the indoor operative temperature of air-conditioned rooms," 2020, doi: 10.1016/j.jobe.2020.101373.

[126] X. Zheng, T. Dai, and M. Tang, "An experimental study of vertical greenery systems for window shading for energy saving in summer," 2020, doi: 10.1016/j.jclepro.2020.120708.

[127] A. B. Besir and E. Cuce, "Green roofs and facades: A comprehensive review," *Renew. Sustain. Energy Rev.*, vol. 82, no. October 2017, pp. 915–939, 2018, doi: 10.1016/j.rser.2017.09.106.

[128] A. Nagase and N. Dunnett, "Amount of water runoff from different vegetation types on extensive green roofs: Effects of plant species, diversity and plant structure," *Landsc. Urban Plan.*, vol. 104, pp. 356–363, 2012, doi: 10.1016/j.landurbplan.2011.11.001.

[129] L. Zhang *et al.*, "Outdoor Thermal Comfort of Urban Park-A Case Study," doi: 10.3390/su12051961.

[130] M. Ottelé, *The Green Building Envelope Vertical Greening*. 2011.

[131] M. R. Seyedabadi, U. Eicker, and S. Karimi, "Plant selection for green roofs and their impact on carbon sequestration and the building carbon footprint," *Environ. Challenges*, vol. 4, no. April, p. 100119, 2021, doi: 10.1016/j.envc.2021.100119.

[132] M. Shafique, X. Xue, and X. Luo, "An overview of carbon sequestration of green roofs in urban areas," 2019, doi: 10.1016/j.ufug.2019.126515.

[133] T. Kuronuma *et al.*, "CO2 Payoffof extensive green roofs with different vegetation species," *Sustain.*, vol. 10, no. 7, pp. 1–12, 2018, doi: 10.3390/su10072256.

[134] A. Marie and G. Palmyra, "The Potential Carbon Offset Represented by a Green Roof," 1996.

[135] L. J. Whittinghill, D. B. Rowe, R. Schutzki, and B. M. Cregg, "Quantifying carbon sequestration of various green roof and ornamental landscape systems," *Landsc. Urban Plan.*, vol. 123, pp. 41–48, 2014, doi: 10.1016/j.landurbplan.2013.11.015.

[136] H. Luo *et al.*, “Carbon sequestration potential of green roofs using mixed-sewage-sludge substrate in Chengdu World Modern Garden City,” *Ecol. Indic.*, vol. 49, pp. 247–259, 2015, doi: 10.1016/j.ecolind.2014.10.016.

[137] S. Ondoño, J. J. Martínez-Sánchez, and J. L. Moreno, “The inorganic component of green roof substrates impacts the growth of Mediterranean plant species as well as the C and N sequestration potential,” *Ecol. Indic.*, vol. 61, pp. 739–752, 2015, doi: 10.1016/j.ecolind.2015.10.025.

[138] T. Kuronuma and H. Watanabe, “Relevance of Carbon Sequestration to the Physiological and Morphological Traits of Several Green Roof Plants during the First Year after Construction,” *Am. J. Plant Sci.*, vol. 08, no. 01, pp. 14–27, 2017, doi: 10.4236/ajps.2017.81002.

[139] J. Heusinger and S. Weber, “Extensive green roof CO2 exchange and its seasonal variation quantified by eddy covariance measurements,” *Science of the Total Environment*, vol. 607–608. pp. 623–632, 2017, doi: 10.1016/j.scitotenv.2017.07.052.

[140] S. Cascone, F. Catania, A. Gagliano, and G. Sciuto, “A comprehensive study on green roof performance for retrofitting existing buildings,” *Build. Environ.*, vol. 136, no. February, pp. 227–239, 2018, doi: 10.1016/j.buildenv.2018.03.052.

[141] M. J. M. Davis, M. J. Tenpierik, F. R. Ramírez, and M. E. Pérez, “More than just a Green Facade: The sound absorption properties of a vertical garden with and without plants,” *Build. Environ.*, vol. 116, pp. 64–72, 2017, doi: 10.1016/j.buildenv.2017.01.010.

[142] G. Pérez *et al.*, “Acoustic insulation capacity of Vertical Greenery Systems for buildings,” 2016, doi: 10.1016/j.apacoust.2016.03.040.

[143] S. Gonsalves, O. Starry, A. Szallies, and S. Brenneisen, “Correction to: The effect of urban green roof design on beetle biodiversity (Urban Ecosystems, (2021), 10.1007/s11252-021-01145-z),” *Urban Ecosyst.*, 2021, doi: 10.1007/s11252-021-01155-x.

[144] E. V. White and B. Gatersleben, “Greenery on residential buildings: Does it affect preferences and perceptions of beauty?,” *J. Environ. Psychol.*, vol. 31, no. 1, pp. 89–98, 2011, doi: 10.1016/j.jenvp.2010.11.002.

[145] M. El Bachawati, R. Manneh, R. Belarbi, T. Dandres, C. Nassab, and H. El Zakhem, “Cradle-to-gate Life Cycle Assessment of traditional gravel ballasted, white reflective, and vegetative roofs: A Lebanese case study,” *J. Clean. Prod.*, vol. 137, pp. 833–842, 2016, doi: 10.1016/j.jclepro.2016.07.170.

[146] P. Vacek, K. Struhala, and L. Matějka, “Life-cycle study on semi intensive green roofs,” *J. Clean. Prod.*, vol. 154, pp. 203–213, 2017, doi: 10.1016/j.jclepro.2017.03.188.

[147] S. Bozorg Chenani, S. Lehvävirta, and T. Häkkinen, “Life cycle assessment of layers of green roofs,” *J. Clean. Prod.*, vol. 90, pp. 153–162, 2015, doi: 10.1016/j.jclepro.2014.11.070.

[148] M. Shafique, A. Azam, M. Rafiq, M. Ateeq, and X. Luo, “An overview of life cycle assessment of green roofs,” *J. Clean. Prod.*, vol. 250, p. 119471, Mar. 2020, doi: 10.1016/J.JCLEPRO.2019.119471.

[149] G. M. J. A. Salah and A. Romanova, "Life cycle assessment of felt system living green wall: Cradle to grave case study," *Environ. Challenges*, vol. 3, no. February, p. 100046, 2021, doi: 10.1016/j.envc.2021.100046.

[150] K. Perini and P. Rosasco, "Cost–benefit analysis for green façades and living wall systems," *Build. Environ.*, vol. 70, pp. 110–121, Dec. 2013, doi: 10.1016/J.BUILDENV.2013.08.012.

[151] K. Perini, "Life Cycle Assessment of Vertical Greening Systems," *Nat. Based Strateg. Urban Build. Sustain.*, pp. 333–340, Jan. 2018, doi: 10.1016/B978-0-12-812150-4.00030-6.

[152] "Urban Farm - University Business Services - Ryerson University." https://www.ryerson.ca/university-business-services/urban-farm/ (accessed May 18, 2021).

[153] N. Hafizah, "green roof gap____," *Ekp*, vol. 13, no. 3, pp. 1576–1580, 2017.

[154] "Green Roofs for Healthy Cities." https://greenroofs.org/ (accessed Nov. 24, 2021).

[155] P. Bevilacqua, D. Mazzeo, R. Bruno, and N. Arcuri, "Experimental investigation of the thermal performances of an extensive green roof in the Mediterranean area," *Energy Build.*, vol. 122, pp. 63–79, 2016, doi: 10.1016/j.enbuild.2016.03.062.

[156] City of Toronto, "Green Roof Bylaw," *Green Roofs*, pp. 1–17, 2012.

[157] Canada Green Building Council, "Toronto: LEED Supplement Summary Comparison," 2014, [Online]. Available: https://www.cagbc.org/cagbcdocs/leed/Toronto_LEED_Supplement_for_NC_2009_Oct2014.pdf.

[158] S. Cooper, "Planning Green Roofs in Toronto: Overcoming Obstacles to Private Investment," 2014, [Online]. Available: http://yorkspace.library.yorku.ca/xmlui/handle/10315/30259.

[159] eralesso T. Lib, C. Oliveira Cruz, C. Matos Silva, and M. Manso, "Green infrastructure and public policies: An international review of green roofs and green walls incentives," *Land use policy*, vol. 96, no. June 2019, p. 104693, 2020, doi: 10.1016/j.landusepol.2020.104693.

[160] J. Lee, "'Making Green Roofs Happen' in Toronto: Policy Analysis," 2017, [Online]. Available: https://qspace.library.queensu.ca/bitstream/handle/1974/22027/Lee_Joanne_201708_MPL.pdf?sequence=1.

[161] G. Proksch, "Urban Rooftops as Productive Resources Rooftop Farming versus Conventional Green Roofs," *ARCC Considering Res. Reflecting upon Curr. themes Archit. Res.*, pp. 497–509, 2011, [Online]. Available: http://citeseerx.ist.psu.edu/viewdoc/download?doi=10.1.1.847.5504&rep=rep1&type=pdf%0Ahttp://www.arcc-journal.org/index.php/repository/article/view/358.

[162] E. Grala da Cunha *et al.*, "Characterizing leaf area index of rooftop farm to assess

thermal-energy performance by simulation," *Energy Build.*, vol. 241, p. 110960, 2021, doi: 10.1016/j.enbuild.2021.110960.

[163] F. Orsini *et al.*, "Exploring the production capacity of rooftop gardens (RTGs) in urban agriculture: the potential impact on food and nutrition security, biodiversity and other ecosystem services in the city of Bologna," doi: 10.1007/s12571-014-0389-6.

[164] "Urban Farming: A Budding Investment Opportunity in Real Estate | Millionacres." https://www.millionacres.com/real-estate-investing/articles/urban-farming-budding-investment-opportunity-real-estate/ (accessed Sep. 27, 2021).

[165] "Facilities Management and Development - Ryerson University." https://www.ryerson.ca/facilities-management-development/ (accessed May 16, 2021).

[166] S. Permpituck and P. Namprakai, "The energy consumption performance of roof lawn gardens in Thailand," *Renew. Energy*, vol. 40, no. 1, pp. 98–103, 2012, doi: 10.1016/j.renene.2011.09.023.

[167] J. A. Coma, G. P. Erez, C. Sol, A. Castell, and L. F. Cabeza, "Thermal assessment of extensive green roofs as passive tool for energy savings in buildings," 2015, doi: 10.1016/j.renene.2015.07.074.

[168] H. M. Imran, J. Kala, A. W. M. Ng, and S. Muthukumaran, "Effectiveness of green and cool roofs in mitigating urban heat island effects during a heatwave event in the city of Melbourne in southeast Australia," 2018, doi: 10.1016/j.jclepro.2018.06.179.

[169] S. C. M. Hui and S. C. Chan, "Integration of green roof and solar photovoltaic systems," *Jt. Symp. 2011 Integr. Build. Des. New Era Sustain.*, vol. 2011, no. November, pp. 1–12, 2011.

[170] "(2) 'Biosolar Roofs' by Nathalie Baumann and Dusty Gedge - YouTube." https://www.youtube.com/watch?v=-W4j28cuykM&t=2s (accessed Oct. 05, 2021).

[171] D. Chemisana and C. Lamnatou, "Photovoltaic-green roofs: An experimental evaluation of system performance," *Appl. Energy*, vol. 119, pp. 246–256, 2014, doi: 10.1016/j.apenergy.2013.12.027.

[172] M. J. Alshayeb and J. D. Chang, "Variations of PV Panel Performance Installed over a Vegetated Roof and a Conventional Black Roof," doi: 10.3390/en11051110.

[173] A. Jahanfar, B. Sleep, and J. Drake, "Energy and Carbon-Emission Analysis of Integrated Green-Roof Photovoltaic Systems: Probabilistic Approach," *J. Infrastruct. Syst.*, vol. 24, no. 1, p. 04017044, 2018, doi: 10.1061/(asce)is.1943-555x.0000399.

[174] M. S. Penaranda Moren and A. Korjenic, "Hotter and colder – How Do Photovoltaics and Greening Impact Exterior Facade Temperatures: The synergies of a Multifunctional System," *Energy Build.*, vol. 147, pp. 123–141, 2017, doi: 10.1016/j.enbuild.2017.04.082.

[175] A. Medl, R. Stangl, and F. Florineth, "Vertical greening systems – A review on recent technologies and research advancement," *Build. Environ.*, vol. 125, pp. 227–239, 2017, doi: 10.1016/j.buildenv.2017.08.054.

[176] F. Ascione, R. F. De Masi, M. Mastellone, S. Ruggiero, and G. P. Vanoli, “Green walls, a critical review: Knowledge gaps, design parameters, thermal performances and multi-criteria design approaches,” *Energies*, vol. 13, no. 9, 2020, doi: 10.3390/en13092296.

[177] L. Malys, M. Musy, and C. Inard, “A hydrothermal model to assess the impact of green walls on urban microclimate and building energy consumption,” *Build. Environ.*, vol. 73, pp. 187–197, Mar. 2014, doi: 10.1016/J.BUILDENV.2013.12.012.

[178] A. B. Daemei, E. Shafiee, A. A. Chitgar, and S. Asadi, “Investigating the thermal performance of green wall: Experimental analysis, deep learning model, and simulation studies in a humid climate,” *Building and Environment*, vol. 205. 2021, doi: 10.1016/j.buildenv.2021.108201.

[179] F. Olivieri, R. C. Grifoni, D. Redondas, J. A. Sánchez-Reséndiz, and S. Tascini, “An experimental method to quantitatively analyse the effect of thermal insulation thickness on the summer performance of a vertical green wall,” *Energy Build.*, vol. 150, pp. 132–148, 2017, doi: 10.1016/j.enbuild.2017.05.068.

[180] J. S. Carlos, “Simulation assessment of living wall thermal performance in winter in the climate of Portugal,” *Build. Simul.*, vol. 8, no. 1, pp. 3–11, 2015, doi: 10.1007/s12273-014-0187-2.

[181] X. C. Pan and Y. X. Xiao, “Simulation analysis of building green facade eco-effect,” *Appl. Mech. Mater.*, vol. 548–549, pp. 1701–1705, 2014, doi: 10.4028/www.scientific.net/AMM.548-549.1701.

[182] “EnergyPlus.” https://energyplus.net/ (accessed Nov. 26, 2021).

[183] City of Toronto, “Toronto’s first resilience strategy,” p. 159, 2019, [Online]. Available: https://www.toronto.ca/ext/digital_comm/pdfs/resilience-office/toronto-resilience-strategy.pdf.

[184] F. Manzano-Agugliaro, F. G. Montoya, A. Sabio-Ortega, and A. García-Cruz, “Review of bioclimatic architecture strategies for achieving thermal comfort,” *Renew. Sustain. Energy Rev.*, vol. 49, pp. 736–755, Sep. 2015, doi: 10.1016/J.RSER.2015.04.095.

[185] K. Perini, M. Ottelé, A. L. A. Fraaij, E. M. Haas, and R. Raiteri, “Vertical greening systems and the effect on air flow and temperature on the building envelope,” *Build. Environ.*, vol. 46, no. 11, pp. 2287–2294, Nov. 2011, doi: 10.1016/J.BUILDENV.2011.05.009.

[186] H. Ţundrea and M. Budescu, “Bioclimatic Architecture, a Sensible and Logical Approach Towards the Future of Building Development.,” *Citefactor*, vol. 59, no. 6, pp. 109–117, 2013, [Online]. Available: http://ezproxy.uniandes.edu.co:8080/login?url=http://search.ebscohost.com/login.aspx?direct=true&db=a9h&AN=97179860&lang=es&site=eds-live&scope=site.

[187] A. B. Daemei, S. R. Eghbali, and E. M. Khotbehsara, “Bioclimatic design strategies: A guideline to enhance human thermal comfort in Cfa climate zones,” *J. Build. Eng.*, vol. 25, p. 100758, Sep. 2019, doi: 10.1016/J.JOBE.2019.100758.

[188] A. Tamaskani Esfehankalateh, M. Farrokhzad, F. Tamaskani Esfehankalateh, and F.

Soflaei, *Bioclimatic passive design strategies of traditional houses in cold climate regions*, no. 0123456789. Springer Netherlands, 2021.

[189] B. Ozarisoy and H. Altan, "Systematic literature review of bioclimatic design elements: Theories, methodologies and cases in the South-eastern Mediterranean climate," *Energy Build.*, vol. 250, p. 111281, Nov. 2021, doi: 10.1016/J.ENBUILD.2021.111281.

[190] T. A. de L. Martins, S. Faraut, and L. Adolphe, "Influence of context-sensitive urban and architectural design factors on the energy demand of buildings in Toulouse, France," *Energy Build.*, vol. 190, pp. 262–278, 2019, doi: 10.1016/j.enbuild.2019.02.019.

[191] H. Sanaieian, M. Tenpierik, K. Van Den Linden, M. Seraj, S. Majid, and M. Shemrani, "Review of the impact of urban block form on thermal performance, solar access and ventilation," 2014, doi: 10.1016/j.rser.2014.06.007.

[192] Y. Tian, H. Yuan, C. Wang, H. Wu, and Z. Xing, "Numerical investigation on mass and heat transfer in an ammonia oil-free twin-screw compressor with liquid injection," *Int. J. Therm. Sci.*, vol. 120, pp. 175–184, Oct. 2017, doi: 10.1016/J.IJTHERMALSCI.2017.06.007.

[193] S. Frankenstein and G. Koenig, "FASST Vegetation Models," *Cold Reg. Res. Eng. Lab.*, no. December, p. 56, 2004.

[194] "Sellers_1986_J._Atmos._Sci.pdf." .

[195] M. V. B. de Morais, E. R. Marciotto, V. V. Urbina Guerrero, and E. D. de Freitas, "Effective albedo estimates for the Metropolitan Area of São Paulo using empirical sky-view factors," *Urban Clim.*, vol. 21, pp. 183–194, Sep. 2017, doi: 10.1016/j.uclim.2017.06.007.

[196] "Green Roof Model (EcoRoof): Engineering Reference — EnergyPlus 8.3." https://bigladdersoftware.com/epx/docs/8-3/engineering-reference/green-roof-model-ecoroof.html (accessed May 17, 2021).

[197] P. A. Hughes *et al.*, "A mathematical model for the prediction of temperature of man-made and natural surfaces," *Int. J. Remote Sens.*, vol. 14, no. 7, pp. 1383–1412, 1993, doi: 10.1080/01431169308953964.

[198] L. K. Balick, R. K. Scoggins, and L. E. Link, "Inclusion of a simple vegetation layer in terrain temperature models for thermal infrared (IR) signature prediction.," no. 3, 1981.

[199] J. W. Deardorff, "Efficient prediction of ground surface temperature and moisture, with inclusion of a layer of vegetation," *J. Geophys. Res.*, vol. 83, no. C4, p. 1889, 1978, doi: 10.1029/jc083ic04p01889.

[200] G. L. Guymon, R. L. Berg, and T. V Hromadka, "Mathematical Model of Frost Heave and Thaw Settlement in Pavements," no. April, 1993.

[201] A. N. On and T. H. E. B. Profiles, "A note on the businger-dyer profiles," vol. 42, pp. 145–146, 1988.

[202] J. Coma, G. Pérez, A. de Gracia, S. Burés, M. Urrestarazu, and L. F. Cabeza, "Vertical

greenery systems for energy savings in buildings: A comparative study between green walls and green facades," *Build. Environ.*, vol. 111, pp. 228–237, Jan. 2017, doi: 10.1016/J.BUILDENV.2016.11.014.

[203] A. Yazdanseta, "Designing Green Walls : An Early-design Framework to Estimate the Cooling Impact of Indirect Green Walls on Buildings in Six Different Climates," 2017.

[204] L. Zhang *et al.*, "Thermal behavior of a vertical green facade and its impact on the indoor and outdoor thermal environment," *Energy Build.*, vol. 204, p. 109502, Dec. 2019, doi: 10.1016/J.ENBUILD.2019.109502.

[205] EnergyPlus v9.1.0, "Input Output Reference," *Encycl. Ref. to EnergyPlus Input Output*, no. c, pp. 1996–2016, 2010.

[206] C. Berretta, S. Poë, and V. Stovin, "Reprint of 'Moisture content behaviour in extensive green roofs during dry periods: The influence of vegetation and substrate characteristics,'" *J. Hydrol.*, vol. 516, pp. 37–49, Aug. 2014, doi: 10.1016/J.JHYDROL.2014.04.001.

[207] S. Cascone, J. Coma, A. Gagliano, and G. Pérez, "The evapotranspiration process in green roofs: A review," *Build. Environ.*, vol. 147, no. October 2018, pp. 337–355, 2019, doi: 10.1016/j.buildenv.2018.10.024.

[208] "Chapter 2 - FAO Penman-Monteith equation." https://www.fao.org/3/X0490E/x0490e06.htm#aerodynamic resistance (ra) (accessed Nov. 09, 2021).

[209] W. F. Change, "Vertical forests."

[210] A. Decruz, J. Darkwa, K. Yuan, and P. Strachan, "Development of databases for facilitating green roof energy simulation assessments," *2nd Asia Conf. Int. Build. Perform. Simul. Assoc.*, pp. 1–8, 2014.

[211] "PostgreSQL Tutorial - Learn PostgreSQL from Scratch." https://www.postgresqltutorial.com/ (accessed Feb. 02, 2022).

[212] J. Schiefelbein, A. P. Javadi, M. Lauster, V. Group, and P. Remmen, "Development of a City Information Model to support Data Management and Analysis of Building Energy Systems within Complex City," *Proc. CISBAT 2015 - Futur. Build. Dist. - Sustain. from Nano to Urban Scale*, no. September, 2015, doi: 10.5075/epfl-cisbat2015-949-954.

[213] K. Brassel, "Parameter Catalogs for Simulation," pp. 1–42, 2021.

[214] C. S. Technology and C. Paradigms, "Concepts and Paradigms of Object-Oriented Programming Expansion of Oct 400PSLA-89 Keynote Talk Peter Wegner, Brown University 1."

[215] "UML 2 Class Diagrams: An Agile Introduction." http://agilemodeling.com/artifacts/classDiagram.htm (accessed Oct. 28, 2021).

[216] "Eclipse (software - Wikipedia." https://en.wikipedia.org/wiki/Eclipse_(software (accessed Nov. 03, 2021).

[217] "Eclipse Modeling Project | The Eclipse Foundation."

https://www.eclipse.org/modeling/emf/ (accessed Nov. 02, 2021).

[218] "EcoreTools - Graphical Modeling for Ecore." https://www.eclipse.org/ecoretools/ (accessed Nov. 02, 2021).

[219] "Sirius | Home." https://www.eclipse.org/sirius/ (accessed Nov. 02, 2021).

[220] "Lecture 11: Object Oriented Modelling," 2004.

[221] V. Costanzo, G. Evola, and L. Marletta, "Energy savings in buildings or UHI mitigation? Comparison between green roofs and cool roofs," *Energy Build.*, vol. 114, pp. 247–255, Feb. 2016, doi: 10.1016/J.ENBUILD.2015.04.053.

[222] Eduardo Grala da Cunha *et al.*, "Growing Food on Green Roofs: The First Step of an Interdisciplinary Approach," *J. Civ. Eng. Archit.*, vol. 13, no. 11, 2019, doi: 10.17265/1934-7359/2019.11.004.

[223] S. Poddar, D. Park, and S. Chang, "Energy performance analysis of a dormitory building based on different orientations and seasonal variations of leaf area index," 2053, doi: 10.1007/s12053-016-9487-y.

[224] K. A. Byrne, G. Kiely, and P. Leahy, "CO2 fluxes in adjacent new and permanent temperate grasslands," *Agric. For. Meteorol.*, vol. 135, no. 1–4, pp. 82–92, 2005, doi: 10.1016/j.agrformet.2005.10.005.

[225] Z. H. Wang, X. Zhao, J. Yang, and J. Song, "Cooling and energy saving potentials of shade trees and urban lawns in a desert city," *Appl. Energy*, vol. 161, pp. 437–444, Jan. 2016, doi: 10.1016/J.APENERGY.2015.10.047.

[226] H. Demirsoy, L. Demirsoy, and A. Öztürk, "Improved model for the non-destructive estimation of strawberry leaf area," *Fruits*, vol. 60, no. 1, pp. 69–73, Jan. 2005, doi: 10.1051/FRUITS:2005014.

[227] "Principles of Environmental Physics: Plants, Animals, and the Atmosphere - John Monteith, Mike Unsworth - Google Books." https://books.google.ca/books?hl=en&lr=&id=EhLtk6hkLogC&oi=fnd&pg=PR1&dq=+Principles+of+Environmental+Physics:+Plants,+An&ots=Qv6pX-4qIl&sig=GPHbPS5ejRqMte7fyN9tadE6lNI#v=onepage&q=Principles of Environmental Physics%3A Plants%2C An&f=false (accessed Nov. 11, 2021).

[228] A. Capozzoli, A. Gorrino, and V. Corrado, "Thermal characterization of green roofs through dynamic simulation," *Proc. BS 2013 13th Conf. Int. Build. Perform. Simul. Assoc.*, pp. 3630–3637, 2013.

[229] H. W. Gausman and W. A. Allen, "Optical Parameters of Leaves of 30 Plant Species," *Plant Physiol.*, vol. 52, no. 1, pp. 57–62, 1973, doi: 10.1104/pp.52.1.57.

[230] A. Gagliano, F. Nocera, M. Detommaso, and G. Evola, "Thermal behavior of an extensive green roof: Numerical simulations and experimental investigations," *Int. J. Heat Technol.*, vol. 34, no. Special Issue 2, pp. S226–S234, 2016, doi: 10.18280/ijht.34S206.

[231] F. F. Blanco and M. V. Folegatti, "A new method for estimating the leaf area index of

cucumber and tomato plants," *Hortic. Bras.*, vol. 21, no. 4, pp. 666–669, 2003, doi: 10.1590/s0102-05362003000400019.

[232] E. Ahn, D. Yeom, and K. I. Lee, "Experimental research on the indoor environment performance of complex natural insulation material: Carbonized rice hull and rice hull," *Journal of Asian Architecture and Building Engineering*, vol. 16, no. 1. pp. 239–246, 2017, doi: 10.3130/jaabe.16.239.

[233] A. P. L. Duarte, "Avaliação de Propriedades Termo-Hidráulicas de Solos Requeridas na Aplicação da Técnica de Dessorção Térmica," pp. 1–290, 2004.

[234] A. Pianella, L. Aye, Z. Chen, and N. S. G. Williams, "Substrate depth, vegetation and irrigation affect green roof thermal performance in a mediterranean type climate," *Sustainability (Switzerland)*, vol. 9, no. 8. 2017, doi: 10.3390/su9081451.

[235] B. Polly, "Improving the Accuracy of Software-Based Energy Analysis for Residential Buildings," no. July, 2011.

[236] I. Caetano, L. Santos, and A. Leitão, "Computational design in architecture: Defining parametric, generative, and algorithmic design," *Front. Archit. Res.*, vol. 9, no. 2, pp. 287–300, 2020, doi: 10.1016/j.foar.2019.12.008.

[237] "Ladybug Tools | Home Page." https://www.ladybug.tools/ (accessed Jan. 06, 2022).

[238] "Grasshopper - algorithmic modeling for Rhino." https://www.grasshopper3d.com/?overrideMobileRedirect=1 (accessed Jan. 06, 2022).

[239] "Rhino - About McNeel." https://www.rhino3d.com/mcneel/about/ (accessed Jan. 06, 2022).

[240] "Ladybug Tools | Publication." https://www.ladybug.tools/publication.html (accessed Jan. 06, 2022).

[241] "EnergyPlus." https://energyplus.net/ (accessed Feb. 25, 2022).

[242] "OpenStudio." https://openstudio.net/ (accessed Jan. 06, 2022).

[243] "DesignBuilder Software Ltd - Home." https://designbuilder.co.uk/ (accessed Feb. 11, 2022).

[244] *Geographical Names Data Base*. Natural Resources Canada.

[245] "Quebec Construction Code, Chapter I.1 – Energy Efficiency of Buildings, and National Energy Code of Canada for Buildings 2015 (amended)," 2015, [Online]. Available: Quebec Construction Code, Chapter I.1 – Energy Efficiency of Buildings, and National Energy Code of Canada for Buildings 2015 (amended).

[246] "Bath Inventory of Carbon and Energy (ICE) | Greenhouse Gas Protocol." https://ghgprotocol.org/Third-Party-Databases/Bath-ICE (accessed Feb. 11, 2022).

[247] "Explaining Your Québec Electricity and Natural Gas Rates – EnergyRates.ca." https://energyrates.ca/quebec/explaining-your-quebec-electricity-and-natural-gas-rates/ (accessed Feb. 25, 2022).